8th International Symposium on Focused Ultrasound

October 23-27, 2022
Bethesda North Marriott Hotel & Conference Center
Bethesda, MD, USA

Program and Abstracts

Part 2: GYN-01 through OPT-01

FOCUSED ULTRASOUND FOUNDATION

Oral Abstracts

Part 2 contains abstracts GYN-01 through OPT-01.

The following abstracts were withdrawn by the authors:

BRT-41	END-03	NDG-08
BST-01	IMM-07	SDT-02
BST-07	MOV-10	URO-04

BRT-38 has been omitted as a duplicate of BRT-39, the latter having more complete author information.

GYN-01

Topic: Gynecologic
Presentation Type: Oral

The Impact of Machine Learning Classifiers in Predicting the Treatment Outcome of High-Intensity Focused Ultrasound Ablation of Uterine Fibroids with an Immediate Nonperfused Volume Ratio of at Least 90%

Emine Akpinar[1], Chandran Nadarajan[2], Nguyen Minh Duc[3], Bilgin Keserci[2]

[1]Yildiz Technical University, Istanbul, Istanbul, Turkey
[2]Universiti Sains Malaysia, Kubang Kerian, Kelantan, Malaysia,
[3]Pham Ngoc Thach University School of Medicine, Ho Chi Minh City, [Sai Gon], Vietnam

Background: Well-informed medical decisions require comprehensive information supported with higher scientific accuracy data. This can be achieved with artificial intelligence (AI) capabilities, which incorporates wider statistically valid evidence-based predictors available through advanced magnetic resonance imaging (MRI) technology. Machine learning (ML) methods are able to increase the granularity of data analysis, category distinctions, and associated tissue responsiveness information. Such capabilities are particularly relevant and essential for the complete assessment of the success of the high-intensity focused ultrasound (HIFU) procedure. Therefore, the aim of this study was to comparatively evaluate the role of Gradient boosting (GBM) classifier to find the most informative anatomical features and tissue characteristics of lesion outlining its cellularity, diffusivity, and vascularity in predicting the treatment outcome of HIFU ablation with an immediate non-perfused volume (NPV) ratio of at least 90%.

Materials and Methods: The screening MR examinations of 73 women (mean age, 38.8 years; range, 22?49 years) were included in the analysis. Dataset was split into two disjoint sets of training-set (x_tr ain, y_train) and testing-set (x_test, y_test) which contain 67% and 33% of data, respectively. The relationship between the MRI features and the immediate NPV ratio of 90% was evaluated using Pearson's correlation coefficients to measure feature importance. Furthermore, we have investigated the best performing features from each multi-parametric (mp) MRI group in predicting the treatment outcome of HIFU ablation with an immediate NPV ratio of 90%, calculated with GBM Classifier. The diagnostic ability of ML classifier was performed by means of standard performance metrics, including the area under the receiver operating characteristic curve (AUROC), accuracy, sensitivity, and specificity.

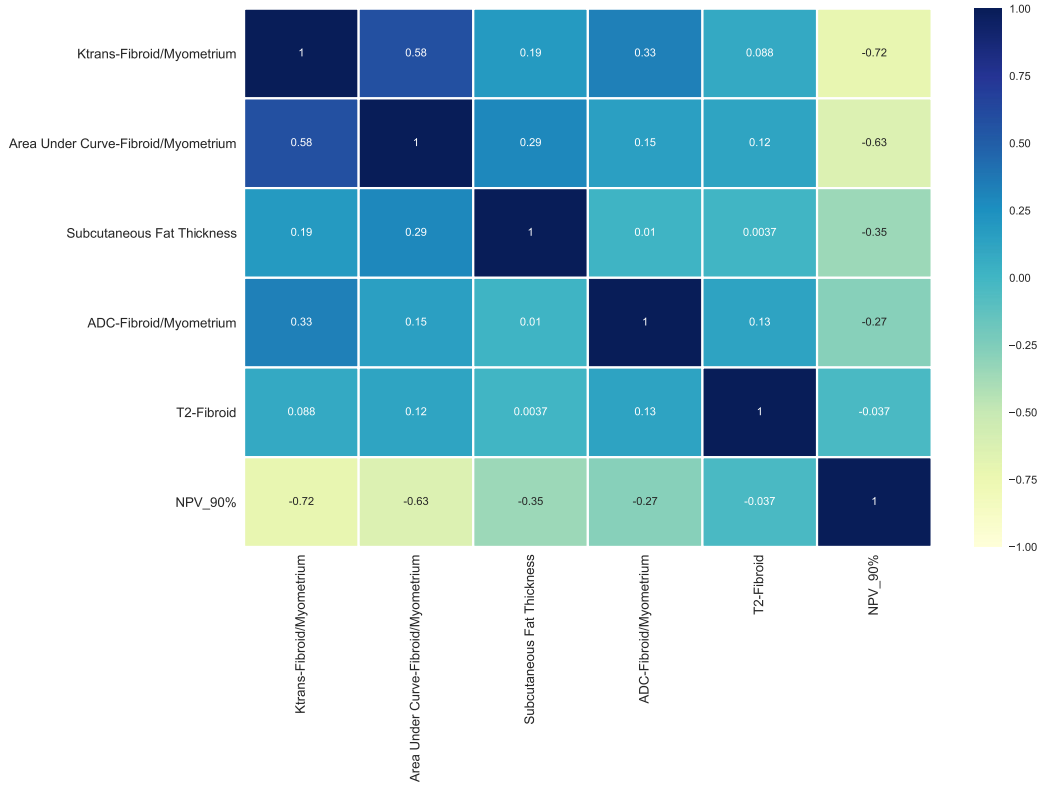

Figure 1. The pairwise Pearson's correlation coefficients among the best performing features from each mpMRI group

Results: The mpMRI features were assessed on the following subgroups: : (i) anatomical, (ii) T2 signal intensity (SI), (iii) Diffusion-weighted (DW) MRI, (iv) quantitative perfusion MRI, and (v) semiquantitative perfusion MRI. The best features suggested by ML voting system were: (1) Ktrans ratio of fibroid to myometrium (Ktrans_FIB_MYO); (2) The ratio of area under the curve (AUC) of fibroid to myometrium (BEF_AREA_FIB_MYO); (3) Subcutaneous fat thickness (Sub_fat), (4) The ratio of ADC value of fibroid to myometrium (ADC_BEF_FIB_MYO); (5) T2-SI of fibroid (T2_FIB). Ktrans ratio of the fibroid to the myometrium showed the highest negative correlations with NPV ratio of at least 90% ($r = -0.72$, $P<0.0001$; Pearson's correlation test). The ratio of AUC of fibroid to myometrium ($r = -0.63$, $P < 0.0001$) had a statistically significant negative correlation with NPV ratio of at least 90%. Furthermore, the ratio of ADC value of fibroid to myometrium ($r = -0.28$, $P = 0.0184$) and subcutaneous fat thickness ($r = -0.35$, $P = 0.0026$) were negatively correlated with NPV ratio of at least 90% while no statistically significant correlation was found between T2-SI of fibroid and NPV ratio of at least 90% ($r = -0.037$, $P = 0.7585$). Ktrans ratio of fibroid to myometrium had the highest AUROC (0.97), followed by the ratio of ADC value of fibroid to myometrium (0.83), the ratio of AUC of fibroid to myometrium (0.82), subcutaneous fat thickness (0.5), T2-SI of fibroid (0.5). The AUROC ranged from 0.5 to 0.97, accuracy ranged from 0.34 to 0.97, specificity ranged from 0.56 to 1.0, and sensitivity ranged from 0.87 to 1.0.

Conclusions: This preliminary study indicates that accurate analysis of the disease that influences the treatment responsiveness using the combination of mpMRI to assess tissue cellularity, diffusivity, and vascularity simultaneously is critical for understanding the suitability of treatment and the likely effectiveness of HIFU with MRI guidance.

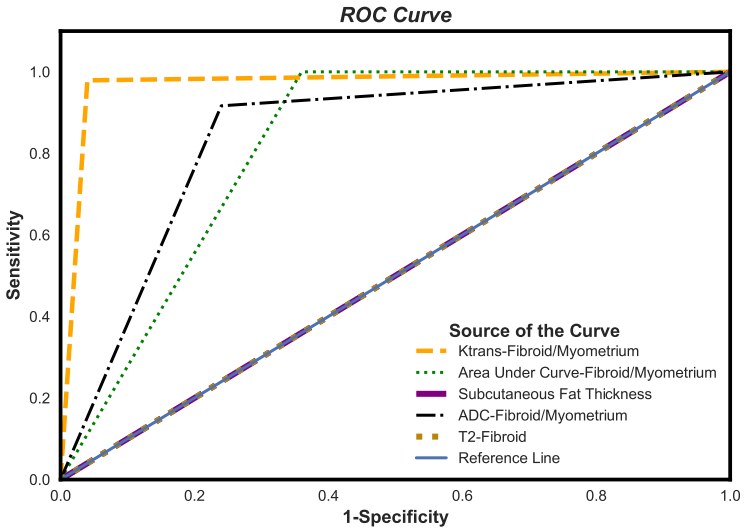

Figure 2. The performance of best performing features from each mpMRI group in predicting the treatment outcome of HIFU ablation with an immediate NPV ratio of 90%, calculated with GBM classifier.

GYN-02

Topic: Gynecologic
Presentation Type: Oral

The Comparison of Traditional and Tree Based Machine Learning Methods in Predicting the Treatment Outcome of High-Intensity Focused Ultrasound Ablation of Uterine Fibroids with an Immediate Nonperfused Volume Ratio of at Least 90%

Emine Akpinar[1], Bilgin Keserci[2]

[1]Yildiz Technical University, Istanbul, Istanbul, Turkey
[2]Universiti Sains Malaysia, Kubang Kerian, Kelantan, Malaysia

Background: Well-informed medical decisions require comprehensive information supported with higher scientific accuracy data. This can be achieved with artificial intelligence (AI) capabilities, which incorporates wider statistically valid evidence-based predictors available through advanced magnetic resonance imaging (MRI) technology. Machine learning (ML) methods are able to increase the granularity of data analysis, category distinctions, and associated tissue responsiveness information. Such capabilities are particularly relevant and essential for the complete assessment of the success of the high-intensity focused ultrasound (HIFU) procedure. Therefore, the aim of this study was to comparatively evaluate the traditional and tree-based machine learning methods in predicting the treatment outcome of high-intensity focused ultrasound ablation of uterine fibroids with an immediate nonperfused volume ratio of at least 90%.

Materials and Methods: We, in this study, used mpMRI features including anatomical characteristics of patients and tissue characteristics of lesion outlining its cellularity, diffusivity, and vascularity. The screening MR examinations of 73 women (mean age, 38.8 years; range, 22-49 years) were included in the analysis. Nine traditional ML methods; Logistic Regression (LR) classifier, Passive Aggressive classifier, SGDC classifier, Linear Discriminant Analysis classifier, Quadratic Discriminant Analysis classifier, LinearSVC classifier, Support Vector Machine (SVM) classifier, K-Nearest Neighbor (KNN) classifier, Gaussian Naive Bayes classifier, and three tree ML based methods, Decision Tree classifier, Random Forest (RF) classifier, Extra Tree classifier were used. The diagnostic ability of the ML classifiers was evaluated using standard performance metrics, including the area under the receiver operating characteristic curve (AUROC), accuracy, sensitivity, and specificity and F1-score. The whole data set of 73 patients was split into 5 groups by performing the 5-fold cross validation to evaluate generalizability and accuracy of the model.[1]

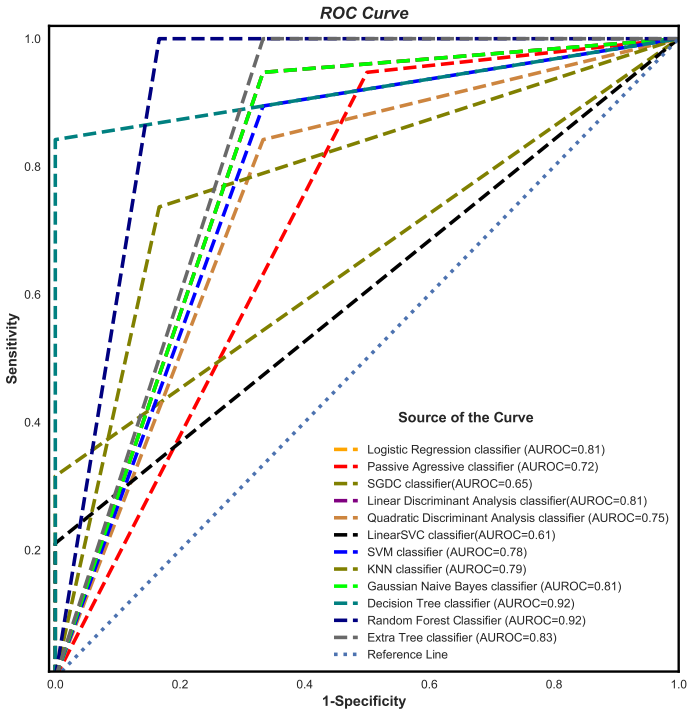

Figure 1. The performance of the 12 ML techniques in predicting the treatment outcome of HIFU ablation with an immediate NPV ratio of 90%.

Results: The most efficient ML classifiers with the highest AUROC were determined as the predictive model, which was used to predict the treatment outcome of HIFU ablation for uterine fibroids with an immediate NPV ratio of at least 90%. For twelve classifiers, the area under receiver operating characteristic curve (AUROC), accuracy, specificity, and sensitivity ranged from 0.65 to 0.92, 0.4 to 0.96, 0.5 to 1.0, and 0.21 to 1.0, respectively. The random forest (RF) classifier demonstrated the best predictive performance with an AUROC of 0.92 and accuracy of 0.96, followed by decision tree classifier, an AUROC of 0.92 and accuracy of 0.88.

Conclusions: This preliminary study indicates that ML algorithms should be considered in assisting physicians to fully evaluate the outcome of the HIFU therapy.

Acknowledgment/Funding Sources: This project is funded by The Scientific and Technological Research Council of Turkey (2020-2023).

Reference

1. Javatpoint. *K-Nearest Neighbor(KNN) Algorithm for Machine Learning*. 2022. Accessed 1 June 2022. https://www.javatpoint.com/k-nearest-neighbor-algorithm-for-machine-learning

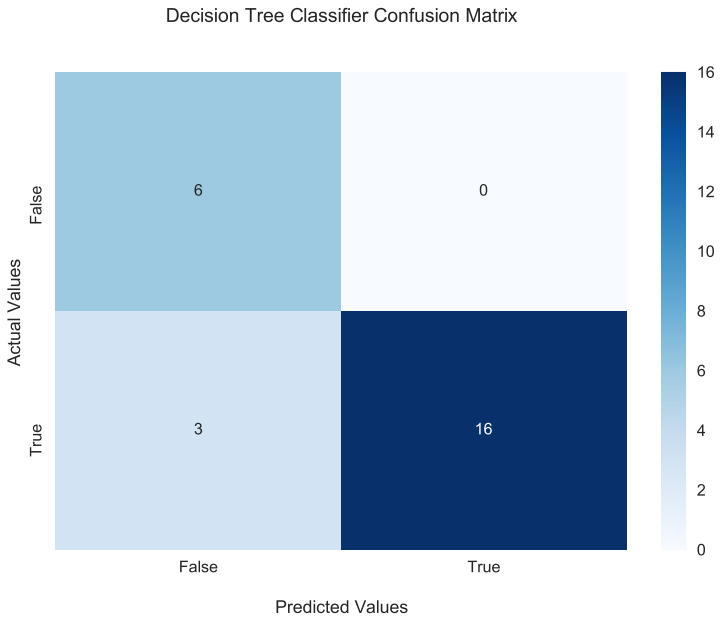

Figure 2. Confusion matrices of the best performing classifiers

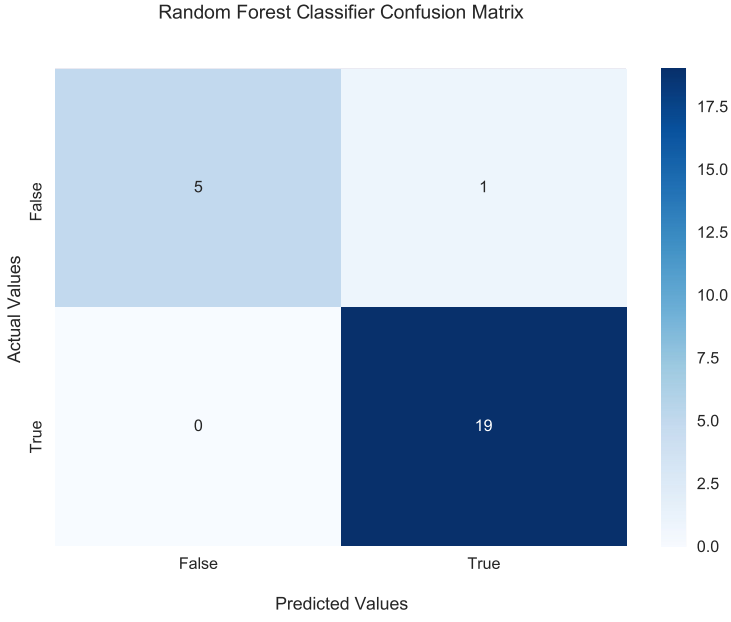

Figure 3. Confusion matrices of the best performing classifiers

GYN-03

Topic: Gynecologic
Presentation Type: Oral

Sustainability of the MR-HIFU Treatment of Uterine Fibroids

Kimberley Anneveldt, Martijn F. Boomsma, Ingrid Nijholt

Isala Hospital, Zwolle, Overijssel, Netherlands

Background: The healthcare systems is responsible for large CO2 emissions contributing to global warming. This has a negative impact on our environment and can lead to sickness itself. Besides clinical effectiveness and cost-effectiveness evaluations, more attention should be paid to the environmental impact of different treatments for the same disease. To assess the multifactorial impact of a treatment, a Life Cycle Assessment (LCA), which provides information from cradle-to-grave of all elements involved in the treatment, should be performed. Life Cycle Inventory (LCI) databases, to perform such an assessment, currently lack healthcare data. Therefore we took the first steps in collecting data to evaluate the CO2 emission of a single uterine fibroid MR-HIFU treatment performed in our hospital.

Materials and Methods: In this evaluation we took a single uterine fibroid MR-HIFU treatment (performed on a Sonalleve V2 device, Profound Medical Inc.) as our functional unit and included relevant data from the moment the patient entered the MRI examination room until she left, which were our boundaries of investigation. We retrospectively collected data of 25 treatments on the average energy use of the MRI-scanner (1.5T Philips Ingenia) and the MR-HIFU device during a treatment and the amount and type of medication used. Data on solid waste amount and type of waste were prospectively collected during 5 treatments.

Results: The energy use of the MRI scanner and the MR-HIFU device during a MR-HIFU treatment was on average 60 kWh and 13.6 kWh respectively. This corresponds with a CO2 equivalent of 15.9 kg. A total of 16 different medication types were used during a treatment, however of only two types the CO2 emission is known. The oxygen use during a MR-HIFU treatment led to 15.5 g of CO2 emission. The total amount solid waste after a MR-HIFU treatment ranged between 727 – 1228 g, with an average of 998 g.

Conclusions: When implementing a new treatment, sustainability and environmental impact should be evaluated besides (cost-) effectiveness to face the paradoxal effect of healthcare on the health of people worldwide. This information should be provided to patients and their physicians before deciding on which treatment the patient should undergo. However, at this point LCI databases including medical data are lacking and therefore performing an official LCA to calculate the multifactorial environmental impact of a treatment, is barely feasible. We performed the first steps in evaluating the CO2 emission of the MR-HIFU treatment. This information can be used in a future LCA and compared with the CO2 emission of other uterine fibroid treatments.

Acknowledgment/Funding Sources: Supported by the Hilly de Roever-Bonnet Fund of the Dutch Association of female doctors (VNVA)

GYN-04

Topic: Gynecologic
Presentation Type: Oral

Clinical Experience Using Sonalleve MR-Guided High-Intensity Focused Ultrasound System for the Treatment of Adenomyosis in China

Chenchen Bing[1], Kang Zhou[2], Haifeng Shi[2], Jintang Ye[2], Yu Zhang[2], Ari Partanen[3]

[1]Profound Medical, Beijing, China
[2]Peking Union Medical College Hospital, Beijing, China
[3]Profound Medical, Mississauga, ON, Canada

Background: Adenomyosis is a common disease featuring the abnormal growth of endometrium into the muscle wall of the uterus. It can result in enlarged uterus and painful, heavy menstrual bleeding. The cause of adenomyosis is not clear but the disease usually resolves after menopause. The average age at diagnosis is between 35 to 50 but recent cases among younger women have been observed. Hormonal treatments are considered for adenomyosis, and for extreme cases the removal of the uterus (hysterectomy) can be performed. In the past few decades, magnetic resonance imaging-guided high-intensity focused ultrasound (MR-HIFU) has been shown as an effective, non-invasive intervention for uterine diseases such as uterine fibroids. MR-HIFU can preserve the uterus and maintain fertility, which is ideal for younger patients. As adenomyotic lesions are often more vascularized, however, there are technical barriers for a successful treatment. The goal of this study was to evaluate MR-HIFU efficacy to treat adenomyosis in China.

Materials and Methods: Women (n = 57, age 28-53) diagnosed with adenomyosis (with or without coexistence of uterine fibroids) were included in this study. After MR screening, the eligibility for MR-HIFU treatment was determined by experienced radiologist and gynecologist. The uterus size was measured during patient screening for treatment planning. Depending on the lesion size and perfusion, 1-4 doses of gonadotropin-releasing hormone agonists (GnRH-a) were administered to reduce uterus size and blood flow for improved clinical outcomes. The ideal uterus size for treatment was considered as 7 cm or less. Treatment planning, ablation treatment, and post-op evaluation were performed with clinical Sonalleve V2 MR-HIFU system (Profound Medical, Canada). After sonication, contrast-enhanced T1w MRI were acquired, and the non-perfused volume ratio (NPVr) was calculated to evaluate the immediate clinical outcome. After treatment, the patient received 2 courses of GnRH-a. At 3-month follow-up, Uterine Fibroid Symptoms-Quality of Life (UFS-QoL) and Symptom Severity Score (SSS) were recorded and compared to baseline. MR images were also obtained at 3-month timepoint.

Results: 93% (53/57) of treatments had NPVr higher than 80%, considered as a good clinical outcome. A median of 2 courses of GnRH-a per patient were administered prior to therapy. The average uterus size was 6.1 ± 1.2 cm upon treatment. Average acoustic power used for ablation was 303 ± 55 W and the average sonication energy was 6.5 ± 1.9 kJ. The average treatment duration was 122 minutes. One adverse event of leg numbness (resolved) was reported due to sonication performed too close to the spine. There were no serious adverse events. At 3-month follow-up, symptom relief in terms of UFS-QoL and SSS was observed in 81% (46 of 57) of the patients.

Conclusions: The efficacy of using a clinical MR-HIFU system for treating adenomyosis has been confirmed in a clinical setting in China. With the administration of GnRH-a drug, the clinical outcomes were further optimized. Satisfactory treatment performance was shown by the immediate post-treatment NPVr and the 3-month follow-up results.

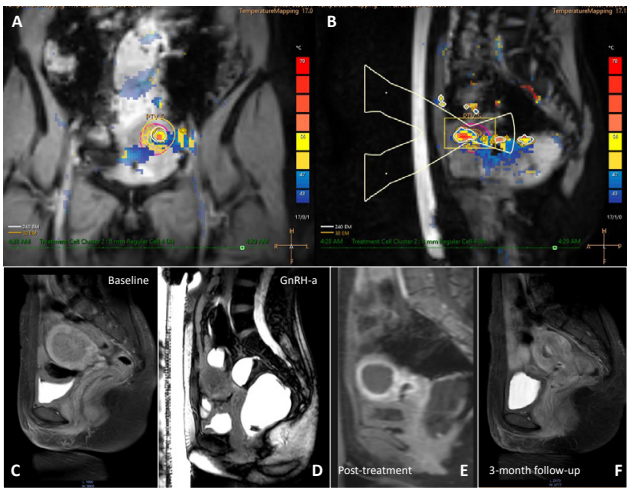

Figure 1. Temperature map acquired during the treatment (A, B). T2-weighted image upon patient screening was shown in (C). The size of uterus reduced after 2 courses of GnRH-a (D). Post-treatment CE T1-weighted images and follow-up at 3-months shown in (E) and (F).

Acknowledgment/Funding Sources: We thank the anesthesiologists Dr. Xiaoyu Yang and Dr. Qiujun Li from Peking Union Medical Center Hospital; the administrative officers Mrs. Ying Wang, Ms. Taolin Zhong; the MR technician director Mr. Chengyu Yang, technicians, and nurses.

GYN-05 -YI

Topic: Gynecologic
Presentation Type: Oral

A Fully Electronically Steerable Modular MR-Guided Focused Ultrasound Phased Array System

Ryan M. Jones[1], Yuexi Huang[1], Benjamin Lucht[2], Samuel Gunaseelan[1], Tyler Portelli[2], Elizabeth David[1], Kullervo Hynynen[1]

[1]Sunnybrook Research Institute, Toronto, ON, Canada
[2]Arrayus Technologies Inc., Burlington, ON, Canada

Background: MR-guided focused ultrasound (MRgFUS) for non-invasive thermal therapy has been demonstrated in various clinical applications. Phased array FUS applicators provide electronic control over the beam geometry and direction, and can be tailored to provide optimal energy deposition patterns for a given therapeutic indication. Existing commercial body MRgFUS systems employ large-element spherically-curved arrays that have limited electronic steering ranges and rely on mechanical translation to treat large tissue volumes. Here we describe a flat fully-populated modular MRgFUS phased array system with increased electronic steering capabilities. The feasibility of using this novel design for image-guided thermal ablation over larger target volumes was demonstrated in pre-clinical and clinical studies.

Materials and Methods: PZT transducer elements were grouped into 8 x 8 square modules with a half-wavelength inter-element spacing at the driving frequency (f = 518 kHz, lateral vibration mode) [Song et al IEEE UFFC 2012; Ellens et al PMB 2015; Aslani et al IEEE TBME 2020]. A flat 170 mm-diameter 96-module (6144-element) array was fabricated in house. Custom driving electronics were developed using Application-Specific Integrated Circuit (ASIC) technology, enabling element-wise phase and amplitude control over the therapy beam. The MRI-compatible transducer array and driving system were designed to mount on the standard bed of a 3T MRI scanner (MAGNETOM Prisma, Siemens Healthcare, Erlangen, Germany). Online 3D visualization of the estimated in-situ acoustic pressure field distribution was integrated within the driving system software for treatment planning. Multi-planar MR-thermometry and thermal dose mapping were carried out for intraoperative treatment monitoring. A sparse 64-element receiver array was integrated for cavitation monitoring. The device underwent extensive pre-clinical testing, and is currently being evaluated in an ongoing clinical trial of MRgFUS for the treatment of uterine fibroids (NCT03323905). Patients were followed (clinical/MR imaging, symptom surveys) for 12 months post-treatment.

Results: Acoustic Characterization: Hydrophone measurements of the acoustic field generated by the phased array demonstrated ellipsoidal focal volumes; at a target depth of 6 cm the focal beam width and depth of field (pressure full width at half maximum) were 2.7 mm and 11.0 mm, consistent with numerical simulations [Ellens et al PMB 2011]. The system was shown capable of rapid electronic beam steering at 250 treatment points/second, with the targets distributed arbitrarily across the array aperture. Pre-Clinical Testing: FUS exposures were performed in in-vivo porcine muscle tissue. Over 860 sonications targeting ablation were carried out across 29 animals. Volumetric tissue ablation was demonstrated via both single- and multi-point exposures, and confirmed via gross pathology and histology. Clinical Trial: Patients received 23 ± 9 sonications (power = 141 ± 63 W, duration = 39 ± 12 s) during MRgFUS treatment sessions (74 ± 35 [143 ± 30] min FUS [MRI] time) resulting in thermal dose volumes of 24 ± 21 cm3 (240 cumulative equivalent minutes at 43oC). Active cooling and the low operating frequency permitted sequential sonications in quick succession with minimal near-field heating, shortening treatment times. The mean nonperfused tissue volume measured immediately post-treatment via contrast-enhanced T1-weighted MR imaging was 75 ± 129 cm3. Increases observed in quality of life scores improved throughout the year post-treatment. Symptom severity scores improved 1 month post-treatment and were durable throughout the year. There were no serious adverse events (i.e. off-target effects, near-field damage) related to the use of the MRgFUS device.

Conclusions: Volumetric thermoablation with a fully-populated phased array appears safe and effective for the treatment of uterine fibroids. The MRgFUS system is capable of large volume tissue ablation without the need for mechanical translation, and the high element count provides increased control over the beam geometry for improved ultrasound energy delivery. The technology is extensible, stackable, and modular, allowing custom MRgFUS device development tailored to any indication.

Acknowledgment/Funding Sources: Canada Foundation for Innovation, Canadian Institutes of Health Research, Federal Development Grant, Ontario Institute of Cancer Research, Ontario Research Fund, National Institutes of Health, Natural Sciences and Engineering Research Council of Canada.

ID-01

Topic: Infectious Disease
Presentation Type: Oral

Optimization of Histotripsy Dose for the Non-invasive Treatment of Biofilms in Catheter-Based Medical Devices

Ryan Morse, Chris Childers, Elizabeth Nowa[2], Jayasimha Rao, Eli Vlaisavljevich

Virginia Tech Carilion School of Medicine, Roanoke, VA, USA

Background: Medical catheter contamination with biofilms is a major issue in the inpatient hospital setting that results in adverse effects and increased mortality through catheter-associated infections. Histotripsy is a noninvasive, nonthermal focused ultrasound ablation method. Recent studies by our group have shown that histotripsy is capable of removing biofilms from the lumen of medical catheters. However, these studies have relied on relatively more conservative treatment parameters than may be required clinically, with prior studies requiring approximately 5 minutes of treatment per centimeter of catheter, corresponding to ~3-4 hours for the treatment of a standard length urinary catheter (44 cm). In this study, we investigate the minimum required dose of histotripsy to achieve biofilm removal from the lumens of medical catheters in order to optimize histotripsy parameters for future clinical translation.

Materials and Methods: A previously established P. aeruginosa (PA14) model was used to culture biofilm in catheter mimics with a length of 2.5 cm. Histotripsy was applied using a custom designed 16-element, 1MHz transducer with single cycle pulses applied at a pulse repetition frequency (PRF) of 200 Hz. A computer-guided 3-D positioning system was used to provide a predetermined number of histotripsy pulses to several discrete points on the catheter. Dosage of histotripsy was altered through three independent factors in separate studies; pulses per point (PPP), step size, and scanning speed. Biofilm was quantified post-treatment through crystal violet staining and spectrophotometry, with treated catheters compared to controls to determine the percentage of biofilm removed. All histotripsy settings were tested in triplicate, with results compared to three untreated control catheters per experiment.

Results: Results from initial testing compared biofilm removal from histotripsy at a range of treatment doses from 100-500 PPP with results showing near complete biofilm removal for all treatments (Fig 1a). Next, a second set of experiments looked at increasing the step size between treatment points to further enhance treatment efficiency (Fig. 1b), with step size ranging from 0.1 mm to 2 mm. Once again, the percent of biofilm removed was maintained for all treatment conditions. A final study was then conducted using a continuous scanning approach in order to further increase the treatment speeds beyond what was feasible using treatments of a discrete number of points. In this final set of experiments, treatment dosage was modified by varying the scanning speed applied by the motorized positioning system while histotripsy was continuously applied to the catheter lumens, with scanning speeds ranging from 0.41 mm/s to 5 mm/s tested. Results showed near complete removal of biofilms for all speeds until the speed was increased to 2.5 mm/s (Fig.1c). At scanning speeds above this point, a significant reduction in treatment efficacy was observed, with significantly more biofilm remaining after treatment.

Conclusions: The results of this study demonstrate that the minimum required dose of histotripsy to successfully ablate biofilm is substantially lower than previously established protocols. The methods implemented in this study were able to increase the histotripsy application speed from ~0.032 mm/s to 1.5 mm/s, while still removing nearly all biofilm from catheter lumens. Based on these findings, our newly developed parameters would be

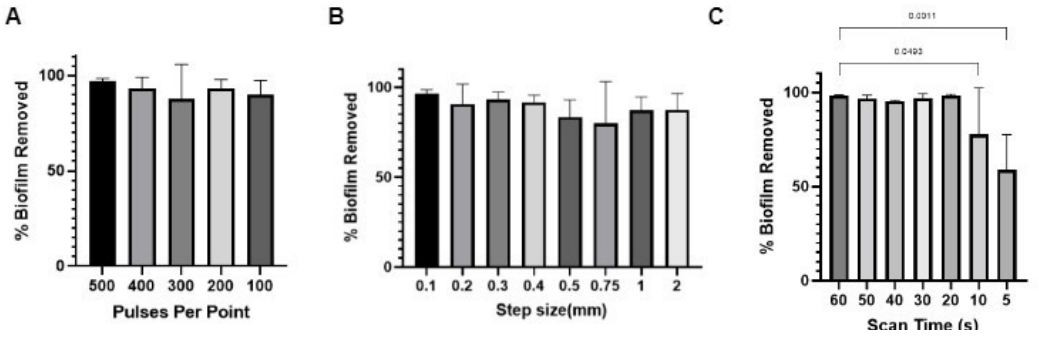

Figure 1. The effects of histotripsy dose on the percentage of biofilm removed from the lumens of catheter mimics. Total pulse variations were achieved through alteration of (A) pulses per point, (B) step size between points, and (C) scanning speed.

capable of reducing the expected histotripsy treatment time for treating a clinical urinary catheter from 3-4 hours down to just under 5 minutes. Ongoing studies are underway to further optimize histotripsy treatment parameters by utilizing higher PRFs. Overall, these findings suggest histotripsy has the potential to be used for the non-invasive removal of medical catheter biofilms in a clinically applicable timeframe.

Acknowledgment/Funding Sources: Virginia Tech Carilion School of Medicine.

IMM-01

Topic: Immunotherapy
Presentation Type: Oral

Focused Ultrasound and Low-Dose Gemcitabine to Augment Immune Control of Early-Stage Breast Cancer, UVA B-54 Clinical Trial

David R. Brenin, Patrick Dillon, Jonathan Nguyen, Christiana Brenin, Trish Millard, Carrie Rochman

University of Virginia, Charlottesville, VA, USA

Background: Focused ultrasound ablation (FUSA) induces immune responses to thermally damaged tissue. Its use for breast cancer is appealing due to ease of access to most breast tumors and its non-invasive nature. When combined with immunotherapy for metastatic breast cancer in humans, FUSA has demonstrated precision in tumor demarcation and safety in a human clinical trial (UVA-B-48) for breast cancer. However, the effects on systemic immune priming have not been explored. This study investigates the local and systemic effects of FUSA + gemcitabine (GEM) in patients with breast cancer, with the expectation that treatment prior to breast surgery will result in decreased circulating and intra-tumoral monocyte-derived suppressor cells (MDSC) and increased circulating effector T cell responses compared to either treatment alone.

Materials and Methods: Target accrual for this phase I study conducted at the University of Virginia is 42 patients. The study has three arms (see figure). Participants on Arm A will receive GEM only. Participants on Arm B will receive FUSA of tumor only. Participants on Arm C will receive both GEM and FUSA of tumor. Following the experimental therapy, all subjects will undergo standard surgical and adjuvant therapy. The EchoPulse device, manufactured by Theraclion will but used for FUSA.

Results: Primary endpoints: safety of FUSA, GEM, and FUSA+GEM therapy. Secondary endpoints: estimation of effect of FUSA, GEM, and FUSA/GEM on the MDSC/CD8 ratio in the tumor, estimation of effect of FUSA, GEM, and FUSA/GEM on circulating activated T cells, estimation of effect of FUSA, GEM, and FUSA/GEM on dendritic cell maturation in tumor, and impact of treatment on residual cancer burden in the breast. Exploratory endpoints: Explore whether the treatments induce T cell specificity to known breast cancer antigens; explore whether the treatments affect the maturity of dendritic cells within the sentinel node; estimate the effect on the frequency and phenotype of circulating myeloid populations; estimate the effect on the intra-tumoral immune landscape; estimate the effect on cytokine expression in the tumor microenvironment; estimate the effect on the function of intra-tumoral T cells; estimate the effect on systemic cytokine expression.

Conclusions: The UVA B-54 clinical trial, Focused Ultrasound and Low-Dose Gemcitabine to Augment Immune Control of Early-Stage Breast Cancer, is currently open to accrual at the University of Virginia with expected completion in three years.

Acknowledgment/Funding Sources: Theraclion, Focused Ultrasound Foundation, UVA Focused Ultrasound Immuno-Oncology Center

Figure 1. Schema

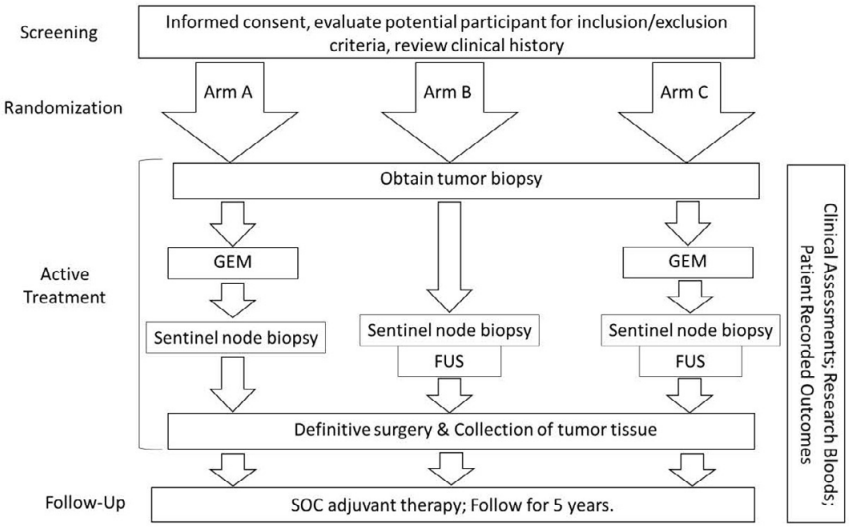

IMM-02

Topic: Immunotherapy
Presentation Type: Oral

MRgFUS Mediated Combination Chemotherapy and Innate Immune Blockade for Glioblastoma

Victoria (Tor) R. Breza, Katherine M. Nowa, Catherine Gorick, Wilson Miller, Richard J. Price

University of Virginia, Charlottesville, VA, USA

Background: Glioblastoma (GBM) is a complex primary brain tumor characterized by tumor cell invasion into surrounding tissue, heterogeneous and leaky blood-brain and blood-tumor barriers (BBB & BTB), and tumor-immune evasion. The current standard-of-care therapy includes surgery, radiotherapy, and temozolomide (TMZ) chemotherapy, but despite intervention, patients are faced with the survival expectancy of only ~16 months post diagnosis. Magnetic resonance image-guided focused ultrasound (MRgFUS) has emerged as a targeted technique for BBB/BTB opening to enhance the delivery of cancer therapies. We recently established that FUS potentiates anti-CD47 (mCD47) antibody delivery, significantly increasing therapeutic efficacy and tumor control. mCD47 targets a ubiquitously overexpressed "don't eat me" signal on GBM that enables innate immune cell evasion. Recent studies highlight combining TMZ with mCD47 in the absence of FUS to increase pro-phagocytic mediators on cell surfaces to induce an adaptive anti-tumor immune response. The goal of this study was to assess therapeutic efficacy of combined TMZ with MRgFUS-mediated delivery of mCD47 in a model of GBM.

Materials and Methods: GL261-Luc2 GBM cells (1x105 cell/2ul) were implanted into the right striatum of C57BL/6 mice. On days 11-13, 16, and 19 post-implantation, mice were treated with temozolomide (20mg/kg i.p., Cayman Chemical). Mice were sonicated (microbubbles i.v., four-spot grid, 1.1MHz, 0.4MPa, 10ms burst, 2 min duration) on day 14, 17, and 20 post-implantation. 15 min post sonication, mCD47 (MIAP410, 8mg/kg i.v.) was injected. Tumor growth was monitored by serial T1w 1.5T and 9.4T MRI. Mouse behavior and weight were monitored weekly to determine humane survival endpoints.

Results: TMZ+mCD47 induced tumor growth control and improved survival with and without FUS (Fig.1A-B). While regression occurred in two mice, the FUS-treated tumor's regression occurred well after treatments had ceased (Fig.1C, day 25-day 48), while the non-FUS-treated tumor (Fig.1D) was not visible on 1.5T MRI by day 14, suggesting that the regression was due to the cytotoxic effects of TMZ alone. The late regression of the FUS-treated tumor is consistent with generation of a systemic anti-tumor immune response. Further, the FUS-treated tumor reoccurred (day 66-day 75), suggesting acquisition of adaptive resistance.

Conclusions: TMZ+FUS+mCD47 promotes increased survival and growth control over untreated control. The regression pattern of the FUS-treated tumor vs the non-FUS-treated tumor suggests the addition of FUS may potentiate an anti-tumor immune response. Future studies will assess systemic immunity to elucidate mediators of the TMZ+FUS+mCD47 induced anti-tumor immune response.

Acknowledgment/Funding Sources: Supported by NIH R21NS118278 and NIH R01EB030409.

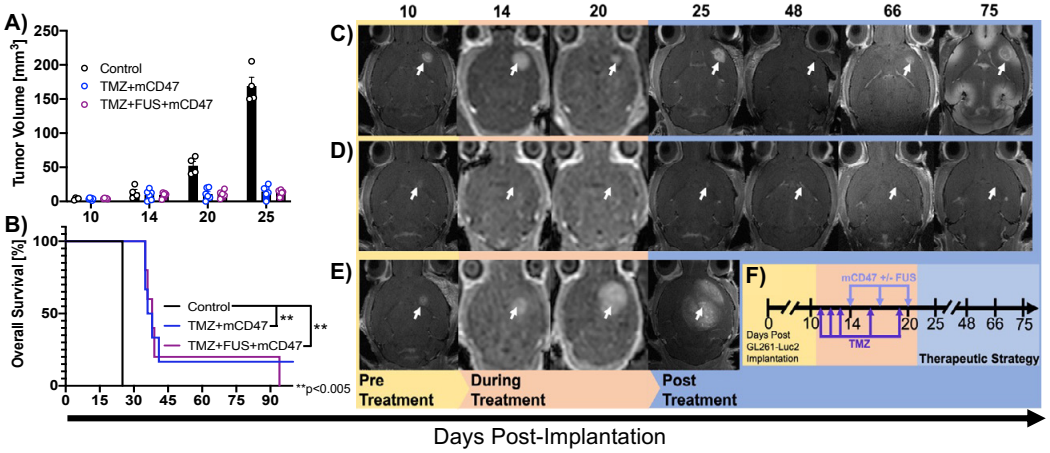

Figure 1. A) Tumor outgrowth. B) Kaplan-Meier curve of overall survival. 1.5T and 9.4T serial MRI images of C) TMZ+FUS+mCD47 responder, D) TMZ+mCD47 responder, and E) representative control mouse. F) Overview of therapeutic strategy.

IMM-03

Topic: Immunotherapy
Presentation Type: Oral

Effect of Murine Vendor on Anti-tumor Immune Responses to Non-ablative Pulsed Focused Ultrasound

Parwathy Chandran, Scott R. Burks, Joseph A. Frank

National Institute of Health, Bethesda, MD, USA

Background: Non-ablative image guided pulsed focused ultrasound (pFUS) has shown promise in murine tumor models as an immunomodulatory strategy for altering tumor microenvironment (TME). However, studies to date have demonstrated efficacy only in murine models procured from a single vendor. To determine whether differences in inbred mice obtained from 3 vendors would alter tumor growth and TME, we evaluated temporal expression of cytokine, chemokine and trophic factor (CCTF), and immune cell profiles following non-ablative pFUS to murine B16 melanoma flank tumors established in C57BL/6J mice.

Materials and Methods: Murine B16 cells (1×106 cells) were sub-cutaneously, bilaterally implanted into C57BL/6J mice (n=6/group/time-point) obtained from 3 vendors [Jackson Laboratories (JAX; n=36), Charles River (CR; n=36), Taconic Biosciences (Tac; n=36)]. Once tumors reached ~5 mm in size, ultrasound guided pFUS (VIFU 2000, Alpinion) was administered at 1 MHz, at 6 MPa peak negative pressure (PNP; ISATP=2683 W/cm2; mechanical index=5.6). Entire tumor volume was sonicated point-by-point along a 2´2 mm matrix with 20 msec pulse length, 10% duty cycle and a 5 Hz pulse repetition frequency. At days 1, 3, and 5 post-sonication, spleens (Sp), lymph nodes (LN) and tumors were harvested, processed and evaluated by proteomic (CCTF) and flow cytometry analyses.

Results: pFUS treatment demonstrated variable, vendor-dependent effects on tumor growth, CCTF and immune cell profiles. B16 volumes in CR mice showed significant reduction ($p<0.05$; 2-way ANOVA) starting at day 2 through day 5, but not in JAX or Tac mice. Proteomic analyses revealed a similar trend wherein CR TME exhibited upregulation of pro-inflammatory cytokines (TNFa, IL-1b, IL-12p70) on days 1 and 3, and downregulation of anti-inflammatory cytokines (VEGF, IL-10) over 5 days. Comparatively, less robust expression of anti-tumoral cytokines were observed in Tac and JAX TME over the study period. Flow cytometry data corroborated tumor growth and molecular analyses, showing significant tumor infiltration of helper and cytotoxic T cells (Th, Tcyt), M1 macrophages and dendritic cells (DC) on days 3 and 5, compared to untreated controls. Day 5 CR spleen also exhibited a pro-inflammatory profile with T cells, macrophages and DC. The profiles of Tac and JAX tumors over days 1, 3 and 5 were comparatively unchanged by pFUS with major, anti-tumoral immunological activity restricted to draining LN on days 5 and 3 in Tac and JAX, respectively. Moreover, molecular and immune cell differences were observed in B16 tumors from control animals on days 1, 3 and 5.

Conclusions: Collectively, B16-bearing CR mice exhibited a more pronounced anti-tumor response to pFUS, resulting in reduced tumor growth and pro-inflammatory CCTF and immune cell profiles as compared to B16 tumors in Tac and JAX mice. Despite using the same mouse strain, tumor type, and pFUS parameters, profound vendor-dependent variability was observed, suggestive of the possible role of inherent genetic disparities among C57BL/6J mice from different vendors. These results suggest that vendor choice may be critical in evaluating anti-tumor effects of pFUS.

Acknowledgment/Funding Sources: Intramural Research Programs at the NIH Clinical Center and the National Institute of Biomedical Imaging and Bioengineering.

IMM-04

Topic: Immunotherapy
Presentation Type: Oral

Abdominal Low-Intensity Pulsed Ultrasound Moderates Pro-inflammatory Phenotype and Improves Therapeutic Outcomes in Murine 4T1 Breast Tumors

Parwathy Chandran, Erik Paletzki, Scott R. Burks, Joseph A. Frank

National Institute of Health, Bethesda, MD, USA

Background: Accumulating evidence have highlighted vagus nerve (VN) as the link serving the bi-directional communication between the nervous and immune systems to regulate inflammatory response and maintain homeostasis. Vagal immunomodulatory effects, also known as the cholinergic anti-inflammatory pathway, can alter the immune system's activity via innervation of lymphoid organs such as the spleen. This pathway can also be activated by non-pharmacological stimulation of the VN or sympathetic splenic nerve, which subsequently suppresses splenic macrophages from secreting pro-inflammatory cytokines such as tumor necrosis factor-alpha (TNF?), interleukin (IL)-1b and IL-6, through the ?7 nicotinic acetylcholine receptor (?7nAChR). Experimental studies in animal cancer models have demonstrated the beneficial effect of VN activity in tumor development by preventing immune suppression and enhancing cytotoxic immunity in the tumor microenvironment (TME). Moreover, vagotomy studies have confirmed the protective effect of an intact VN on cancer progression. However, evidence for an interaction of the VN and immune cells relevant to the TME is scarce and not fully understood. In this study, we utilized low-intensity pulsed ultrasound (LIPUS) as a non-invasive and non-pharmacological approach to modulate the immunological profile of a murine 4T1 breast cancer flank model.

Materials and Methods: Briefly, 4T1 tumor cells were subcutaneously inoculated (106 cells/100µl) into both flanks of each mouse under anesthesia. Once the tumor diameter reached ~5 mm in size, mice were given LIPUS treatment to the abdomen. Preceding the LIPUS treatment, mice were shaved over the abdomen and then placed on a 37 °C heating pad. A transducer was placed over the abdomen's right side with a clamp holder on top of a water-based ultrasound gel. Animals were treated for a total of 10 days (days 1-5 and days 8-12) with a 1 MHz transducer (5 cm2 diameter, Mettler 740x; Anaheim, CA) at US burst 1ms, 10% duty cycle and intensity of 2 W/cm2 for 7 min. On defined time points, mice were euthanized through isoflurane anesthesia and cervical dislocation and tumors, spleens, inguinal lymph nodes (LN), and brains were harvested for further analysis.

Results: Our findings reveal that LIPUS stimulation of the vagus nerve-to-spleen circuit could acutely shift the immunological profile of a murine TME to an immunosuppressive milieu. In comparison to time-matched controls, an overall attenuation of pro-inflammatory markers as well as significant decrease in tumor growth rate were observed in wild type tumor-bearing mice following 2 weeks of abdominal LIPUS stimulation. Immunohistochemistry data revealed double-positive immunoreactivity of choline acetyltransferase (ChAT)/c-Fos within the dorsal motor nucleus of the VN (DMX) in the brain stem area of LIPUS treated wild type (WT) mice brains validating the activation of the immune-regulatory 'inflammatory reflex' via VN stimulation. ?7nAChR and F4/80 double-positive immunoreactivity was observed within LIPUS-treated WT mice tumor sections compared to TMC implying the role of spleen in the anti-inflammatory effect associated with LIPUS and correlating ?7nAChR expressing macrophages to the observed effect. Moreover, associated anti-inflammatory response was abolished in mice with splenectomy suggestive of the crucial role of spleen in VN stimulation mediated by abdominal LIPUS stimulation.

Conclusions: These results provide insight into the neuro-immune communication of the cholinergic anti-inflammatory pathway and highlight the potential use of LIPUS, in combination with conventional cancer treatments, to modulate spleen-mediated inflammatory responses relevant to anti-cancer immunity.

Acknowledgment/Funding Sources: Intramural Research Programs at the NIH Clinical Center and the National Institute of Biomedical Imaging and Bioengineering

IMM-05

Topic: Immunotherapy
Presentation Type: Oral

Focused Ultrasound Induced Blood-Brain Barrier Opening and Systemic Anti-CD40 Agonist Enhances Monocyte Infiltration of Intracranial Melanoma

Vinton W. Cheng, Catherine Gorick, Eric A. Thim, Victoria (Tor) R. Breza, Wilson Miller, Timothy Bullock, Richard J. Price

University of Virginia, Charlottesville, VA, USA

Background: Melanoma brain metastases (MBM), when symptomatic, have a limited response to immune modulating systemic agents and carry a poor prognosis. We hypothesised that focused ultrasound (FUS) with microbubbles (MB) for blood-brain barrier (BBB) opening in a two-site model of metastatic melanoma, combined with an anti-CD40 agonist (aCD40), would enhance CD8 T cell infiltration of the MBM and lead to improved intracranial (i.c.) tumor control.

Materials and Methods: A two-site syngeneic model of metastatic melanoma was established in C57BL/6 mice. Briefly, B16F1cOVA melanoma cells were subcutaneously (s.c.) inoculated in the right flank, followed 5 days later by i.c. inoculation of the same cell line. The following conditions were tested: (1) systemic aCD40 vs. IgG isotype control; and (2) systemic aCD40 with/without FUS+MB vs. IgG with FUS+MB. Systemic aCD40/IgG was administered on days 5 and 7 post-i.c. inoculation; MRI guided FUS (MRgFUS) with MB was co-administered with systemic treatment on day 7. On day 9 post-i.c. inoculation, animals were sacrificed; tumors and draining lymph nodes were harvested for flow cytometry to assess immune cell infiltration. Separate animal cohorts were used to assess for differences in survival by Kaplan-Meier analysis.

Results: Treatment with aCD40 alone or in combination with FUS+MB did not improve survival compared to the other cohorts. Systemic aCD40 significantly increased circulating myeloid and dendritic cells (DC) with associated reductions in T lymphocytes and NK cells compared to the IgG cohort. Higher numbers of inflammatory monocytes were observed in i.c. tumors treated with aCD40 with FUS+MB compared to aCD40 alone or IgG with FUS+MB cohorts. There was no significant difference in CD8 T cell infiltration of the i.c. tumour. Following FUS+MB for BBB opening, there was an increase in SIRPa+ DC with an associated reduction in XCR1+ DC in the i.c. tumors of aCD40 treated animals compared to the IgG treated group.

Conclusions: Anti-CD40 agonists have diverse roles in regulating anti-tumor immune activation. In the context of the two-site model of melanoma brain metastasis, aCD40 alone and in combination with FUS+MB did not improve survival. Moreover, aCD40 appeared to cause a shift to higher levels of circulating myeloid cells. Contrary to our original hypothesis, the addition of FUS+MB did not increase CD8 T cell infiltration, but instead enhanced infiltration of inflammatory monocytes to the i.c. tumor. Therefore, ongoing work will focus on stimulating a monocyte driven anti-tumor response against MBM.

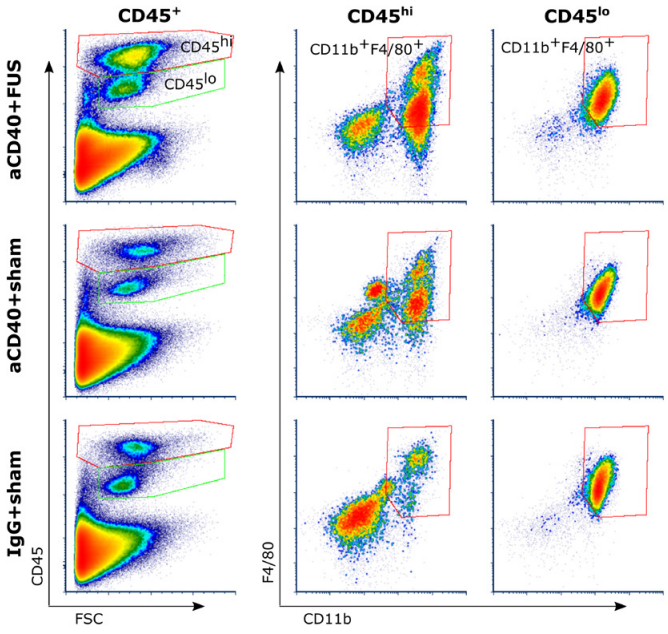

Figure 1. Representative flow cytometry plots of intracranial tumor cells treated with anti-CD40 agonist (aCD40)+FUS, aCD40+sham or IgG+FUS Cell populations of interest: bone marrow derived macrophages (CD45hiCD11b+F4/80+) and microglia (CD45loCD11b+F4/80+)

Acknowledgment/ Funding Sources: We thank the Focused Ultrasound Foundation for funding this research and the UK National Institute of Health and Care Research (NIHR) for funding Dr VWT Cheng to conduct this work.

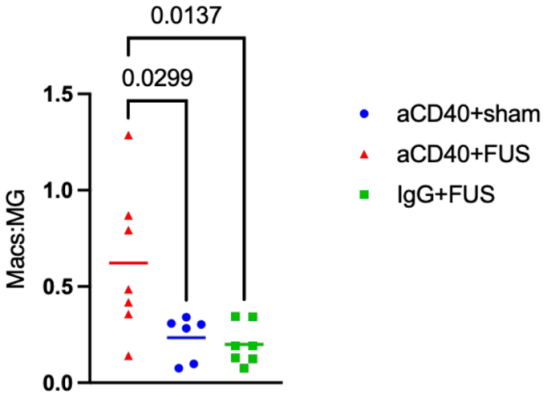

Figure 2. Graph showing increased infiltrating macrophages (Mac), when normalised to microglia (MG), in intracranial tumors from mice treated with aCD40+FUS compared to aCD40+sham or IgG+FUS. Statistical significance assessed by post-hoc Tukey test (One way ANOVA).

IMM-06

Topic: Immunotherapy
Presentation Type: Oral

Immunotherapy of Brain Tumors via Ultrasound-Targeted Delivery of Antibody-Encoding mRNA: Initial Evaluation in a Murine Orthotopic Model of Glioma

Beata Chertok[1], Wilson Miller[1], Richard J. Price[1], David Boczkowski[2], Smita Nair[2]

[1]University of Virginia, Charlottesville, VA, USA
[2]Duke University School of Medicine, Durham, NC, USA

Background: Intracranial gliomas are among the deadliest types of cancer known. New approaches are urgently needed to challenge the status quo – a dismal prognosis with a median survival of only ~15 months despite treatment with existing therapeutic modalities. Antibody-based immunotherapy (e.g. check point inhibitors) has revolutionized treatment of several advanced cancers. This promising modality is being explored for brain tumor therapy, yet with little success to date. Pre-clinical studies show encouraging efficacy when therapy with antibody-based drugs is initiated at early stages of brain tumor development. Unfortunately, combating established intracranial gliomas at more advanced stages - a scenario that better reflects the clinical presentation at diagnosis - remains difficult, likely due to exacerbated transport barriers that impede intra-tumoral access of antibody drugs. The Chertok lab at the University of Michigan has previously developed a novel approach that has the potential to address this challenge. This approach utilizes engineered nanoparticles and non-invasive focused ultrasound to facilitate minimally-invasive, ultrasound-enhanced delivery of a genetic protein precursor, messenger RNA (mRNA), to tumor-resident cells for generation of therapeutic proteins within tumors in situ. Collaborative efforts of the Chertok lab and the Nair lab (Duke University) have previously demonstrated a promising therapeutic proof of concept of this approach in subcutaneous tumor models, using mRNA that encodes for an immunotherapeutic antibody, aCTLA-4. The objective of the current study is to assess the therapeutic potential of this approach against established brain tumors, leveraging MRI-guided Focused Ultrasound technology for precise targeting of orthotopic brain tumors in mice.

Materials and Methods: Therapeutic efficacy was assessed in a pre-clinical murine orthotopic model of glioma, GL261. Tumor volumes were monitored longitudinally by T2-weighted MRI using a 9.4T small animal scanner. Treatments were performed using an MR-guided Focused Ultrasound system (MRgFUS) equipped with a 1MHz single-element transducer and positioned in a clinical 1.5T MRI scanner. On the treatment day, tumors were detected with a contrast-enhanced T1-weighted MRI and the MRgFUS system was programmed to target the tumor. Nanoparticles and microbubbles were co-injected intravenously prior to sonications. mRNA encoding for aCTLA-4-IgG (mRNA-Ab) and recombinant aCTLA-4-IgG antibody (rAb) were used as experimental therapeutics. Changes in tumor volumes and animal survival were used as metrics of therapeutic efficacy.

Results: We report initial results from this ongoing study. Treatments commenced on day 12-14 post-inoculation, at an advanced stage of tumor growth when tumors reach volumes of ~5 μL. In a pilot experiment (n=3), we compared outcomes in subjects treated with a multi-dose regimen of rAb versus non-treated controls. We found that rAb treatment failed to improve the outcomes compared to the non-treated cohort, consistent with previous reports where rAb treatments were initiated at similar stages of tumor progression (J Immunotherapy, 2012, v35: p. 385). We next proceeded to evaluate treatment with mRNA-Ab nanoparticles and MRgFUS (n=5) against non-treated controls (n=8). Strikingly, this treatment resulted in pronounced anti-tumor effects. We observed a nearly 2-fold reduction in tumor volumes at day 18 post-inoculation (day 4 post-treatment) in the treated group vs controls ($p=0.012$), followed by a significant extension of median survival ($p=0.037$). Pilot evaluation of a control treatment with nanoparticles encapsulating non-therapeutic mRNA and MRgFUS (n=2) yielded no significant effects on tumor growth compared to non-treated controls.

Conclusions: Our early results suggest that FUS-targeted delivery of antibody-coding mRNA may have the potential to unlock the benefits of antibody-based immunotherapy for intracranial gliomas, warranting further evaluation of this promising approach.

IMM-08

Topic: Immunotherapy
Presentation Type: Oral

iFOCUS: Phase I Study of High-Intensity Focused Ultrasound Histotripsy and Immune Checkpoint Inhibition in the Treatment of Advanced Cancer

Mirjam de Visser[1], Roel Deckers[1], Josanne S. de Maar[1], Miranda P. Dierselhuis[2], Max M. Van Noesel[2], Clemens Bos[1], Manon N. Braat[1], Willem P. Mali[1], Ari Partanen[3], Stefan Nierkens[1], Chrit T. Moonen[1], Karijn P. Suijkerbuijk[1]

[1]University Medical Center Utrecht, Utrecht, Netherlands
[2]Prinses Maxima Centrum, Utrecht, Netherlands
[3]Profound Medical, Mississauga, ON, Canada

Background: Immune Checkpoint Inhibition (ICI) has led to significant improved survival for some cancers, yet failed to demonstrate substantial benefit in many metastatic malignancies. Limited efficacy of ICI is seen particularly in "cold tumors", characterized by a paucity of T cells. Converting cold tumors into hot tumors could improve the efficacy of ICI. A promising technique that has the potential to sensitize these cold tumors is boiling histotripsy (BH), a novel high-intensity focused ultrasound modality. BH results in non-invasive mechanical fractionation of tissue using pulsed waves at high pressures (55-90 MPa positive, and 14-17 MPa negative pressure), and low duty cycles (<5%). The sharp transition from peak-positive to peak-negative pressure produces a shock wave, resulting in a bubble. Interaction of this bubble with subsequent shock waves leads to rapid tissue lysis, release of tumor-associated antigens and danger-associated molecular patterns (DAMPS) leading to a sudden sterile local inflammation and activation of dendritic cells in the sentinel lymph node.

In collaboration with the Children's National Medical Center and NIH we have shown that ultrasound-guided BH worked synergistically with ICI in a neuroblastoma animal model leading to increased survival, abscopal and vaccination effects. In this model, BH caused increase of dendritic cells, tumor infiltrating T-cells, proinflammatory cytokines, and DAMPs, while reducing pro-tumor regulators such as regulatory T-cells. This approach is further supported by similar in-vivo experiments conducted in other tumor models including melanoma, pancreatic adenocarcinomas and breast cancer. BH has been used clinically in patients with benign prostate hyperplasia and primary and secondary liver malignancies. To date, no clinical studies on the combination of BH and ICI antibodies have been reported. iFOCUS is a first-in-human phase I study of combined ICI and MR-guided boiling histotripsy.

Materials and Methods: Singular histotripsy treatment will be used to boost the effect of combination ICI therapy (anti-CTLA4 ipilimumab; anti-PD1 nivolumab). Patients with metastatic or unresectable advanced solid tumors without standard of care treatment options are eligible to participate if they have a lesion accessible for BH and measurable disease according to RECIST 1.1 . Especially patients with subcutaneous, lymph node, muscle, peritoneal and abdominal wall metastases will be suitable candidates. The first cycle of ICI will be administered one week before BH. After four doses of ICI combination therapy, treatment will be continued as monotherapy (nivolumab) every four weeks until progressive disease, dose-limiting toxicity, or a total treatment duration of two years. The study is divided in three cohorts (Figure 1). Boiling histotripsy procedure

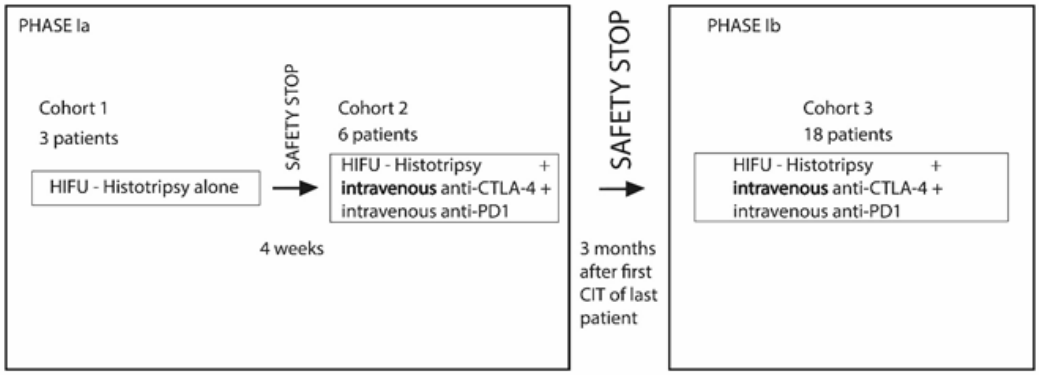

Figure 1. Study design iFOCUS. CIT = cancer immunotherapy.

BH will be performed as an out-clinic procedure. Patients will undergo procedural sedation and will be discharged after three hours of observation. Treatment is planned and executed using the Sonalleve interface by placing 5 mm BH cells with an ellipsoid shape, evenly distributed over the tumor volume. At each focal position, a BH pulse is emitted with 18.000 cycles per pulse at a US frequency of 1.2 MHz and an acoustic power of 750-900 W. The sonication trajectory is repeated for 210 seconds for each focal position. This will be repeated until approximately 10% of the total volume of the tumor is fractionated or until a duration of 60 minutes has been reached.

Results: Primary endpoints: Safety will be assessed by incidence and severity of adverse events, dose-limiting toxicity, and treatment discontinuation rates. Tolerability will be evaluated by patient reported outcome questionnaires. Feasibility will be assessed by reporting the number of technically effective procedures, the percentage screening failures, and the time burden of the study procedures.

Secondary endpoints: Systemic and local response will be evaluated with RECIST1.1 on CT and MRI or PERCIST on PET-CT. RNA-sequencing, multicolor flow cytometry and functional assay analysis will be used to analyze immunological infiltration in tumor biopsies and to assess immunological response in blood samples.

Conclusions: Study design of iFOCUS

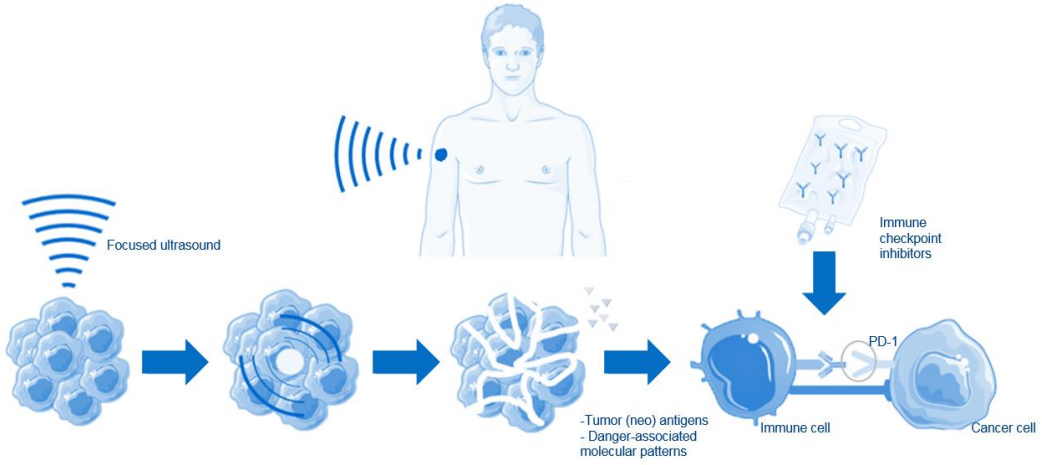

Figure 2. Graphic representation of the combination of BH and ICI. At the focal point, formation of a bubble occurs, which leads to mechanical fractionation, release of tumor-associated antigens and DAMPS. ICI prevents the T-cells from being inactivated.

IMM-09

Topic: Immunotherapy
Presentation Type: Oral

Ex-vivo Validation of HIFU Histotripsy System and Procedure in Preparation for a First Clinical Study on the Combination of Boiling Histotripsy and Immune Checkpoint Inhibition

Mirjam de Visser[1], Ari Partanen[2], Cyril Ferrer[3], Avinash Eranki[4], Clemens Bos[3], Chrit T. Moonen[3], Roel Deckers[3]

[1]University Medical Center Utrecht, Amsterdam, Noord-Holland, Netherlands
[2]Profound Medical, Mississauga, ON, Canada
[3] University Medical Center Utrecht, Utrecht University, Utrecht, Netherlands
[4]IIT Hyderabad, Hyderabad, Uttar Pradesh, India

Background: Immune Checkpoint Inhibition(ICI) has led to significantly improved survival for some cancers yet failed to demonstrate substantial benefit in many metastatic malignancies. Limited efficacy of ICI is seen particularly in immunologically "cold" tumors. Boiling histotripsy(BH) is a promising HIFU technique that has the potential to sensitize cold tumors to ICI. BH employs pulsed waves at high pressures(55-90 MPa peak-positive and 14-17 MPa peak-negative pressure), and low duty cycles(<5%) to liquefy tumor tissue which may aid anti-tumor immune response when combined with ICI. We are planning a first-in-human phase 1 study (iFOCUS) to assess the combination of ICI and MR-guided BH using a clinical HIFU system. To ensure safe and controlled BH treatment, the system must be characterized for different BH parameters and tissue types. This is important since BH lesions are found to vary as a function of tissue type and sonication parameters.The primary aim of this study was to validate the clinical HIFU system targeting accuracy and efficacy for different powers, depths, and tissue types. The second goal was to assess the correlation of BH lesion dimensions on MR imaging and pathology.

Materials and Methods: Fresh ex-vivo porcine liver and skeletal muscle, and bovine heart were degassed in phosphate buffer saline. All tissues were sonicated using a Sonalleve V2 system(Profound Medical, Canada) operated at 1.2MHz with varying sonication powers(600, 750 and 900W) and depths(15 and 30 mm). Other relevant sonication parameters were: 18,000 cycles/pulse, 1Hz pulse repetition frequency, and 210 s sonication duration. MR thermometry(MRT) was performed during BH using the PRFS-method. Immediately before and after BH, T1-weighted-gradient echo(TR=4ms; TE=1.87ms; FA=10°; resolution = 1.6×1.6×3mm3) and T2*-weighted (Gradient Echo; TR=512ms; TE=13.8; FA=90°; resolution = 1×1×3mm3) MR images were obtained to visualize the BH lesion. After sonication, tissue blocks were fixed in formaldehyde, frozen, and sectioned using a cryomacrotome to visualize the BH lesion on pathology. BH lesion location on the MR images was compared to BH target location and the location of maximum temperature measured by MRT. The lesion dimensions on MR images and histopathological slides were measured and compared.

Results: Figure 1 shows the difference between the BH target location and i) the center of mass of maximum temperature increase during a sonication(panel A and B) and ii) the center of mass of the hyper-intense lesion on T2*-weighted MR images(panel C and D) for different powers and depths. For all settings, the differences remained well below 2 mm.

Next, we analyzed the temperature in the focal spot during BH as function of time. All settings demonstrated similar exponential temperature increase and

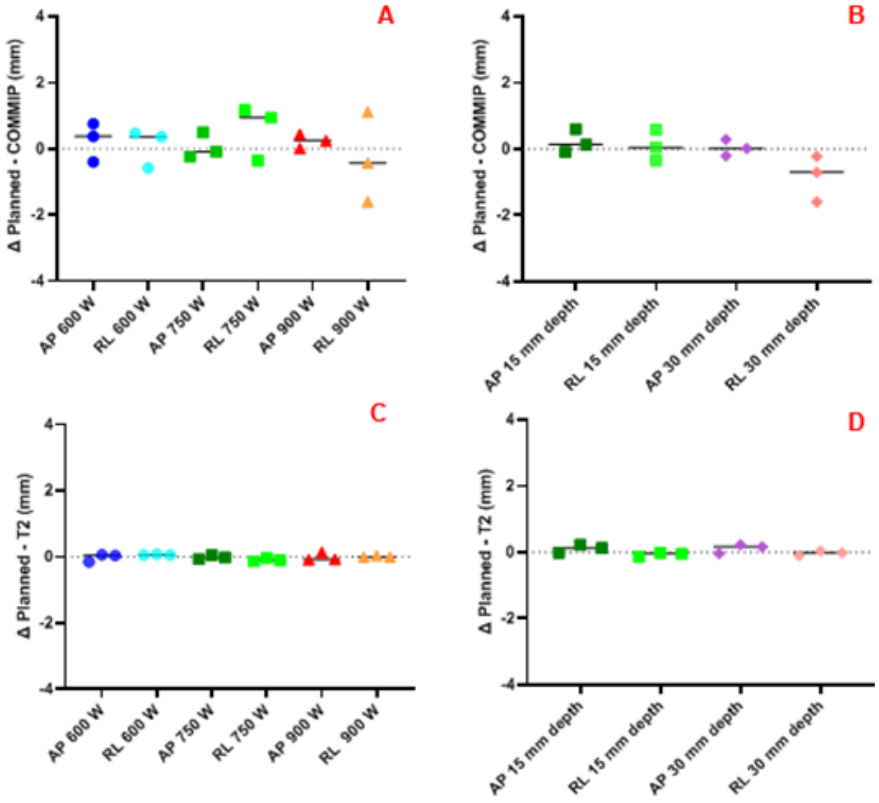

Figure 1. Column scatter graph displaying spatial targeting accuracy of the center of mass of temperature (A+C) and lesion at T2*(B+D) in porcine liver for different powers at a fixed depth of 15 mm (A-B) and for different depths at a fixed power of 750 W (C-D).

decrease, though with different maximum temperature changes. The maximum temperature change increased with increasing power (figure 2D) was lower for deeper sonications and higher for bovine heart compared to porcine liver (data not shown). Successful BH lesions visible on gross pathology were visible as hyper-intense lesions on T2*-wt MRI (figure 3A+B). Lesion dimensions on T2*-wt images corresponded with the size of the BH target. A threshold power to create a BH lesion was observed, though above this threshold the applied power did not substantially influence the lesion dimensions.

Table 1: Mean lesion diameters on T2*–weighted MRI of porcine liver sonicated at different powers and depths. N.v.=not visible on T2*–weighted MRI

Size on T2*–coronal slice			
Power (W)	Depth (mm)	Minor Axis (mm)	Major Axis (mm)
600	15	n.v.	n.v.
750	15	5.9 (5.6 – 6.4)	8.0 (7.0 – 8.6)
750	30	4.8 (2.5 – 6.4)	6.8 (4.8 – 9.1)
900	15	3.0 (1.2-4.9)	6.4 (6.0 – 6.9)

Conclusions: The clinical MR-HIFU system allows for spatially accurate BH lesions in different ex-vivo tissue types and at different powers and depths.The BH lesion dimensions on MRI and on pathology corresponded closely. These results are part of the Investigational Medical Device Dossier for the Institutional Review Board and guides initiation of a safe phase I study on histotripsy combined with ICI.

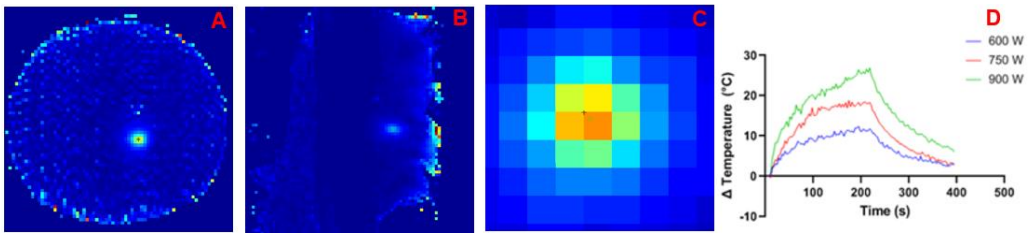

Figure 2. A&B) Maps of max temperature over time based on MRT. Target location(black cross), and COMTmax(green) on coronal(A) and sagittal slices(B); C) Close up of panel A; D) Temperature change in focal spot in porcine liver at room temperature with different powers

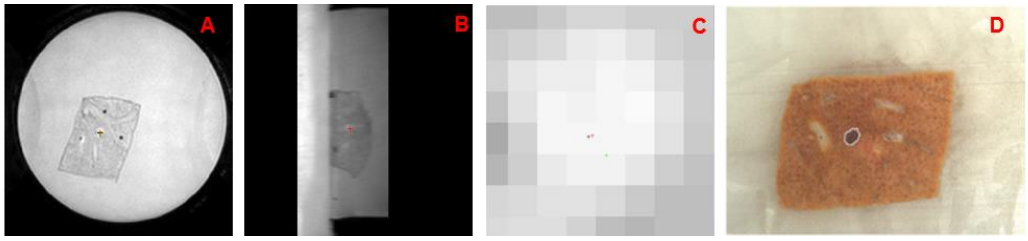

Figure 3. A&B) Target location(black cross), COMTmax(green) and center of mass of lesion atT2(red) on T2*-weighted MRI in coronal(A) and sagittal(B) direction; C) Close up of panel A; D) Cryomacrotome photo with BH lesion automatic segmentation (white line)

IMM-10

Topic: Immunotherapy
Presentation Type: Oral

FUS Mediated Therapeutic Responses in Breast Cancer

Edward P. Griffin, Sean Le, Riya Jai, Wilson Miller, Kumari Andarawewa

University of Virginia, Charlottesville, VA, USA

Background: Breast cancer is the most common invasive cancer in females worldwide. It accounts for 16% of all female cancers and 22.9% of invasive cancers in women. 18.2% of all cancer deaths worldwide, including both males and females, are from breast cancer. The current standard therapies are inadequate to subvert the existing local and systemic immune suppression characteristic for patients with metastatic cancer. Current clinical evidence suggests that strategies aimed to elicit an anti-tumor immune response may be effective in advanced breast cancer, where tumor infiltration with T lymphocytes is associated with improved clinical outcomes. However, until recently, such strategies have not demonstrated success despite tremendous efforts to harness the anti-tumor properties of the immune system. The redundancy within the multiple signaling pathways activated in breast cancer, along with the likelihood of drug resistance and immune tolerance, suggests that combination therapy strategies will be required for effective disease management. However, not all patients treated with immunotherapies demonstrate durable responses. It is essential to develop novel combination therapy regimes with less/no toxicity.

We suggest that it is possible to immunize patients against their own tumor by using Focused Ultrasound (FUS) therapy to augment tumor antigen release. We hypothesize that low energy deposition into tumors by FUS will lead to mechanical damage to initiate an immune response through release of tumor antigens and enhancing immunogenic cell death (ICD). Further we hypothesize that FUS combined with immune checkpoint (PD-1) inhibitors will enhance systemic therapeutic response to mediate rejection of both FUS treated and untreated tumors (abscopal effect).

Materials and Methods: 4T1 orthotopic tumors were treated with pulsed mode FUS (44W pulsed for 120 seconds, spot-interleaved every 1 s, and pulse duration 40 ms, up to 1-4 sonication spots). All tumor tissues were harvested and processed for histological analysis 48h post treatment and stained for H&E as well as Caspase3. Multiplexed immunofluorescence staining was performed to quantify immune cell subtypes in tumors.

Results: Staining for Caspase 3 gave rise to increase apoptosis in FUS treated tumors when compared to the controls. Tumors treated with pulsed mode FUS had higher counts of CD8+ T cells as well as CD11c+ cells when compared to the control tumors. Our experiments show that there is a decrease in the size of primary tumors as well as secondary tumors in animals that were treated with FUS when compared to non-treated controls. We also observed that the metastatic sites were significantly decreased in FUS treated lungs when compared to the controls.

Conclusions: Preliminary evidence shows FUS may evoke a beneficial immune response which may be responsible for tumor control. Next, we plan to perform the same experiments by combining with PD-1 inhibitors.

Acknowledgment/Funding Sources: Funding for this work was provided by the US Department of Defense.

IMM-11

Topic: Immunotherapy
Presentation Type: Oral

Effects of FUS Thermal Exposure on T Cell Infiltration in Anti-PD-1 Checkpoint Inhibitor Combination Immunotherapy in a TNBC Model

Sara Johnson[1], Pavitra Viswanath[2], Nicholas Richards[1], Joshua Hillyard[1], Jill Shea[1], Elaine Hillas[1], Alana Welm[2], Allison Payne[1]

[1]University of Utah, Salt Lake City, UT, USA
[2]Huntsman Cancer Institute, Salt Lake City, UT, USA

Background: Triple-negative breast cancer (TNBC) is a promising candidate for aPD-1 immunotherapy due to limited treatment options, high immunogenicity, and PD-L1+/PD-1+ expression. Overall response rates for aPD-1/PD-L1 monotherapy have been modest (5-22%)1, potentially due to insufficient "Signal 1" effector T cells. Focused ultrasound (FUS) can induce anti-tumor immune response, including enhanced Signal 1, in numerous cancers. However, the response varies widely with FUS modality and exposure parameters. In this study, we investigated the effects of thermal FUS exposure on tumor-infiltrating T cells in a murine TNBC model as a monotherapy and in combination with aPD-1.

Materials and Methods: MMTV-PyMT tumor cells (1x104) were injected orthotopically into female mice (FVB-NJ) and grown to a diameter of ~1 cm. Mice were assigned to control, ?PD-1 only, FUS-only and FUS+aPD-1 treatment groups. FUS-treated groups were further divided into dense (FUS-D) and sparse (FUS-S) ablation schemes (Figure 1a). Over 15-days, aPD-1 drug was administered on Day 0 and every 3rd day (4 mg/kg/dose). FUS was administered on Day 3, under guidance of 3D MR thermometry (3 MHz, annular array transducer; IGT). Tumor volume was measured with calipers (V=0.5*L*W2). On Day 15, tumors were harvested and surface markers were stained for flow cytometry. Live cell populations were manually gated (FlowJo™) and statistical significance between groups was determined by two-tailed t-tests (?=0.05). MR thermometry was co-registered to T2-weighted segmentations of FUS-treated mouse tumors to calculate percentage of tumor volume receiving at least 240 CEM (%TD¬240) and exposed to maximum temperatures between 37-60°C (%Hyper). Significant correlations between flow cytometry populations and FUS exposure were determined by Pearson's R statistical test for linear correlation (?=0.05).

Results: N=32 mice were included in the study with 5-6 mice/group. FUS exposure metrics for ablation (%TD240), and hyperthermia (%Hyper) were greater in the FUS-D than FUS-S groups on average (Figure 1b). Although tumor growth progressed in all experimental groups, percent change in tumor volume between Day 0 and Day 15 was significantly lower in FUS-D+aPD-1 vs. FUS-D tumors (p=0.0403, Figure 2a). At Day 15, the immune infiltrate to tumor cell ratio (CD45+/EpCAM+) was highest in FUS+aPD-1 groups, but not significant (Figure 2b). Total TILs and % of CD4+ T cell populations were similar across groups, but % of CD8+ T cells was significantly higher in FUS-D+aPD-1 than FUS-D monotherapy tumors (p = 0.0369, Figure 2a). In the subset of tumors treated with FUS (n=22), we found that CD4+ and CD8+ tumor-infiltrating T cells correlated modestly with FUS exposure (Figure 3, top). However, when separating tumors into FUS-only (green) and FUS+aPD-1 (red) groups, significant opposing correlations were observed (Figure 3, middle). In FUS-only tumors, %CD8+ was negatively correlated with %TD240 (R=-0.68, p=0.0218) and %CD4+ was positively correlated with %Hyper (R=0.65, p=0.0292). Conversely in FUS+aPD-1 tumors, %CD8+ and %CD4+ T cells were modestly positively and negatively correlated with %Hyper, respectively (R=0.27, p>0.05 and R=-0.027, p>0.05). Therefore, high CD8+ expression in the FUS-D+aPD-1 group may be attributed to high mean %Hyper in FUS-D tumors (Figure 1) combined

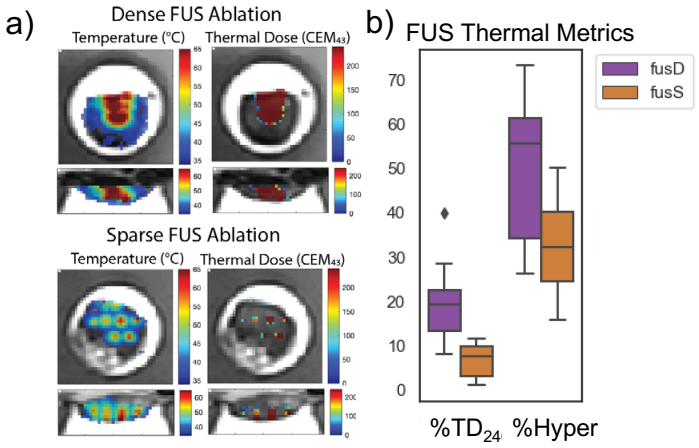

Figure 1. a) Example maximum temperature and thermal dose (CEM@43°C) in FUS-D and FUS-S ablation schemes, overlaid on T2-weighted images b) Box-and-whiskers plots of %TD240 and %Hyper in FUS-D (purple) and FUS-S (orange) tumors (n=11/group).

with the presence of aPD-1 drug. FUS-only versus FUS+aPD-1 correlations did not track with FUS-D (purple) versus FUS-S (orange) correlations, indicating that the aPD-1 effect was not due to differences in ablations schemes (Figure 3, bottom).

Conclusions: In a pre-clinical TNBC model, tumor growth was slowed and % of CD8+ T cells was greater after thermal ablation FUS+aPD-1 combination treatment compared to monotherapy and control groups. CD8+ infiltration is an increasingly recognized positive prognostic factor in patients with TNBC. We demonstrated that intra-tumoral CD4+ and CD8+ T cells may be modulated by intensity and extent FUS exposure, and that immunomodulation of FUS can change in the presence of aPD-1 drug. With MR thermometry-driven analysis, this study demonstrated a novel approach for discerning the complex interactions between the immune tumor environment, immunotherapy drugs, and FUS parameters.

Acknowledgment/Funding Sources: We would like to acknowledge the Office of the Vice President for Research at the University of Utah for funding this research.

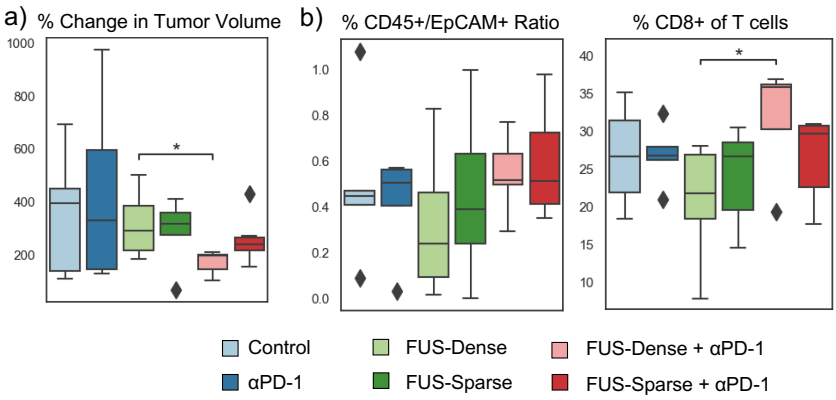

Figure 2. Box-and-whiskers plots of a) percent change in tumor growth between Day 0 and Day 15 of treatment across groups and b) immune cell populations in the tumor tissue at Day 15 across groups (n=5-6 mice/group).

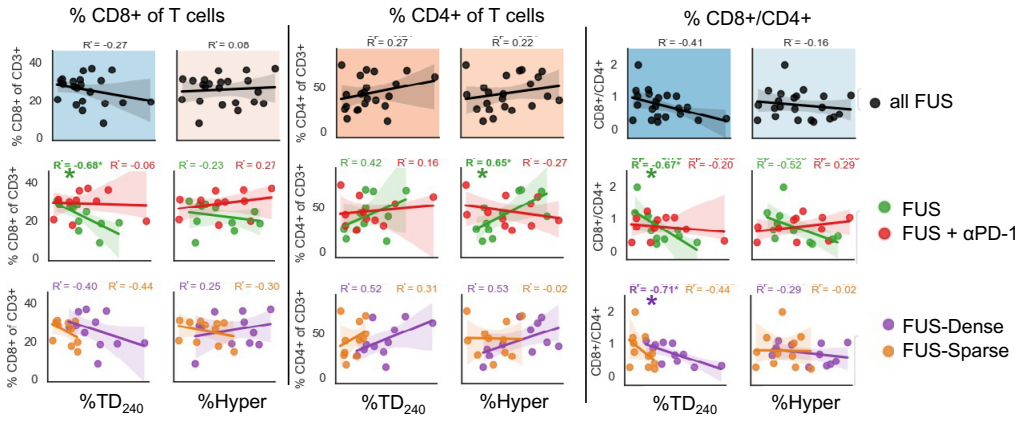

Figure 3. Scatter plots of intra-tumor T cell populations versus FUS exposure metrics in all FUS-treated mice (top), in FUS-only and FUS+?PD-1 tumors (middle), and in FUS-D and FUS-S groups (bottom). (*) denotes significant Pearson's correlation coefficient.

IMM-12

Topic: Immunotherapy
Presentation Type: Oral

Focused Ultrasound Therapy and Photodynamic Priming Improve Delivery of Immune Checkpoint Inhibitors in Head and Neck Cancer

Ryan Margolis, Chanda Bhandari, Junjie Li, Girgis Obaid, Kenneth Hoyt

The University of Texas at Dallas, Richardson, TX, USA

Background: Fluorescently labeled antibodies that target overexpressed receptors have recently shown promise for cancer diagnostic and therapeutic approaches. However, the tumor microenvironment provides physical barriers that prevent optimal drug delivery. One approach, termed photodynamic priming (PDP), uses sub-therapeutic doses of photodynamic therapy (PDT) to modulate the tumor microenvironment to improve drug delivery. Another approach uses focused ultrasound (FUS) in combination with gas-filled microbubbles (MBs) to improve vascular permeability. The goal of this research project was to investigate the combined therapeutic effect of low–intensity FUS and PDP on improved drug delivery.

Materials and Methods: C3H/HeJ mice were implanted with AT84 cells (2.0 × 106 cells) subcutaneously in the flank. Mice were randomly divided into three groups (N=9): control (no PDP or FUS), PDP only, and PDP + FUS. Experiments began once tumors reached 6.0 – 8.0 mm in size. All mice were intravenously injected with 200 μL (0.25 mg/kg) of liposomal benzoporophyrin derivative (nal BPD) followed by 50 μL of anti-PD-L1-IRDye800 and MBs (Definity, Lantheus Medical Inc.) one hour later. For the FUS group, US therapy was immediately performed after the microbubble injection using three-dimensional FUS therapy using a programmable ultrasound system (Vantage 256, Verasonics Inc.) equipped with a dual configuration for interleaved imaging and therapy. Both the imaging and therapeutic transducers are 128 element arrays with center frequencies of 3.5 and 2.0 MHz, respectively. The latter is a concentric array that enables beam steering in volume space. FUS therapy was performed at a pressure of 0.7 MPa (MI = 0.45), pulse repetition frequency of 10 Hz, duty cycle of 10%, pulse duration of 10 ms, 9 focal zones with 0% overlap, and 19 repetitions per focal zone. For the PDP group, PDP was performed at 690 nm activation directly after FUS therapy. The tumor region was exposed to a sub-therapeutic dose of 75 75 J/cm^2 of 690 nm laser light (Modulight) at an irradiance of 100 mW/cm^2. Mice were given subcutaneous Meloxicam SR analgesia (ZooPharm) prior to PDP to minimize discomfort. Temporal accumulation of anti-PD-L1 and IRDye800 was monitored via in vivo optical imaging (Pearl Trilogy, LI-COR Biosciences) at baseline (0 h) and again at 1, 3, 6, 9, 24, and 48 h. Following humanely euthanizing the mice, histology was performed.

Results: Preliminary data shows that the combinational therapy of FUS and PDP improves delivery by 300.9% compared to 138.6% for PDP alone. At peak uptake of the anti-PD-L1 antibody, mice treated with FUS + PDP showed increased drug enhancement by at least 150% compared to mice treated with and without PDP. Histological results confirmed increased anticancer activity for mice that received FUS + PDP.

Conclusions: The use of low-intensity FUS has the potential to synergize with the PDP therapy to further modulate the tumor microenvironment by increasing microvascular permeability to increase drug delivery and improve treatment efficacy.

IMM-13

Topic: Immunotherapy
Presentation Type: Oral

Combining Thermal Ablative Focused Ultrasound with Gemcitabine to Immunologically Control Triple Negative Breast Cancer: How It Works

Lydia Petricca, Natasha D. Sheybani, Eric A. Thim, Timothy Bullock, Richard J. Price

University of Virginia, Charlottesville, VA, USA

Background: Immunological rejection of triple-negative breast cancer (TNBC) is rare. Thus, there exists a strong precedent for seeking out adjunct treatments that can convert immunologically "cold" tumors into "hot" tumors that are responsive to immunotherapy. Focused Ultrasound (FUS) promotes antitumor immunity by inducing tissue destruction and inflammation. We hypothesized that thermal-ablative FUS (tFUS) would increase the immune response to TNBC, however, TNBC is commonly accompanied by the expansion of immunosuppressive myeloid cells. We have previously shown that combining tFUS and Gemcitabine (GEM), a myeloablative chemotherapy, constrains primary TNBC tumor growth and reduces mortality. This response is dependent on T cell-mediated immunity. However, we do not know how the T cell compartment functions in response to tFUS+GEM therapy to confer this protective advantage. While this treatment remarkably resulted in some cures, the effects were not durable in every case; suggesting immunosuppression may be re-established. For this reason, understanding the basis of T cell mediated tFUS+GEM growth control is crucial for developing a sustainable and durable therapy against TNBC for every individual.

Materials and Methods: BALB/c mice were subcutaneously inoculated with 4x105 4T1 cells in the right flank. Each mouse was given an intraperitoneal (i.p.) injection of GEM (1.2mg/mouse) immediately prior to treatment. tFUS (f0=3.28 MHz, PNP=-12 MPa, 10 seconds/treatment point, 3 mm spacing between treatment points) was applied 14 days post inoculation. On day 21, 7 days post-treatment, mice received an i.p. injection of brefeldin A – to determine and quantify cell-specific cytokine secretion - 4hrs prior to harvesting their tumors and tumor draining lymph nodes (tdLNs). Tumors were enzymatically digested and mechanically homogenized prior to immune cell isolation via density gradient separation. tdLNs were mechanically homogenized. Single cell suspensions of the samples were stained for spectral flow cytometry.

Results: Compared to the control arm, tFUS+GEM treated mice have an increased frequency of CD4+ and CD8+ T cells present within total Live CD45+ Immune cells. Within the CD4+ T cell compartment, we found that tFUS+GEM is leading to a decreased frequency of immunosuppressive Tregs, while increasing the frequency of CD4+ Helper T cells. Additionally, fewer T cells present within the tumor microenvironments of tFUS+GEM treatment group have hallmarks of exhaustion. Decreased co-expression of PD-1/LAG-3 is not accompanied by increased IFN-gamma expression. However, other immune cells are producing more IFN-gamma in response to this therapy. What cell type this might be is currently being examined. This work was done on a GEM background, so further studies are needed to understand how T cells are responding to FUS alone.

Conclusions: tFUS+GEM therapy is altering the T cell compartment, but not towards increased cytolytic activity. The combination therapy is reducing the proportion of regulatory T cells within both the TME and tdLNs, suggesting a possible mechanism for alleviating immunosuppression. tFUS+GEM results in increased expression of the proinflammatory cytokine, IFN-gamma, by CD3- immune cells. IFN-gamma production implicates another anti-tumorigenic mechanism tFUS+GEM might be utilizing to control TNBC outgrowth.

Acknowledgment/Funding Sources: 2T32AI007496-26A1, R01 164985101GB1084641017

IMM-14

Topic: Immunotherapy
Presentation Type: Oral

Tailoring Chemoimmunostimulant Bioscaffolds for Inhibiting Colorectal Cancer Growth and Metastasis after Incomplete Microwave Ablation

Yuting Shen,

Shanghai Tenth People's Hospital, Tongji University School of Medicine, Shanghai, China

Background: Image-guided microwave ablation (MWA) technique has been accepted as a reliable treatment method in numerous solid neoplasms by several clinical guidelines. Notwithstanding the favorable effects of local treatments in some patients, the high incidence of incomplete ablation that could promote the rapid cancer progression still remains a therapeutic dilemma. Importantly, it is the main reason to restrict the wide application of MWA therapy. Thus identifying and further inhibiting the potential causes contributing to the pro-oncogenic effects of incomplete ablation should be especially necessary and urgent.

Materials and Methods: Herein, we report and demonstrate, for the first time, with a preclinical murine model system (establish by microwave ablator (ECO-100E, Yigao Microwave)) that incomplete microwave ablation (iMWA) promotes colorectal cancer progression mainly owing to predominant myeloid cell-mediated immunosuppressive effects. Then, The therapeutic efficacy after iMWA-treat was then observed in multiple models by establishing unilateral colorectal tumor models, bilateral colorectal tumor models (mock metastasis models), lung metastasis models, and long-term memory models in mice with incomplete ablation and applying FDA-approved fibrin gel scaffolds loaded with immunogenic cell death-inducing chemotherapeutic agents (OX) and pharmacological PI3Kγ inhibitors (IPI549).

Results: After local administration, the in situ formation of the biological scaffold allows for uniform distribution of OX/IPI549 drug around the entire colorectal tumor and achieves sustained slow release of the drug, reversing bone marrow-derived suppressive cell-mediated immunosuppression through IPI549 on the one hand, and OX initiating immunogenic cell death to enhance immunotherapeutic efficacy on the other hand, overall resulting in the highest CTL, CTL vs. Tregs, and M1/M2 intratumoral ratios were elevated to the highest. In addition, some negative factors such as granulocytic MDSC and M2 macrophages were significantly reduced, effectively triggering the antitumor immune response.

Conclusions: By constructing a preclinical iMWA mouse model, it was confirmed that iMWA promotes tumor progression mainly due to immunosuppressive effects mediated by bone marrow-derived immunosuppressive cells. A biohydrogel scaffold-supported chemoimmunotherapy strategy was rationally developed to reverse the immunosuppression after ablation in response to the identified cancer-promoting mechanism. Besides, employing several colorectal tumour models, we have revealed that OX&IPI549@Gel-based chemoimmunotherapy can substantially suppress the growth of the primary residual colorectal tumour, and simultaneously evoke robust systemic anticancer immunity to efficiently inhibit metastatic spread, as well as offer strong long-term immunological memory functions against tumour rechallenge. Considering that all components of the drug composition are clinically approved and the simple hydrogel fabrication procedure, our proposed bioscaffold-enabled chemoimmunotherapeutic approach presents tremendous potential for next-generation post-ablation therapy.

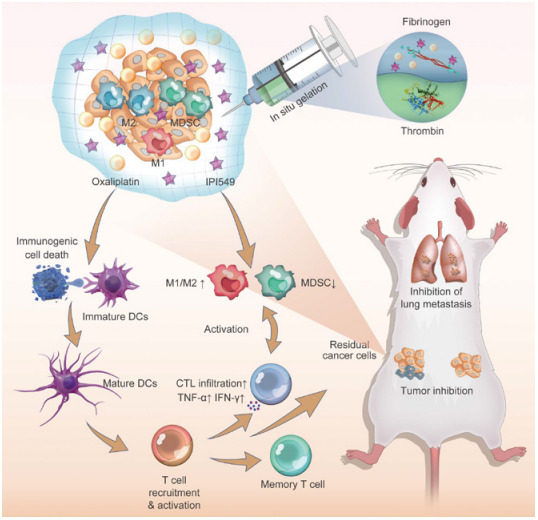

Figure 1. Schematic illustration of the formation and application of bioscaffold-enabled chemoimmunotherapeutic strategy for inhibiting tumour growth and metastasis after incomplete microwave ablation.

Acknowledgment/Funding Sources: the National Natural Science Foundation of China (Grants 81900491, 81601502, 81801802, 81901752 and 81725008), Science and Technology Commission of Shanghai Municipality (19DZ2251100), Shanghai Municipal Health Commission (2019LJ21 and SHSLCZDZK 03502)

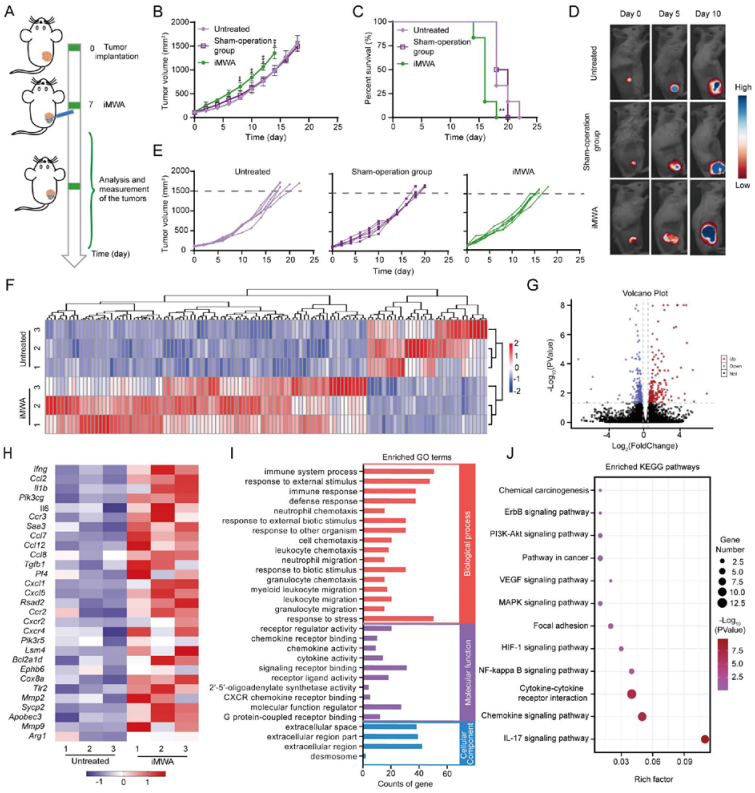

Figure 2. iMWA accelerates tumour progression and induces immune suppression.

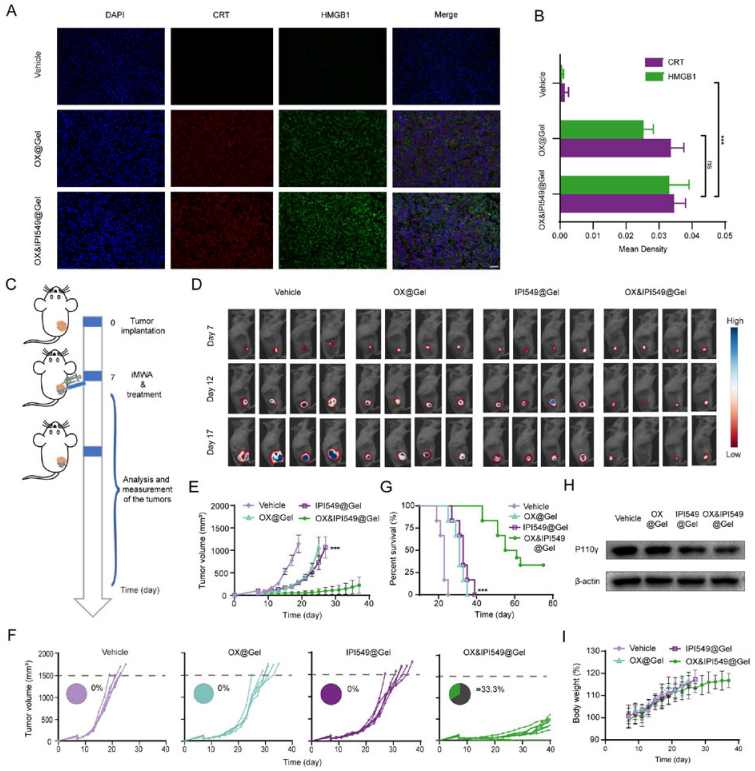

Figure 3. In situ immunotherapeutic scaffold to elicit immunogenic tumour phenotypes and inhibit tumour progression after iMWA treatment.

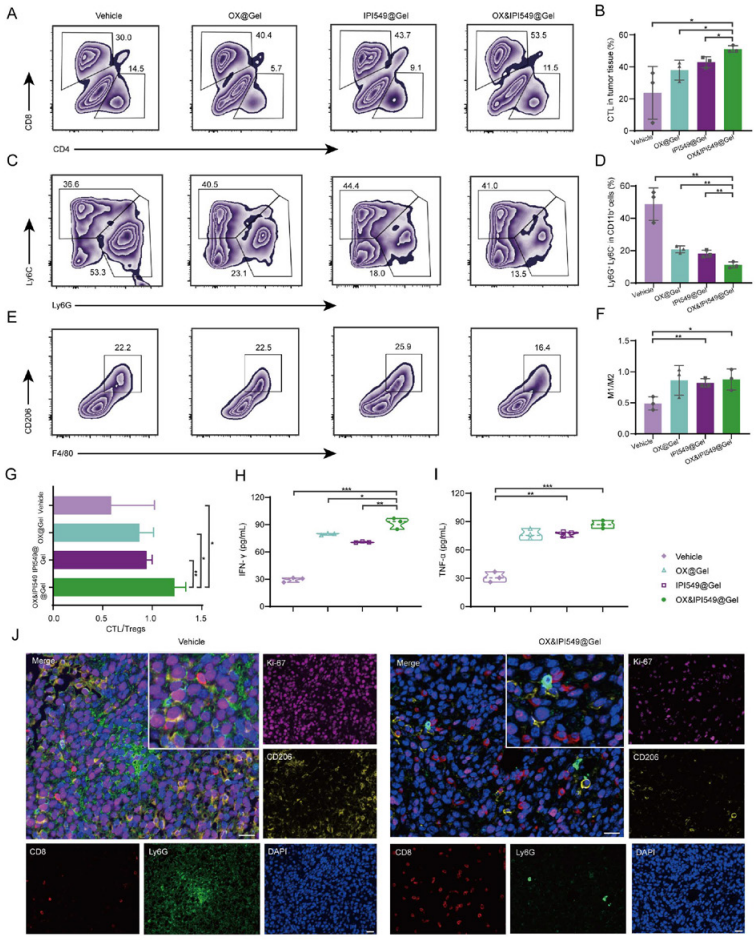

Figure 4. Mechanism of the antitumor immunity elicited by combination therapy strategy.

IMM-15-YI

Topic: Immunotherapy
Presentation Type: Oral

Focused Ultrasound Immunomodulation on the Myeloid Compartment of the Brain in Treating GBM and Alzheimer's Disease

Tao Sun, Nathan McDannold

Brigham and Women's Hospital, Boston, MA, USA

Background: Focused ultrasound (FUS)-mediated blood-brain barrier opening is an attractive method of treating neurological diseases, such as glioblastoma (GBM) and Alzheimer's disease (AD). As an established drug delivery approach, FUS has also been associated with the stimulation of neuro-inflammation, including the morphological activation of resident microglia. With growing scientific appreciation in resident microglia and recruited monocyte-derived macrophages in neuro-immune interface, however, FUS effects on the myeloid compartment of the cancerous and aging brain are not clear, including the trafficking and functional changes of monocytes/macrophages and resident microglia.

Materials and Methods: Here, we investigate how FUS modulates the myeloid compartment in murine models of GBM (GL261 and 005) and AD (APP/PS1dE9) in tests with or without passive immunotherapy. In the GBM models, FUS effects were compared with or without anti-PD1 treatment. FUS (690 kHz, 320 kPa, 10-ms pulses at 4-Hz) was applied on Day 14 and Day 20 after the tumor inoculation. In the AD model, we pair FUS with an anti-pGlu3 A? antibody therapy (an Fc-competent anti-pGlu3 A? monoclonal antibody mAb). Optison™ bubbles with 100 ?l/kg intravenous injections were used in all the animal experiments.

Results: In the GBM models, our results demonstrated that FUS enhanced antigen presentation behaviors of tumor-associated macrophages without affecting the microglia. FUS also reprogrammed the macrophages locally towards the anti-cancer phenotype (CD86+CD206-). FUS-anti-PD1 ($n = 8$) provided significantly increased survival benefits compared to anti-PD1 monotherapy ($n = 7$, $P < 0.05$) and the control group ($n = 6$, $P < 0.001$). In the AD model, plaque-associated Ly6G+ phagocytes were only present in FUS-treated areas ($P < 0.01$), while microglia activation was found in both antibody-treated groups. Overall, these effects resulted in greater plaque removal ($P < 0.05$), sparing of synapses (multiple markers, all $P < 0.01$) and improved cognitive function (multiple assessments including Open Field, Water T Maze and Context Fear Conditioning tests, at least $P < 0.05$).

Conclusions: Our results offer new evidence in FUS immunomodulation on the myeloid compartment of the brain in GBM and AD-like mouse models. We discover new mechanisms that low-intensity pulsed FUS recruits and activate peripheral monocyte derived macrophages, instead of direct activation of resident microglia.

Acknowledgment/Funding Sources: We thank the funding supports from FUS Foundation, NIH (NIBIB, NCI, and NIA), and Harvard School of Engineering.

IMM-16

Topic: Immunotherapy
Presentation Type: Oral

Partial Thermal Ablation of Melanoma Shifts Intratumoral IL-1beta mRNA and Immune Cell Protein Levels and Patterns

Eric A. Thim, Lydia Petricca, Alexander S. Mathew, Timothy Bullock, Richard J. Price

University of Virginia, Charlottesville, VA, USA

Background: Approximately 100,000 new melanoma cancer cases are diagnosed per year. Those patients who experience distant metastatic spread of melanoma cancer have a 30% 5-year survival rate, respectively. Current treatment options include pre- and postoperative chemotherapy, surgery, radiation and, more recently, immunotherapy. The stimulation of adaptive immunity against metastatic cancer can be challenging because of a deficiency in anti-tumor immune cells and/or a plethora of pro-tumor immune cells. Thus, the translation of adjunct approaches that enhance T-cell infiltration, lift the immunosuppressive tumor microenvironment and/or increase therapeutic delivery could vastly expand the cancer patient population exhibiting durable responses after immunotherapy and other systemically administered agents. Pyroptosis, a form of immunogenic cell death facilitated by inflammasome signaling, has also been reported because of radiation therapy and certain chemotherapies. The primary product of pyroptosis is the release of IL-1?, a potent cytokine chemotactic for myeloid cells and generally associated with poor prognosis. Blockage of inflammasome signaling via the small molecule inhibitor MCC950, which inhibits NOD-, LRR- and pyrin domain-containing protein 3 (NLRP3), has been shown to improve outcomes in head and neck squamous cell carcinoma due to reduced recruitment of myeloid-derived suppressor cells (MDSCs) and tumor-associated macrophages (TAMs).Focused ultrasound (FUS), specifically thermal ablation (T-FUS), provides a clinically relevant, non-invasive method for altering the tumor immune milieu in conjunction with current drug therapies.

Materials and Methods: C57/Bl6J mice were subcutaneously inoculated with 5x104 or 2x105 B16F10 cells in the right flank and T-FUS (f0=3.28 MHz, PNP=-12 MPa, 10 seconds/treatment point, 2 mm spacing between treatment points) was applied 13 days post inoculation. Post-treatment tumor harvests were performed for RNA sequencing and flow cytometry at 8, 24, 72 and 168 hrs and 24 hrs, respectively. MCC950, an NLRP3 inhibitor, was delivered 1 hr prior to thermal ablation. Parameters used for t-distributed stochastic neighbor embedding (tSNE) dimensionality reduction on flow cytometry data from intratumoral immune cells (gating: Live/CD45+) were as follows: F4/80, CD11b, Ly6G, Ly6C, CD11c, MHCII, XCR1, CD103, CD8a, CD172a (SIRPalpha).

Results: T-FUS transiently controlled primary B16F10 melanoma tumor growth (Figure 1A). Bulk RNA sequencing revealed upregulation of IL-1b and NLRP3 transcripts 8 hrs post T-FUS (Figure 1B, left) but returns to baseline after 24 hrs (Figure 1B, right). Pro-IL-

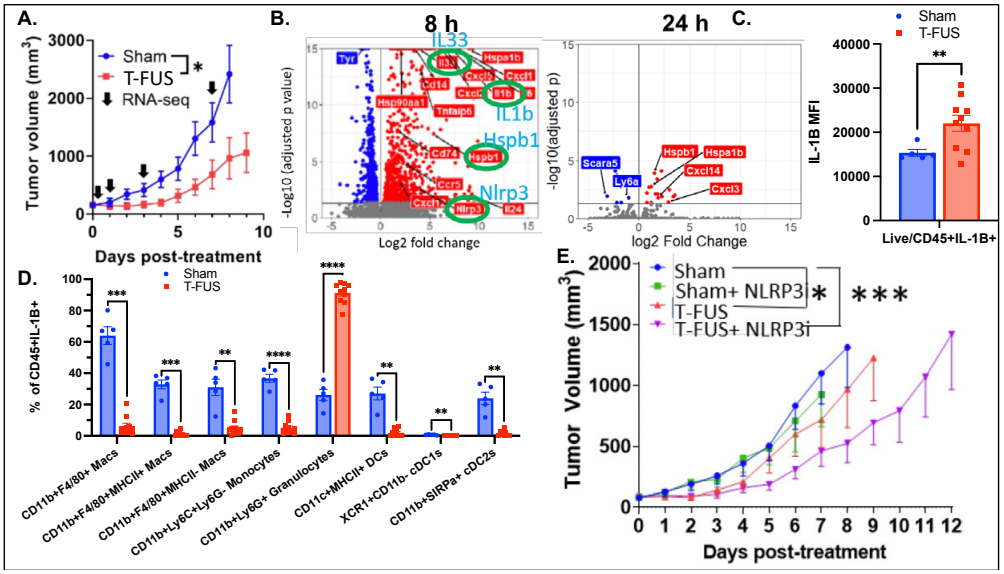

Figure 1. Thermal ablation augments IL-1beta mRNA expression and shifts IL-1beta protein expression in the immune cell compartment, while inhibition of NLRP3 increases tumor growth control.

1b protein level on a per cell basis increased in the CD45+ cell compartment 24 hrs post T-FUS (Figure 1C), with a striking pro-IL-1b expression redistribution to a predominantly granulocytic myeloid cell population (Figure 1D). Systemically inhibiting NLRP3 (upstream upstream regulator of IL-1?) in combination with T-FUS increased tumor growth control beyond either monotherapy (Figure 1E). Furthermore, we saw a dramatic shift in intratumoral immune cell populations 24hrs post T-FUS (Figure 2). The Ly6G+ populations (Figure 2D) appear in the T-FUS treated tumors but F4/80+ populations (Figure 2E) appear in Sham treated tumors. Interestingly, CD11c (Figure 2F) and MHCII (Figure 2G) populations appear almost exclusively in Sham treated tumors.

Conclusions: T-FUS shifts IL-1b expression levels and cell sources in the tumor microenvironment. By inhibiting NLRP3 in combination with T-FUS to increase growth control, we have implicated pyroptosis as a pro-tumorigenic mechanism through the NLRP3-IL-1b pathway. Additionally, we qualitatively show that CD11c+ and MHCII+ cell populations disappear with T-FUS while being replaced by Ly6G+ cells.

Acknowledgment/Funding Sources: Supported by NIH R01EB030007 to RJP and TNJB.

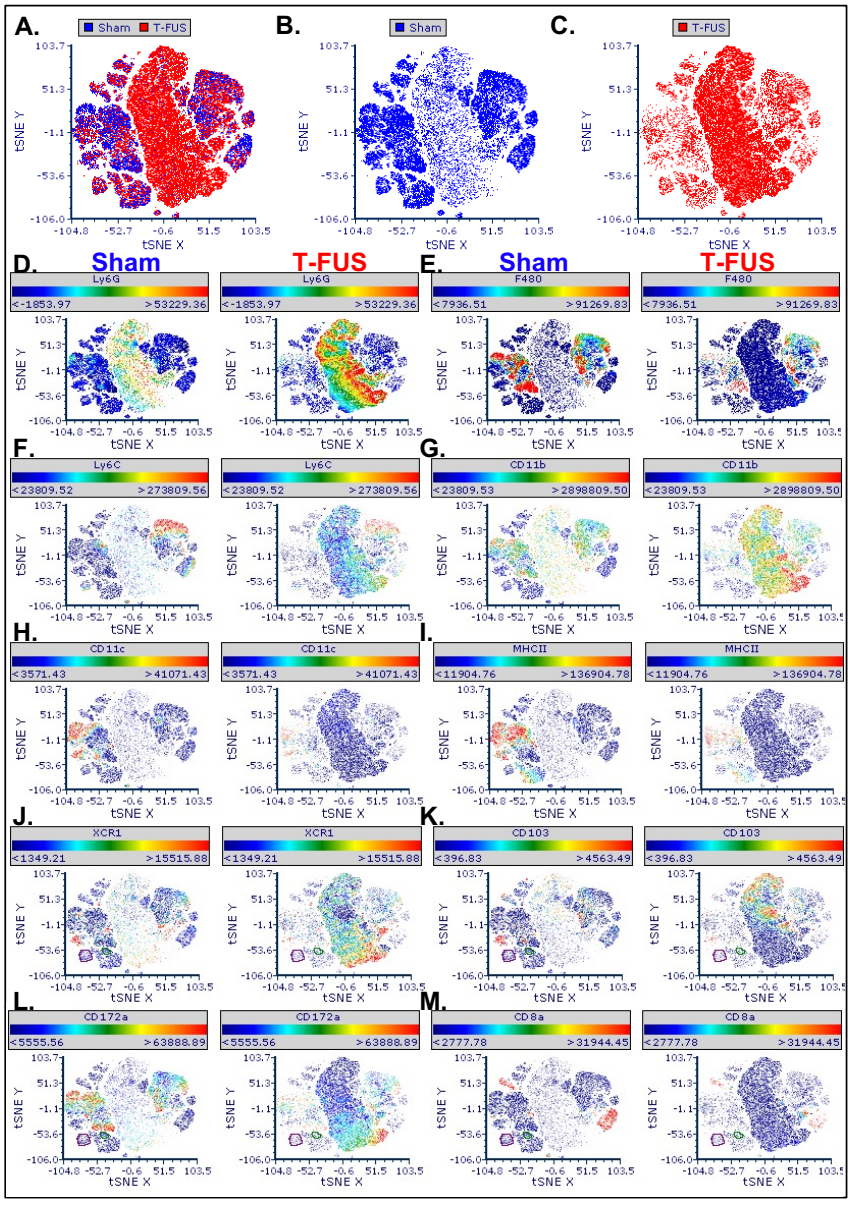

Figure 2. Thermal ablation alters intratumoral immune cell profile as seen in t-distributed stochastic neighbor embedding analysis.

IMM-17

Topic: Immunotherapy
Presentation Type: Oral

TME Heterogeneity Impacts Response to Combined Thermal Ablation and Immunotherapy

James Wang[1], Brett Fite[1], Aris Kare[1], Bo Wu[1], Marina N. Raie[1], Spencer Tumbale[1], Ryan R. Davis[2], Clifford G. Tepper[2], Sharon Aviran[2], Katherine W. Ferrara[1]

[1]Stanford University, Palo Alto, CA, USA
[2]University of California Davis, Sacramento, CA, USA

Background: The tumor microenvironment (TME) immune cell heterogeneity affects immunotherapy, which relies on activating a concerted response from immune cells against tumor. Focused ultrasound ablation is a non-invasive tumor debulking method that transiently reprograms tumor immune cell populations through the means of wound response, tumor antigen and damage associated molecular pattern (DAMP) release and immunogenic cell death.

Materials and Methods: Herein, we studied treatment strategies that combine magnetic resonance guided focused ultrasound ablation (MRgFUS) with immunotherapy such as immune checkpoint inhibitors (aPD-1 and aCTLA-4) and myeloid stimulators (aCD40). To understand the effects of immune cell compositions within the TME, we employed two multi-site murine cancer models, an immune-suppressed KPC (Kras+/LSL-G12D; Trp53+/LSL-R172H; Pdx1-Cre) pancreatic adenocarcinoma model and a neu deletion HER2+ (NDL) mammary adenocarcinoma model with a larger naïve lymphocyte population. We evaluated treatment naïve models with histology and single-cell sequencing and studied treatment effects with survival, bulk-RNA transcriptomics and flow cytometry.

Results: Our initial characterization of the two models indicated a difference in naïve lymphocyte populations based on histology and single cell transcriptomics. The addition of MRgFUS with immunotherapy significantly improved survival in KPC but not in the NDL model. To understand how MRgFUS enhances immunotherapy efficacy in pancreatic cancer, we employed spectral flow cytometry, gene set enrichment analysis (GSEA), and digital cytometry (CIBERSORTx) to study immune cell responses and phenotypes due to the combination treatment. While aCD40 + aPD-1 enhanced dendritic cell activation in KPC, the addition of MRgFUS to aCD40 + aPD-1 + aCTLA-4 (CP4) increased natural killer cells and T cells in non-treated tumors. We found that combining MRgFUS with CP4 upregulated Ly6c myeloid remodeling phenotypes and effector T cell protease secretions. In addition, MRgFUS based combination upregulated signature genes in adaptive immune response to a greater extent than immunotherapy alone.

Conclusions: This work dissects how focused ablation augments immunotherapy combinations by increasing lymphocyte activity and myeloid remodeling and can inform the development of multicomponent treatment combinations.

Acknowledgment/Funding Sources: This work was supported by the Focused Ultrasound Foundation and the National Institutes of Health (R01CA250557, R01CA253316, R01CA112356 and 1R01CA210553 and T32CA118681)

IMM-18

Topic: Immunotherapy
Presentation Type: Oral

Pre-clinical Study of Focused Ultrasound-Mediated Blood-Brain Barrier Opening and Anti-PD-1 for Treatment of Diffuse Midline Glioma

Hong-Jian Wei, Danae Kokossis, Nina Yoh, Nicholas McQuillan, Masih Tazhibi, Xander Berg, Xu Zhang, Luca Szalontay, Robyn Gartrell, Jovana Pavisic, Zhiguo Zhang, Akiva Mintz, Elisa Konofagou, Cheng-Chia F. Wu

Columbia University, New York, NY, USA

Background: Diffuse midline glioma (DMG) is a devastating pediatric high-grade central nervous system (CNS) tumor affecting midline structures (i.e. brainstem, thalamus) with no effective treatment options to date. Prognosis remains poor with a median overall survival of less than one year. Immune checkpoint inhibitors (ICIs) have recently emerged as a highly promising treatment modality in multiple cancer types. Programmed cell death protein-1 (PD-1) is an immune checkpoint molecule found on activated T cells that, by interacting with its ligand PD-L1 on tumor cells, inhibits the activation of effector T cells, blocking effective immune response. Recent phase 1 clinical trials have shown tolerability of ICIs in DMG patients but their effectiveness could not be determined due to the limited number of patients. Due to the molecular size of ICIs, poor blood-brain barrier (BBB) penetration is considered to be a significant obstacle to effective anti-PD1 therapy in CNS tumors. Focused ultrasound (FUS) has been shown to safely and non-invasively open the BBB which can increase ICI delivery. In this study, we hypothesized that FUS-mediated BBB opening (BBBO) can enhance the delivery of anti-PD-1 for a therapeutic benefit in DMG.

Materials and Methods: A syngeneic, orthotopic DMG model was established by injecting mouse DMG cells (PDGFB+, H3.3K27M, p53-/-) intracranially. A single-element, spherical-segment FUS transducer (center frequency: 0.5 MHz) driven by a function generator through a power amplifier was used with concurrent microbubble injection to perform BBBO. Magnetic resonance imaging (MRI) was utilized to evaluate BBBO and tumor progression.

Results: We demonstrated that FUS-mediated BBBO is safe and feasible in mice with DMG tumors by MRI and passive cavitation detection. Western blot showed FUS increases the delivery of anti-PD-1 antibody to DMG tumors in mice by 3.5-fold. The combined treatment of FUS-mediated BBB opening and anti-PD-1 antibody decreased tumor growth by ~50% compared to the anti-PD-1 antibody treatment without FUS. In addition, the combined treatment of FUS+anti-PD-1 preliminarily improved survival in three mice compared to FUS+Isotype IgG or anti-PD1 alone. The overall survival will be further evaluated in ongoing work.

Conclusions: The current results provide evidence that FUS can increase anti-PD-1 delivery to DMG tumors and improve treatment efficacy of anti-PD-1 in a murine model of DMG. This improved response is likely due to the increased local concentration of anti-PD-1 in the tumor when FUS is used with systemic administration. We believe these data establish a strong preclinical rationale to assess the combination of FUS-mediated BBBO with ICIs in pediatric patients with DMG.

IMM-19

Topic: Immunotherapy
Presentation Type: Oral

Ablative focused-ultrasound and cancer immunotherapy: searching for a rational combination

Awndre E. Gamache[1], Frederic Padilla[2]

[1]University of Virginia, Charlottesville, VA, USA
[2]Focused Ultrasound Foundation, Charlottesville, VA, USA

Background: There is a growing body of evidence suggesting that ablative ultrasound therapy can increase the efficacy of cancer immunotherapies. However, the mechanism(s) that underpin these observations remain to be elucidated.

Materials and Methods: This presentation will overview the current state of leveraging ablative focused-ultrasound therapy and cancer immunotherapy in the treatment of cancer.

Results: Topics will include: 1) The limitations of common immunotherapies and how these limitations may be overcome with therapeutic ultrasound. 2) How ablative ultrasound modalities differentially elicit direct immunomodulation of the tumor micro-environment. 3) Determining the most effective therapeutic ultrasound modalities for stimulating an immune response and synergizing with immunotherapy.

Conclusions: There are stil outstanding knowledge gaps and unanswered key questions about the most promising approaches for combination treatment and monitoring of tumor responses.

LUN-01

Topic: Lung
Presentation Type: Oral

Treatment of Lung Cancer Using MRgFUS in a Porcine Model

Jaime Mata[1], Braden Miller[1], David Moore[2], Linda Martin[1], Lauren Powlovich[2]

[1]University of Virginia, Charlottesville, VA, USA
[2]Focused Ultrasound Foundation, Charlottesville, VA, USA

Background: Lung cancer is the second most commonly diagnosed cancer amongst men and the third most commonly amongst women and is the leading cause of cancer related deaths in both sexes with an estimated 142k+ deaths in 2018. Treatment strategy for non-small cell lung cancer (NSCLC) depends on clinical staging, but surgical lobectomy is the primary treatment for stage I/II cancers while also being an accepted treatment for stage III and IV disease. Surgery may be a curative treatment in stage I NSCLC, with a five-year survival rate of 43%-73% compared to a five-year survival rate of 6% for untreated patients. Unfortunately, 20% of patients with stage I/II NSCLC are not eligible for lobectomy, and for those undergoing surgery there is a 1-5% incidence of operative mortality. This project proposes an innovative, minimally invasive procedure for the transcutaneous ablation and subsequent complete removal or significant reduction of lung cancer masses using MRgFUS.

Materials and Methods: Seven Yorkshire pigs (~58Kg) had both main bronchi selectively intubated, and while the right lung was mechanically ventilated, the left lung was purposely collapsed, followed by a controlled left hydrothorax in the chest cavity with saline (1L) via a 2cm incision in order to create an acoustic window for the FUS beam. Animals received two or three transcutaneous MRgFUS ablations of the left lung, in two or three different locations, Fig 1. Each location received a different amount of acoustic power in order to determine the optimal power with minimal side effects, Table 1.

An intercostal approach was used in order to target the transcutaneous beam with minimal distortion and attenuation caused by the ribs. Ablations were performed at maximum inhalation of the non-dependent lung (right lung). At the end of the MRgFUS ablation, Thoracentesis was performed and saline was drained in a method identical to the drainage of a clinical pleural effusion. All pigs remained stable for one week after the ablation, at that time each animal received a complete MRI of the lung using T2, and T1 sequences both pre and post contrast (10mL Gadavist) to assess the success of the ablation, Fig 2. Pigs were then euthanized followed by histopathologic examination to correlate with the results of the MRI, Fig 3.

Results: Ablations were performed successfully in each animal, and there were areas of hyperintensity on T1 MRI corresponding to areas targeted for ablation. Locations and intensity of ablations confirmed by MRI and gross histology aligned well with target locations and applied powers. In all studies the heart and pericardium were without lesions. Pig 1, had a small area of a skin burn but it was remedied in later studies by using a thinner gel pad under the pig allowing the cooling table to have more cutaneous effect; Pigs 2-7 showed no evidence of first degree burns at the areas of entry of FUS beams. In Pig 3 there was a small pneumothorax and in addition to the three ablated spots which were firm, the lung parenchyma had a gelatinous texture. Pigs 2-6 presented with firm, nodular lesions in at the areas of ablation. Pig 5 presented with a unique 3cm cystic lesion filled with pus over the area of ablation. Pig 7 presented with a small lesion in the right lung possibly caused by reflection of the MRgFUS beam. All pigs remained healthy in the week post ablation.

Conclusions: For a pilot project, these results are very encouraging as they demonstrate the ability for transcutaneous MRgFUS ablation in-vivo to induce damage of lung parenchyma

Table 1

	Breed	Weight	Power and Duration of Ablations
Pig 1	Yorkshire	53kg	Ablations performed in 3 spots during a 20 sec breath-hold each. Power per spot: 1) 2x350Watt; 2) 350Watt; 3) 300Watt
Pig 2	Yorkshire	53kg	
Pig 3	Yorkshire	53kg	
Pig 4	Yorkshire	60kg	Ablations performed in 2 distinct spots during a 20 sec breath-hold each. Power per spot: 350Watt.
Pig 5	Yorkshire	60kg	
Pig 6	Yorkshire	63kg	
Pig 7	Yorkshire	53kg	

Figure 1.

behind the rib space. A lot was learned but more work needs to be done to perfect this technique and assess tissue necrosis in real cancer tumors. Each animal model recovered well from this surgery with no poor outcomes related to the new technique. This technique also opens the possibility for intrathoracic delivery of ultrasound for lung cancer tumors that are difficult to reach using an intercostal approach. A therapeutic use for high intensity focused ultrasound (HiFU) has been demonstrated in ex-vivo human cancer models using one-lung flooding (OLF) and in mice models against cisplatin-resistant human lung adenocarcinoma. The risks of OLF in patients with reduced lung function are still in question however.

Acknowledgment/Funding Sources: This work was supported by a grant from the Focused Ultrasound Foundation.

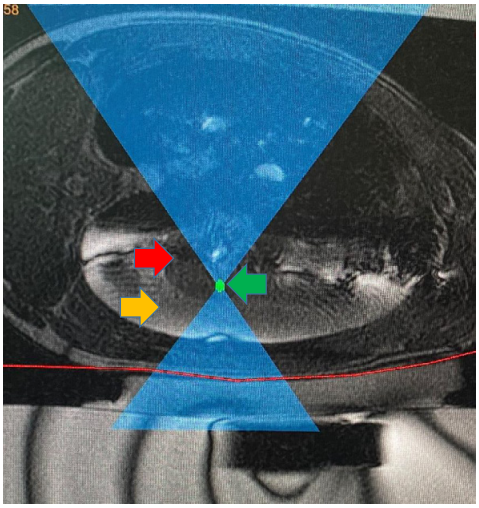

Figure 2. Axial MRI view of pig 6 during MRgFUS treatment planning. Red arrow, collapsed non-ventilated left lung. Orange arrow, thoracic cavity filled with saline to create an acoustic window. Green arrow, FUS focal spot as one of the ablation targets.

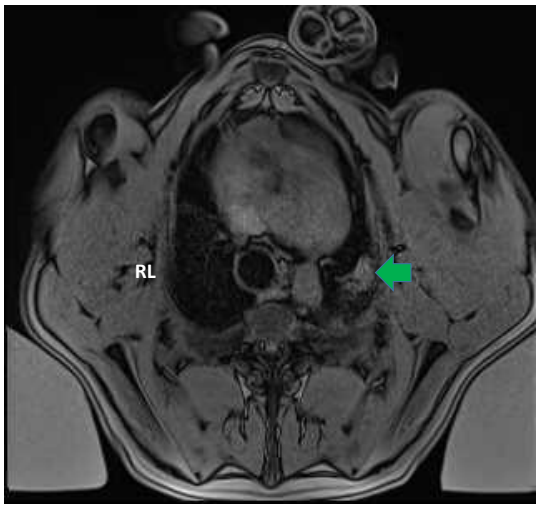

Figure 3. Axial MRI view of pig 6, one-week post MRgFUS ablation treatment. Green arrow, points to the ablated area in the left lung.

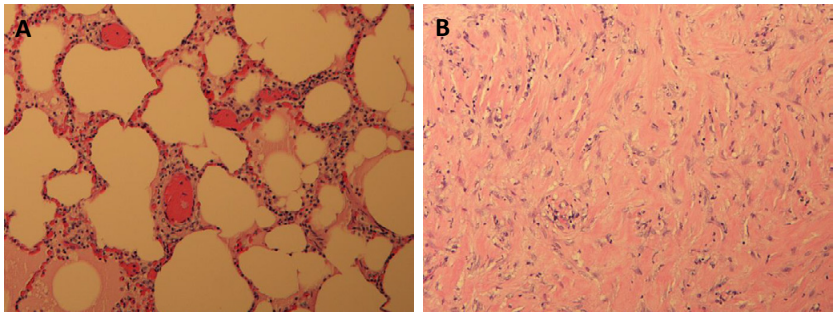

Figure 4. A- Section of normal lung tissue, removed from the right lung middle lobe, where no FUS ablation occurred (control); magnification 10x. B- Section of ablated lung tissue, removed from left lung at the FUS ablation target site; magnification 10x.

LUN-02

Topic: Lung
Presentation Type: Oral

The Vulnerable Alveolar Air-Tissue Interface: Considerations for the Safe Use of FUS in Proximity to Lung

Frank Wolfram, Thomas Lesser

SRH Wald Clinic Gera, Gera, Thueringen, Germany

Background: Therapeutic ultrasound applications are emerging. In some cases, focal ablation is performed in proximity to lung. The thin alveolar air-tissue interface is very sensitive to mechanical stress. Pre-clinical animal studies showed induction of pulmonary capillary hemorrhage (PCH) in lung when exposed to low intensity focused or even sonographic ultrasound. During FUS, the lungs pleural surface is generally not directly targeted, but pre-focal and post-focal intensities can cause unwanted exposure. Even at intensities below destructive thermal or mechanical thresholds PCH is induced. Therefore, this work summarizes novel findings regarding the interaction of ultrasound at the alveolar epithelium-gas interface and gives advices for the save use of therapeutic ultrasound in proximity to lung.

Materials and Methods: A comprehensive literature review related to bio-effects on mechanical waves exposing lung is carried out. This includes current statements of from ultrasound societies (AIUM, EFSUMB) related to the safety of lung ultrasound. Furthermore, recent FUS studies reporting pulmonary complications will be discussed. Finally, recommendations for planning of focal ablation in proximity to lung and monitoring methods will be discussed.

Results: Ventilated lung tissue is much more vulnerable to mechanical stress than solid tissue. This has been intensively investigated in animal models during blast and sonographic ultrasound exposure. The likelihood of PCH induction arises from peak negative pressure below 1.5 MPa with exposure time. The cause of such pulmonary bleeding remains still unknown, although it has been shown that neither cavitation nor thermal effects are involved. The extent of hemorrhage in lung is depending on physiological conditions such as pulmonary vascular pressure, inflation status as well as acoustic parameters (amplitude, pulse length) and is therefore not entirely predictable.

Conclusions: When focusing therapeutic ultrasound in the upper abdomen or chest wall, awareness for possible PCH related complications in proximal lung should be raised. Those may cause asymptomatic or symptomatic adverse events. Therefore, FUS treatment planning should avoid pre-focal lung exposure and consider sufficient safety margin between focal position and lung to ensure pressure values below 1.5MPa (rarefactional). In the therapeutic regime the risk should be minimized and balanced with the clinical benefit of the intervention. Some evidence exists that proper positioning and ventilation management can reduce the extent of hemorrhage. Further research should be done, evaluating risk strategies and monitoring capabilities for minimizing the ultrasound effects on the alveolar air tissue interface and therefore avoiding FUS related complications.

Acknowledgment/Funding Sources: The authors would like to thank the ECMUS Safety committee and Douglas Miller. No funding received.

MIS-01

Topic: Other Indications
Presentation Type: Oral

Radiotherapy Synergizes with PD-L1 Blockade to Limit Post-ablation Cancer Recurrence and Metastasis

Xin Guan

Shanghai Tenth People's Hospital, Tongji University, Shanghai, China

Background: Inadequate ablation remains an important cause of tumor recurrence after local-regional percutaneous thermal ablation therapy. Changes in the microenvironment of the residual foci after ablation that are important in determining post -ablation outcome remain poorly understood.

Materials and Methods: 1. Constituted a mouse melanoma model with insufficient microwave ablation and observed the local tumor progression after ablation. Explored the infiltration of myeloid cells and hypoxia state in the periablation zone via flow cytometry and immunofluorescence. 2. Synthesized IPI549@HMP and evaluate its physicochemical properties. The cytotoxicity and biotoxicity of IPI549@HMP was tested in B16F10 cells and C57BL6 mice, respectively. 3. Evaluated radiosensitization effect and hypoxia relieve capacity of IPI549@HMP via colony formation experiments and photoacoustic imaging. 4. Established local post-ablation model, distant metastasis model and memory model to receive combined radioimmunotherapy. Changes in mice tumor volume were monitored and immune indexes were further explored 13 days after treatment.

Results: 1. Compared to tumors pre-treated without ablation, recurrent tumors after ablation progress more rapidly with more myeloid cells infiltration and exacerbated hypoxia. 2. IPI549@HMP has uniform morphology with average particle size of 143 nm and exhibits superior biosafety within 200 ppm concentration. 3. IPI549@HMP enables to target myeloid cells and catalyze endogenous hydrogen peroxide into oxygen for enhanced radiotherapy. 4. After combined IPI549@HMP with radiotherapy, the residual tumors exhibited slowest outgrowth speed and all the mice survived for 40 days, with complete response in 50%. Immune analyses revealed that the combination therapy not only increases the proportions of positive immune responders, but also suppresses those negative immune inhibitors. Further combined with PD-L1 checkpoint blockade elicited a systemic immune response against both primary and metastatic tumors. No visible secondary tumor growth was observed in mice after their initial tumors were eliminated by the combined treatment, and all survived for 100 days.

Conclusions: 1. Inadequate ablation creates an immunosuppressive milieu characterized by hypoxia and high-influx of myeloid cells, significantly fostering cancer progression and hindering PD-L1 blockade therapy. 2. The IPI549@HMP-sensitized radiotherapy results in post-ablation tumor microenvironment reprogramming and heightening susceptibility to anti-PDL1 therapy. 3. This combined radioimmunotherapy can suppress/eradicate locally residual and distant tumors, and elicits strong immune memory effects to completely resist tumor rechallenge.

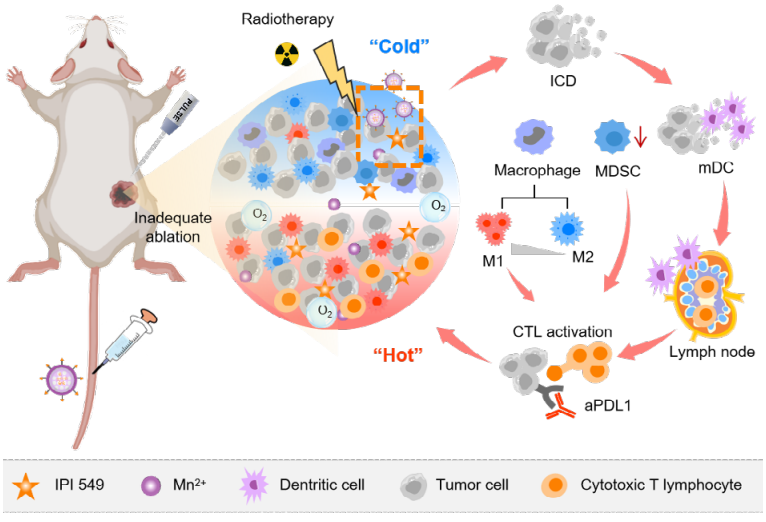

Figure 1. Schematic illustration of engineering radioimmunostimulant nanomedicine synergizing with PD-L1 blockade for postablation cancer immunotherapy.

Acknowledgment/ Funding Sources: National Natural Science Foundation of China (81725008) and Shanghai Municipal Health Commission (2019LJ21)

MIS-02

Topic: Other Indications
Presentation Type: Oral

Streamlining the Research Funding Pipeline at FUSF

Charlie Manning

Focused Ultrasound Foundation, Charlottesville, VA, USA

Background: The Focused Ultrasound Foundation is interested in funding as strategically as possible. A key component of this strategic funding is speed - the timeliness of research dollars can be very important for both individual research entities FUSF is aiming to support as well as the overall momentum of scientific progress in the field. For the last two years, we have been analyzing and adjusting our research funding process in an attempt to minimize unnecessary wait times between steps and increase the speed at which FUSF can process funding requests, make funding decisions, and deliver funding dollars.

Materials and Methods: N/A

Results: N/A

Conclusions: N/A

MIS-03

Topic: Other Indications
Presentation Type: Oral

Non-invasive Thalamic Sonication as a Neuromodulatory Intervention for Patients with a Disorder of Consciousness

Martin M. Monti[1], Joshua Cain[1], Norman Spivak[1] , Paul M. Vespa[1], Caroline Schnakers[2]

[1]University of California, Los Angeles, Los Angeles, CA, USA
[2]Casa Colina Hospital and Centers for Healthcare, Pomona, CA, USA

Background: Disorders of consciousness (DOC) such as Coma, the Vegetative State (VS) and the Minimally Conscious State (MCS) describe conditions of severe disability and complete dependence, typically acquired after severe brain injury, which can last from days to decades. These conditions are also associated with great emotional and financial strain on families, increased burnout rates of care-taking personnel, and pose complex medical, legal, and ethical questions. Yet, despite great advances in our understanding of these conditions, there is no accepted treatment for chronic DOC. Surgical interventions for direct thalamic stimulation (e.g., deep brain stimulation, DBS) have shown remarkable results, but are inapplicable to more than 85% of patients, while non-invasive indirect approaches (e.g., transcranial direct current stimulation; tDCS) show some promise, but remain debated. Low Intensity (i.e., neuromodulatory) transcranial focused ultrasound offers an alternative approach to device-based treatment in these conditions since it is capable of directly targeting key subcortical regions (i.e., central thalamus; unlike tDCS) while being non-invasive and usable at the bedside (unlike DBS). Here, we present evidence from a proof-of-concept first-in-human clinical trial in both acute and chronic DOC patients as well as preliminary data from a follow-up clinical trial in chronic DOC patients.

Materials and Methods: In this first clinical use of focused ultrasound neuromodulation, 21 DOC patients (N=11 and N=10 for the acute and chronic samples, respectively) underwent Low Intensity Focused Ultrasound Pulsation (LIFUP) to central thalamus and clinical testing. . Behavioral assessments were made (Coma Recovery Scale Revised; CRS-R) prior to and following sonication for 12 total time points per subject, while concurrent functional MRI (fMRI) was also recorded. In our ongoing follow-up clinical trial (also open label), chronic DOC patients (to date, N= 9) undergo a 10-day protocol featuring 4 days of baseline measurements, including clinical assessments (i.e., CRS-R), electrophysiology (i.e., EEG) and metabolic (i.e., FDG-PET) recordings, and 6 days of follow-up measurements with the same techniques.

Results: As shown in Figure 1, both acute and chronic samples in our first-in-human trial exhibited a significantly higher maximum CRS-R total score following LIFUP as compared to baseline. Intriguingly, fMRI shows that, in the both acute and chroniccohorts, the degree to which thalamic connectivity (when using the targeted thalamus as seed and not when using the non-targeted thalamus) is modulated by LIFUP during sonication is associated with the degree of clinical improvement measured in the days following LIFUP. The preliminary behavioral data in our follow-up clinical trial shows the same clinical effect – with the best CRS-R score following LIFUP being significantly higher than the best CRS-R at baseline. In addition, electrophysiological data shows two preliminary results. First, LIFUP alters the distribution of power spectrum density in the hour following LIFUP application, leading

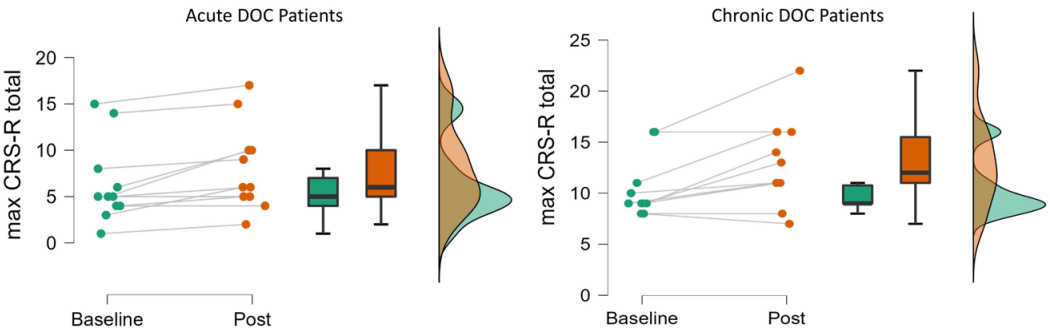

Figure 1. Maximum Coma Recovery Scale Revised (CRS-R) score during baseline and post-sonication periods for acute (left) and chronic (right) DOC patients in our first-in-human clinical trial.

to a proportional reduction of oscillatory power at slower frequencies (i.e., delta) and an increase in faster rhythms (i.e., beta). Second, we find a relationship between the ratio of fast (i.e., beta) to slow (i.e., delta) EEG spectral power density prior to LIFUP and the clinical amelioration (i.e., change in CRS-R) observed over the 6 days following sonication. Finally, no significant adverse events have been observed to date.

Conclusions: These data support the idea that non-invasive thalamic sonication is a promising avenue for neurorestorative intervention in both acute and chronic DOC patients. Importantly, we stress that while it is not unusual for acute DOC patients to show signs of recovery over time, this is not the case for chronic patients, who only show small ameliorations over the span of months or years (i.e., not days, as in the present protocols). The above results should motivate a randomized, double-blind, clinical trial to estimate efficacy. Nonetheless, many questions are yet to be addressed, such as the duration of any sonication-associated improvements.

Acknowledgment/Funding Sources: Tiny Blue Dot Foundation; Dana Foundation

MIS-04

Topic: Other Indications
Presentation Type: Oral

Non-viral Nitric Oxide-Based Gene Therapy Improves Perfusion and Liposomal Doxorubicin Sonopermeation in Neuroblastoma Models

Aditi Bellary[1], Chance Nowak[2], Isabella Iwanicki[3], Fernando Flores-Guzman[3], Lydia Wu[3], Jessica J. Kandel[3], Theodore W. Laetsch[4], Leonidas Bleris[1], Sonia L. Hernandez[3], Shashank R. Sirsi[1]

[1]University of Texas at Dallas, Richardson, TX, USA
[2]University of Texas at Dallas, Boston, MA, USA
[3]University of Chicago Medical Center, Chicago, IL, USA
[4]Children's Hospital of Philadelphia, Philadelphia, PA, USA

Background: Neuroblastoma (NB) is a pediatric malignancy that accounts for 15% of cancer-related childhood mortality. High-risk NB requires an aggressive chemoradiotherapy regimen that causes significant off-target toxicity. In spite of these invasive treatment measures, many patients do not respond adequately or experience relapse after initial therapy. Recent studies suggest that improving tumor perfusion can enhance drug accumulation and distribution within tumor tissue, potentially augmenting treatment effects without systemic toxicity. Accordingly, methods of transiently increasing tumor perfusion prior to treatment may be beneficial in combatting this disease. Here we show the use of gene therapy to confer nitric oxide synthase (NOS) expression solely in the tumor space, using focused ultrasound targeting. NOS catalyzes the reaction that generates nitric oxide (NO), a potent endogenous vasodilator. This study reports the development of a targeted non-viral image-guided platform to deliver iNOS-expressing plasmid DNA (pDNA) to vascular endothelial cells encasing tumor blood vessels. Following transfection, longitudinal quantitative contrast-enhanced ultrasound (qCEUS) imaging revealed an increase in tumor perfusion over 72 hours, attributed to elevated intratumoral iNOS expression.

Materials and Methods: To construct a gene delivery vector, cationic ultrasound responsive agents (known as "microbubbles") were employed to carry pDNA in circulation and transfect tumor vascular endothelial cells in vivo using focused ultrasound (FUS) energy. The post-transfection tumor response was monitored longitudinally using qCEUS imaging to determine relative changes in blood volumes and perfusion rates. Following therapy, ex vivo analysis of tumors was performed to examine the bioeffects associated with iNOS expression.

Results: By combining FUS therapy with cationic ultrasound contrast agents (UCAs), we achieved selective intratumoral transfection of pDNA encoding the iNOS enzyme. While transitory, the degree of expression was sufficient to induce significant increases in tumoral perfusion and to appreciably enhance chemotherapeutic payload and extends survival time in an orthotopic xenograft model. qCEUS imaging was able to monitor changes in tumor perfusion in vivo, allowing identification of an ideal time-point to administer therapy.

Figure 1. Schematic detailing the experimental procedure and proposed mechanisms of action of iNOS gene therapy. Created with BioRender.com

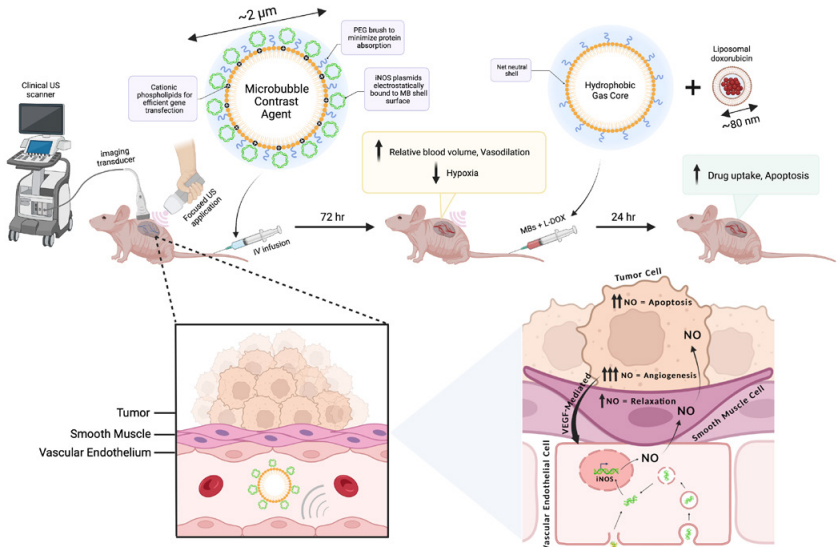

Conclusions: We have demonstrated the ability of a novel targeted non-viral gene therapy strategy to enhance tumor perfusion and improve liposomal doxorubicin delivery. While our results demonstrate that transiently increasing tumor perfusion improves liposome-encapsulated chemotherapeutic uptake and distribution, we expect that our iNOS gene delivery paradigm can also significantly improve radiotherapy and immunotherapies by enhancing delivery of liposome-encapsulated radiosensitizers and immunomodulators, potentially improving upon current neuroblastoma treatment.

Acknowledgment/Funding Sources: The work performed in this study has been supported by the National Institute of Health through the NCI (R01CA235756) as well as the Pediatric Cancer Foundation.

MOV-01

Topic: Movement Disorders

Presentation Type: Oral

Cognitive Outcome of MR Guided Focus Ultrasound for the Treatment of Tremor in Patients with ET and PD

Paolo Amami, Sara Prioni, Elisa Bocchi, Nico Golfre' Andreasi, Roberto Cilia, Luigi M. Romito, Antonio E. Elia, Alessio Novelli, Giuseppe Massina, Vincenzo Levi, Grazia Devigili, Sara Rinaldo, Valentina Gasparini, Marina Grisoli, Mario Stanziano, Francesco Ghielmetti, Elisa F. Ciceri, Maria Grazia Bruzzone, Roberto Eleopra, Sylvie H. Piacentini

Fondazione IRCCS Istituto Neurologico Carlo Besta, Milan, Italy

Background: In the last few years, the technique of magnetic resonance-guided focused ultrasound (MRgFUS) targeting the ventralis intermedius nucleus of the thalamus (VIM) has been demonstrated to be an effective treatment for the management of tremor in patients with either essential tremor (ET) or Parkinson?s disease (PD). Despite VIM is a sensorimotor region of thalamus, the evidence with deep brain stimulation of the same target showed reduction of verbal fluency after the treatment. The few data on cognition after MRgFUS showed a general safety of the technique, but there were conflicting results on the outcome of specific cognitive domain. While some studies reported reductions of memory or verbal fluency, other showed no changes or even improvement. Aim of this study is to assess cognitive status after VIM MRgFUS at one and six months after the treatment. Furthermore, we investigated difference in cognition at six months in patients with ET and PD, and in patients treated on left and right emisphere.

Materials and Methods: Consecutive patients with a diagnosis of ET or PD, treated with monolateral MRgFUS of the VIM were enrolled for this longitudinal study. Patients were regularly evaluated at baseline and during follow-up visits held one and six months post-treatment by a comprehensive neuropsychological battery assessing memory, attention and executive functions and visuo-constructional ability. For re-test we used parallel versions. A within group comparison were performed between baseline, one and six months visitis, furthermore the cognitive status at last follow-up was compared between ET and PD patients and between patients treated on left and right emisphere.

Results: A total of 57 patients, 32 with a diagnosis of ET and 25 with a diagnosis of PD, underwent MRgFUS of VIM and completed the six months follow-up. For all patients the brain target was the VIM: 45 patients were treated on the left emisfere and 12 on the right. At six months follow-up, no patients showed dementia; on avarege the MoCA score improved significantly from baseline to 6 months follow-up by 2 points. Also the accurancy in a task assessing selective attention slightly improved after treatment. A reduction in phonemic and semantic fluencies was observed one month after the treatment, but verbal fluencies increased again to the baseline level in the long term . Verbal memory decreased at 6 months follow-up both in learning and recall abilities, while visuo-spatial memory did not

Table 1. Cognition of patients treated with MRgFUS at baseline and at one and six months follow-up.

	Baseline	1 month	6 months	p-value
MoCA	22.94 (±3.4)	23.69 (±3.1)	24.7 (±3.5)	0.001
Digit span forward	5.8 (±1.2)	-	5.9 (±1.1)	0.223
Digit span backward	4.6 (±1.4)	-	4.6 (±1.4)	0.732
RAVLT – learning	41.2 (±11.1)	-	35.6 (±10.8)	0.001
RAVLT – recall	7.8 (±3.6)	-	6.3 (±3.1)	0.001
ROCF – recall	15.8 (±6.6)	-	16.2 (±5.9)	0.662
MFTC - accuracy	0.94 (±0.06)	-	0.96 (±0.06)	0.001
TMT a	54.1 (±29.9)	51.8 (±36)	49 (±33.2)	0.220
TMT b-a	77.3 (±38.9)	74 (±45.3)	68.9 (±35.8)	0.072
Phonemic fluency	35 (±12.9)	33 (±11.4)	37.4 (±14.3)	0.049
Semantic fluency	41.4 (±10.8)	39.9 (±10.9)	43.3 (±12.5)	0.017
ROCF - Copy	33.1 (±4)	-	33 (±3.5)	0.170

change after treatment. At six months follow-up there were no difference in cognitive status depending on the diagnosis or the treated emisphere.

For within-group comparison, the Friedman test or the Wilcoxon signed-rank test was used. Significant differences ($p < .05$) are expressed in bold.

MFTC, multiple features target cancellation; MoCA, Montreal cognitive assessment; RAVLT, Rey auditory verbal learning test; ROCF, Rey-Osterrieth complex figure; TMT, trial making test.

Conclusions: Our data confirmed that MRgFUS targeting the VIM is a cognitively safe procedure for the treatment of tremor in patients with ET or PD. A decrease in verbal fluency can occur soon after the treatment, but within six months returns to the baseline level. Also a slight reduction of verbal memory was observed in ET and PD patients. Long-term studies are needed to ascertain the outcome of specific cognitive domain after MRgFUS, in particular verbal memory.

MOV-02

Topic: Movement Disorders
Presentation Type: Oral

Unilateral Subthalamotomy by MRgFUS in Asymmetrical Parkinson's Disease (PD)

Laura Armengou Garcia[1], Jorge Guridi[2], Lain Gonzalez[2], Iciar A. Olmos[2], Maria Aranzazu Gorospe[2], Adolfo Jiménez-Huete[3], Antonio Martin-Bastida[3], Maria C. Rodriguez-Oroz[2]

[1]Clinica Universidad de Navarra, Toronto, ON, Canada
[2]Clinica Universidad de Navarra, Pamplona, Navarra, Spain,
[3]Clinica Universidad de Navarra, Madrid, Madrid, Spain

Background: The development of MRgFUS as a minimally invasive technique has revitalized ablation as a treatment for movement disorders. Recently, two pilot studies showed safety and efficacy of MRgFUS unilateral subthalamotomy for the treatment of PD motor features.

Materials and Methods: 20 patients (2 females, mean age 61.5 years were treated with unilateral MRgFUS subthalamotomy and followed up with standardized evaluations including the MDS-UPDRS III for the treated side in Off medication, the Clinical Global Impression of Patient (CGI-P) and a neuropsychiatric evaluation. Treatment-related adverse events (AE) were also recorded.

Results: Mean time of follow up was 16.9 months (range 2.0-28.5). 19, 18 and 12 patients were evaluated at baseline, 6 months and 12 months, respectively. At 6 months, improvement in total score of the treated side was 78.6%, in tremor 91.1%, in bradykinesia 69.4% and in rigidity 82.1% (all $p<0.01$). At 12 months improvement in total score of the treated side was 68.5%, in tremor 88.2%, in bradykinesia 55.5% and in rigidity 79.8% (all $p<0.01$). All patients reported clinical improvement at 6 months (CGI-P 1-3) and 12 months (CGI-P 1-4). A significant improvement of visual memory, depressive, and impulsivity symptoms were seen. Moreover, worse scores were observed in semantic fluency and Stroop Color-Word test. Mean LEDD decreased from 737.5 to 541.8 at 6 months ($p<0.001$) and 554.2 at 12 months (<0.001). Usual treatment-related adverse effects included de novo transient dyskinesia, weakness of the treated side and impulsiveness. Most of the adverse events were mild and completely resolved by the 6-month-follow-up visit.

Conclusions: Our results suggest that unilateral subthalamotomy by MRgFUS is safe and that the benefits on PD motor features are similar to those previously reported. More studies with higher sample sizes are needed to be more conclusive about neuropsychological assessments.

MOV-03

Topic: Movement Disorders

Presentation Type: Oral

MR Compatible Accelerometers for Tremor Monitoring during MRgFUS Essential Tremor Treatments: Early Markers for Tremor Reduction Efficacy

Jean Francois Aubry[1], Thomas Bancel[1], Benoît Béranger[2], Cecile Galea[2], Mathieu D. Santin[2], Melanie Didier[2], Eric Bardinet[2], Itay Rachmilevitch[3], Yeruham Shapira[3], Mickael Tanter[1], Marie Vidailhet[4], David Grabli[4], Elodie Hainque[4], Carine Karachi[4], Nadya Pyatigorskaya[2]

[1]Physics for Medicine Paris, Paris, France
[2]INSERM U 1127, Paris, France
[3]Insightec, Tirat Carmel, Haifa, Israel
[4]Groupe Hospitalier Pitié-Salpêtrière, AP-HP, Paris, France

Background: Currently, the patient subjective feedback plays an important role in the dose escalation procedure during MRgFUS for Essential Tremor treatments. Between sonications, patients are sometimes taken out of the MR bore to better assess the evolution of the tremor during treatment, which are time consuming procedures. We propose here to monitor quantitatively the tremor inside the MR tunnel with MR compatible accelerometers, including during the 15s-40s therapeutic sonications.

Materials and Methods: Seven essential tremor patients were treated with the Exablate Neuro 4000 clinical system manufactured by Insightec Ltd. The transducer is made of 1024 elements distributed on a 30-cm diameter hemisphere and was operated at 650kHz transmit frequency. Patients were instructed to hold postures during treatment and their posture-related tremor was monitored during each ultrasonic thermal sonication with two MR-compatible accelerometers attached to each hand. The tremor power was calculated in the [4 12] Hz band and displayed in real time in the control room on a dedicated computer. The treatment efficacy was assessed by calculating the maximum tremor power change comparing a baseline period before treatment to the same period length during the treatment. During the inclusion and control visits, the tremor was also evaluated by the neurologist using the Fahn-Tolosa-Marin (FTM) scale. Finally, the CSRT (A+B) score reduction between D+7 and M+1 visit was compared to the accelerometry-based maximum tremor power change during the treatment.

Results: On average only 4±1 ablative sonications were necessary to induce 86% tremor reduction on the CSRT scale at D+7. The overall tremor power reduction in the [4 12] Hz band measured with accelerometry during the treatment was 89±14%. The tremor reduction during treatment was correlated to the tremor improvement using clinical rating scales during control visits (R2 = 0.90 at D+7 and R2 = 0.74 at M+1) (Figure 1).

Conclusions: Accelerometry measurements during treatment correlates with clinical outcome. Accelerometry measurements can be displayed in real time to the clinical team and has the potential (i) to improve the clinical outcome; (ii) to reduce the risk of unnecessary ablative sonications, and (iii) to eventually reduce the number of adverse events.

Acknowledgment/Funding Sources: This work was achieved in collaboration and with the financial support of Insightec ltd. It was supported by the Bettencourt Schueller Foundation.

Figure 1. Tremor improvement using clinical rating scales during control visits at D+7 (Left) and M+1 (Right) compared to the tremor reduction calculated during treatment with accelerometry.

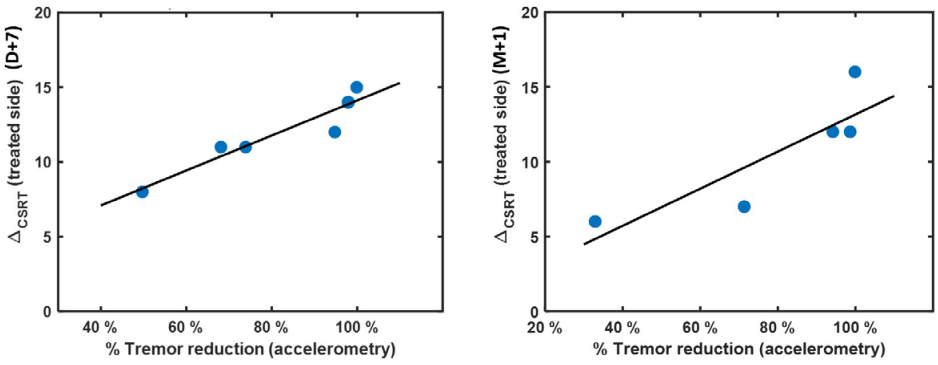

MOV-04

Topic: Movement Disorders
Presentation Type: Oral

First Evidence of a Drastic and Sustained Reduction of Essential Tremor with Low Energy Transcranial Focused Ultrasound Neurostimulation: Clinical Report of 98% Tremor Reduction for More than 25 Minutes

Jean Francois Aubry[1], Thomas Bancel[1], Benoît Béranger[2], Melanie Didier[2], Mathieu D. Santin[2], Itay Rachmilevitch[3], Yeruham Shapira[3], Mickael Tanter[1], Eric Bardinet[2], Cecile Galea[2], Alexandre Dizeux[1], Marie Vidailhet[4], Stephane Lehericy[2], David Grabli[4], Nadya Pyatigorskaya[2], Carine Karachi[4], Elodie Hainque[4]

[1]Physics for Medicine Paris, Paris, Paris, France
[2]INSERM U 1127, Paris, France
[3]Insightec Ltd, Tirat Carmel, Haifa, Israel
[4]Groupe Hospitalier Pitié-Salpêtrière, AP-HP, Paris, Paris, France

Background: Transcranial Ultrasound Stimulation (TUS) is a promising non-invasive technology. Nevertheless, mild effects only have been reported in non-human primates and healthy volunteers so far. Most of the reported work was achieved using single element transducers with high f-number and no aberration correction to compensate for the effect of the skull. We took advantage of the unique high precision ultrasound targeting of the Exablate Neuro 4000 clinical system (Insightec Ltd, Istrael) to investigate the behavioral effect of TUS in the ventral intermediate nucleus (VIM), the relay of the dentato-rubro-thalamic (DRT), in Essential Tremor patients scheduled for MRgFUS treatment.

Materials and Methods: All the sonications were performed with the Exablate Neuro 4000 device (Insightec Ltd, Israel). The transducer is made of 1024 elements distributed on a 30-cm diameter hemisphere and was operated at a 650kHz transmit frequency. Patients were instructed to hold postures inside the MR bore during TUS. Their posture-related tremor was monitored during each ultrasonic low energy sonication with two MR-compatible accelerometers attached to each hand. The tremor power was calculated in the [4 12] Hz band and displayed in real time in the control room on a dedicated computer. The TUS efficacy was assessed by the change in average tremor power between two 6s window periods calculated at the beginning and the end of the TUS stimulation. The TUS stimulations consisted in 3 bursts of 5s followed by a 10s pause, with varying duty cycles. Four stimulations were first performed in the VIM with a total acoustic energy of [52; 15; 47; 8]J respectively. The focal spot was then moved to the DRT and an 8J stimulation was performed.

Results: Figure 1 displays the tremor power measured on the treated hand for each sonication. The average tremor power in the [4 12]Hz band was modulated significantly but not drastically when targeting the VIM. The average power dropped from 3.46±0.4 (m.s-2)2 to 0.003±0.001 (m.s-2)2 for the sonication targeting the DRT, corresponding to a 99.9% tremor reduction in power. The post-effect remained visible after 30 minutes. For the first patient, the tremor power was 0.01±0.01 (m.s-2)2 26 minutes after the DRT stimulation,

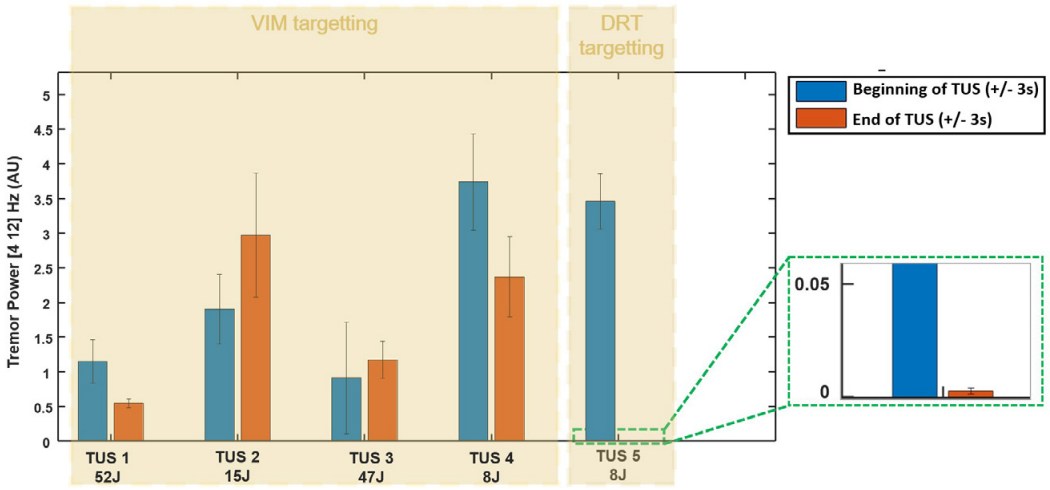

Figure 1. Tremor power for each of the five stimulations in the VIM and the DRT.

corresponding to a 98,1% sustained tremor reduction compared to baseline. No impact on the non-treated hand (left hand) was noted when comparing the tremor to the baseline.

Conclusions: The 26 minutes long 98% tremor reduction reported here immediately after transcranial ultrasound stimulation of the DRT with a low energy (8J) is to our knowledge the most striking evidence of deep brain target engagement with TUS. The exact same stimulation (same ultrasound pulses and same energy) applied to the VIM 5 minutes before induced less than 30% power reduction and its effect was transient (less than 5 minutes). The patient was treated with MRgFUS thalamotomy the same day of the transcranial ultrasound stimulation. For sake of comparison, the acoustic energy used during the last sonication to achieve a thermal lesion was 17,816.5J. The clinical trial is still on-going and the result of TUS on more patients will be presented at the FUS symposium.

Acknowledgment/Funding Sources: This work was achieved in collaboration with Insightec. It was supported by the Bettencourt Schueller Foundation.

MOV-05

Topic: Movement Disorders

Presentation Type: Oral

Feasibility of Accelerometer Measurements for Real-Time Monitoring of Patient's Treatment during MR-Guided Focused Ultrasound Thalamotomy

Hongchae Baek, Daniel Lockwood, Emmanuel Obusez, Matthew Poturalski, Sean Nagel, Stephen Jones

Cleveland Clinic, Cleveland, OH, USA

Background: MR-guided focused ultrasound (MRgFUS) thalamotomy is an FDA-approved treatment for essential tremor (ET) and tremor-dominant Parkinson's disease (PD). We repeated examinations of the patient's kinetic tremor throughout the procedure using the standard drawing sheet to obtain near-real-time feedback on the treatment effect. However, variability in the clinical judgment of the drawings may under or overestimate the outcomes and affect the treatment when updating the treatment plan. Therefore, we adopted intraoperative accelerometers secured to the contralateral upper extremity to objectively measure joint angle during the tremor motion. After each sonication, feedback from the accelerometer measurements provided joint angles at the shoulder, elbow, and wrist. In addition, we have quantitative analyzed patients' drawings and validated the methods by correlating the drawing scores with joint angles measured simultaneously during their drawings.

Materials and Methods: Pre-/post- and intraoperative kinetic tremor tests with simultaneous accelerometer recording A total of 22 tremor patients (12 ET and 10 PD) went through MRgFUS thalamotomy. They performed drawing with simultaneous accelerometer recording in the patient holding room, sitting up before the procedure (pre-test) and after the procedure (post-test). The same drawing test was performed during the procedure after each sonication with simultaneous accelerometer recording in their supine position. Accelerometer set-up and intraoperative analysis Before the procedure, three MR compatible accelerometers were secured to the patient's upper extremity at the arm, forearm, and finger. Tremor motion was measured using three accelerometers during the drawing, examining kinetic tremor. We used custom-made software coded with MATLAB (Mathworks Natick, MA, USA) to calculate the root mean square of angles from each shoulder, elbow, and wrist. Quantitative analysis of the patients' intraoperative drawing tests: post-operative analysis All writing/drawing sheets from the patients were scanned in color and uploaded to PC for analysis. Each figure (signature, spiral, and line) within the sheet was quantitatively analyzed using custom-made code written in IDL (v8.0, L3Harris Geospatial Solutions, Inc, Boulder, CO), yielding four metrics to characterize the tremor severity. A composite score was derived from these metrics for the signature, spiral, and line.

Results: A clear correlation in timing of the treatment response was observed in the clinical evaluation of the intraoperative drawings and a significant reduction of joint angles from simultaneous accelerometer measurements (Fig 1). We found that both joint angle and drawing scores detected significant tremor improvement in ET patients' sitting-up and supine positions during the drawings (Fig 2A,B). However, both joint angle and drawing scores detected significant tremor improvement only in their supine position and not in their sitting-up position in PD patients (Fig 3A,B). The correlation between joint angles and drawing scores was relatively high in the spiral ($r^2=0.66$) and line drawing ($r^2=0.69$) in all ET patients' drawings. Also, the correlation was strong in the spiral ($r^2=0.69$)and in line drawing ($r^2=0.7$) in all PD patients' drawings ($r^2=0.77$) (Fig 4).

Conclusions: We confirmed that the sensitivity of quantitative analysis metrics in detecting the tremor improvement is different depending on the patient's position and tremor etiology. For example, PD patients' supine position inside the MRI magnified their tremor, which allows for observing their treatment response during the procedure. However, we could not detect a meaningful kinetic tremor change in PD patients in their sitting-up position, perhaps due to PD tremor being mostly resting tremor, not kinetics. In summary, quantitative drawings analysis will be particularly useful for follow-up with ET patients. Therefore, we expect to assess the treatment durability by analyzing the patient's follow-up drawings performed at home using the drawing score.

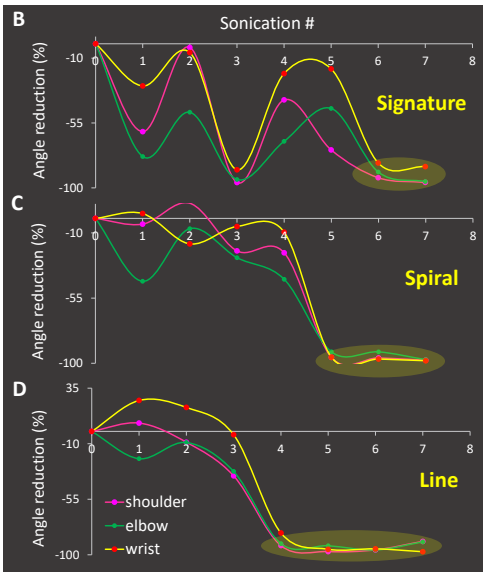

Figure 1. (A) Intraoperative drawing tests from a patient. Intraoperative measurements of simultaneous accelerometer recording during the patient's writing (B), Spiral (C), and line drawing (D).

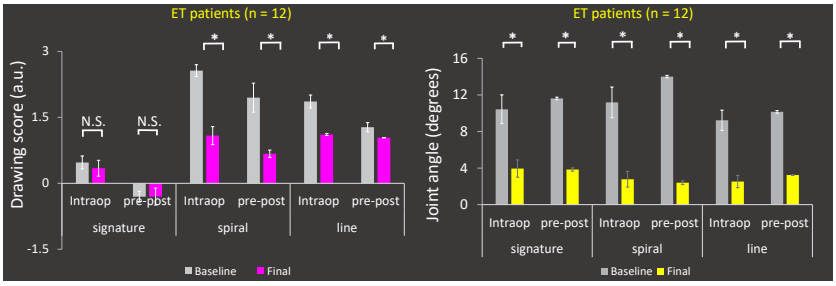

Figure 2. ET patients' tremor improvement was assessed using quantitative drawing analysis (A), and simultaneous accelerometer recording during the drawing tests (B).

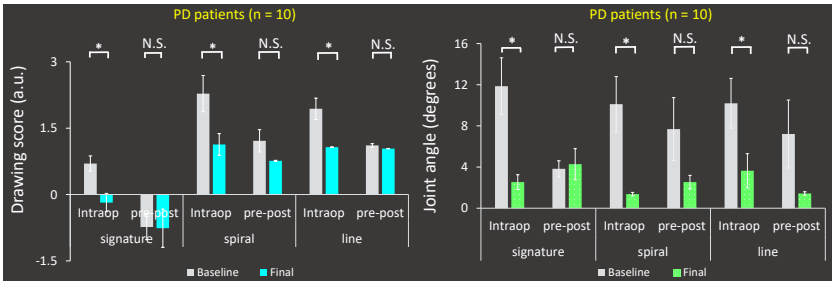

Figure 3. PT patients' tremor improvement was assessed using quantitative drawing analysis (A), and simultaneous accelerometer recording during the drawing tests (B).

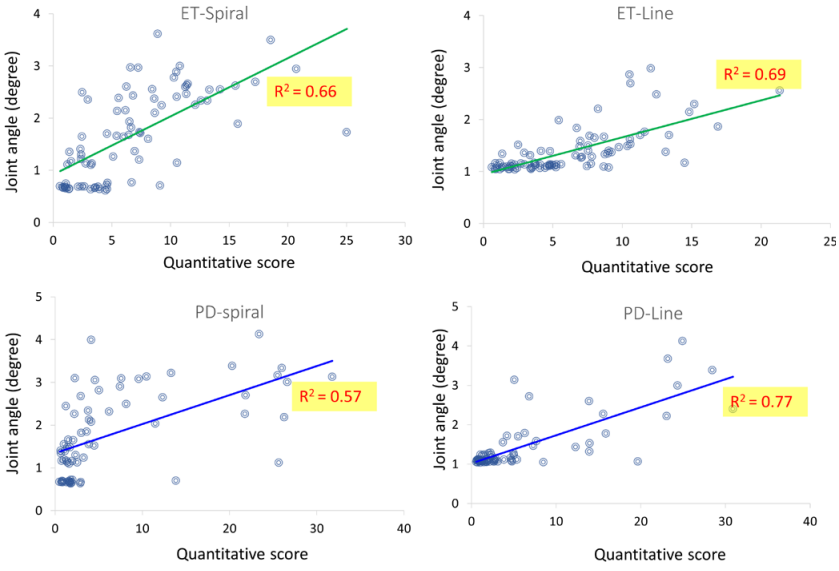

Figure 4. The RMS angle of hand tremor was strongly correlated with the quantitative analysis of Spiral and line drawing in ET patients. We found a strong correlation between spiral and line drawing analysis and RMS angle of hand tremor in PD patients.

MOV-06

Topic: Movement Disorders
Presentation Type: Oral

Correlation of Lesion Persistence and Outcomes in MR-Guided Focused Ultrasound Thalamotomy for Essential Tremor

Sarah Blitz[1], Melissa M. Chua[2], Alfredo Morales Pinzon[3], Michele Cavallari[2], Rees Cosgrove[1], Charles R. Guttmann[2]

[1]Harvard Medical School, Boston, MA, USA
[2]Brigham and Women's Hospital, Boston, MA, USA
[3]Brigham and Women's Hospital & Harvard Medical School, Boston, MA, USA

Background: Treatment of Essential Tremor (ET) with MR-guided focused ultrasound (MRgFUS) thalamotomy is generally successful and has been demonstrated to yield >80% tremor reduction at 1 year at this institution. However, in some patients, there is recurrence of tremor and/or side effects. One potential explanation is lesion volume and location, which may be indicated by persistence of lesion on imaging. We aimed to evaluate the incidence and significance of lesion persistence in a large patient cohort and correlate this with clinical outcomes and side effects.

Materials and Methods: In this retrospective analysis of a large single-surgeon series of MRgFUS thalamotomy for ET, we report the presence of chronic lesions on post-operative imaging and correlate this with tremor control and side effects. After 213 procedures, 212 patients underwent imaging on postoperative day 1. Postoperative MR imaging was obtained in 99 patients at 3 months (89 with follow-up appointments) and in 30 patients at 1 year (29 with follow-up appointments). Axial and coronal T2-weighted MRIs 1 day, 3 months and 1 year post MRgFUS thalamotomy were analyzed manually on a binary scale for persistence of lesion presence. At preoperative and 3-month and 1-year postoperative follow-up visits, Fahn-Tolosa-Marin (FTM) scores were calculated. Side effects were also recorded, including motor and sensory deficits, dysarthria, fatigue and imbalance. Chi-squared test and paired t-tests were used for statistical analyses.

Results: Visible lesions were present in all patients 1 day post MRgFUS. Residual chronic lesions were substantially smaller and detectable in only 53% of patients at 3 months (n = 99) and in 47% of patients at 1 year (n = 30). Lesion presence at 3 months (n = 89) did not correlate with 3-month raw FTM scores (0.9 vs. 0.5, p = 0.265), percent improvement from pre-op FTM score (89.9% vs. 92.3%, p = 0.548), overall presence of side effects (29 vs. 20, p = 0.397), or any specific side effect. Out of 167 patients who had 3-month clinical assessments, there were 6 "partial-responders" (<50% improvement from baseline). Of these, 5 had 3-month imaging, and lesions were present in 3 (60%). Lesion presence at 1 year (n = 29) did

Table 1. Overall Lesion Presence

	Yes lesion	No lesion
1 day, n = 212	212 (100%)	0 (0%)
3 months, n = 99	52 (53%)	47 (47%)
1 year, n = 30	14 (47%)	16 (53%)

Table 2. Follow-ups

	3 months			1 year		
	Yes lesion (n = 46)	No lesion (n = 43)	P value	Yes lesion (n = 13)	No lesion (n = 16)	P value
FTM score at pre-op +/- SD	7.3 +/- 2.8	6.5 +/- 1.9	0.089	7.9 +/- 3.2	6.5 +/- 1.7	0.151
FTM score at follow-up +/- SD	0.9 +/- 1.9	0.5 +/- 1.0	0.265	0.7 +/- 0.9	0.4 +/- 0.5	0.329
FTM improvement +/- SD (%)	89.9 +/- 21.6	92.3 +/- 15.8	0.548	90.7 +/- 12.4	92.8 +/- 9.0	0.608
Any side effect	29	20	0.397	5	7	0.853
Motor deficit	2	3	0.717	0	0	
Sensory deficit	15	11	0.400	3	3	0.817
Dysarthria	3	1	0.296	0	0	
Fatigue	3	3	0/936	0	0	
Imbalance	11	11	0.887	2	4	0.605

not correlate with 1-year raw FTM scores (0.7 vs. 0.4, p = 0.329), percent improvement from pre-op FTM score (90.7% vs. 92.8%, p = 0.608), overall presence of side effects (5 vs. 7, p = 0.936), or any specific side effect.

Conclusions: After MRgFUS thalamotomy for ET, lesions are visible on T2-weighted MRI in only about half of patients at both 3 months and 1 year. Presence of a residual lesion was not found to be correlated with tremor outcomes or side effects at either time point. Future studies should use computational analysis on day 1 imaging and sonication parameters to investigate correlation with lesion persistence.

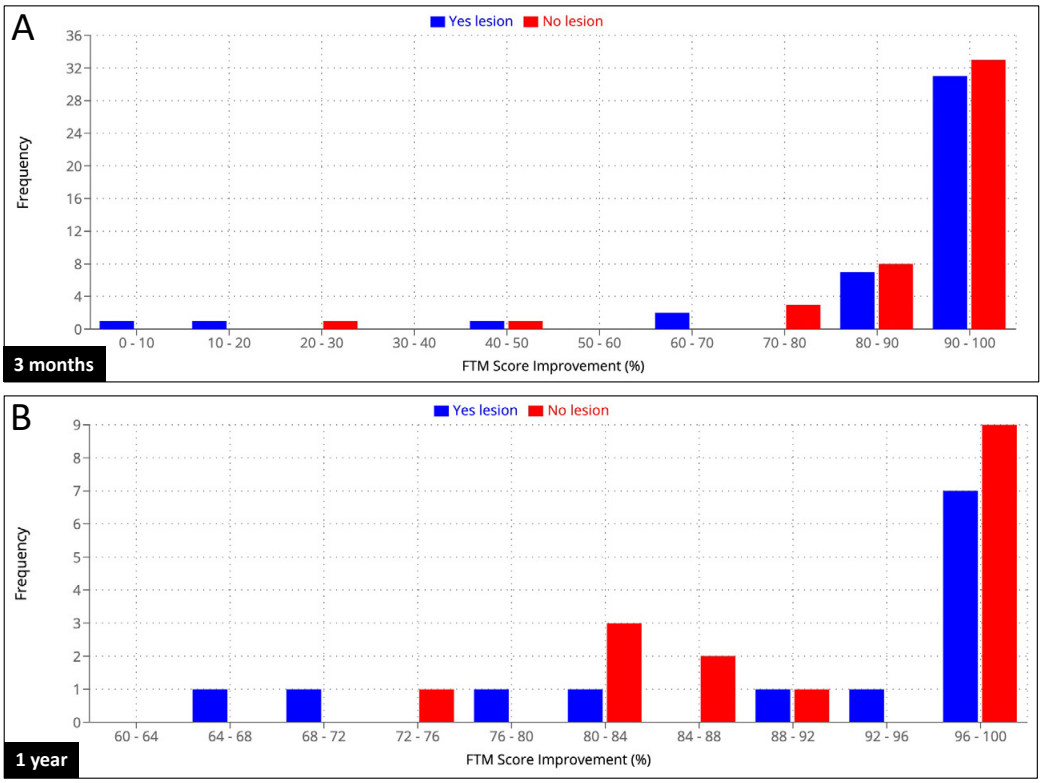

Figure 1. Histogram of Fahn-Tolosa-Marin (FTM) score percent improvement compared to baseline at (A) 3 months and (B) 1 year after MR-guided focused ultrasound thalamotomy for Essential Tremor in patients with lesion present on T2-weighted MRI vs. no lesion visible

MOV-07

Topic: Movement Disorders

Presentation Type: Oral

"Quality over Quantity": Smaller MRgFUS Lesions That Overlap Patient-Fit Normative VIM—Precentral Tracts Improve Quality-of-Life Outcomes in Essential Tremor

Vivek Buch[1], Yosefi Chodakiewitz[1], David Purger[1], Allan Weng[1], Daniel Barbosa[1], Anjali Datta[1], Lior Lev Tov[1], Erika Lim[1], Neha Dhawan[2], Rachelle Bitton[1], Casey Halpern[3], Jaimie Henderson[1], Jennifer McNab[1], Pejman Ghanouni[4]

[1]Stanford University, Palo Alto, CA, USA
[2]Insightec, Dallas, TX, USA
[3]University of Pennsylvania, Philadelphia, PA, USA
[4]Stanford University, Stanford, CA, USA

Background: Essential Tremor (ET) resulting in intention-based trembling of the hand can limit Quality-of-Life (QoL). MRgFUS VIM-thalamotomy is established for reducing tremor in ET. However, despite excellent tremor suppression, possible side-effects may compromise post-MRgFUS QoL. The traditional "canonical" MRgFUS thalamotomy technique is focused on tremor reduction; it involves historical atlas-defined stereotactic coordinates approximately referenced relative to imaging landmarks. More optimized and patient-specific preoperative targeting techniques are desired to enable more accurate and precise lesion targeting, in order to optimize QoL outcomes while achieving efficacious tremor-reduction.

Materials and Methods: An institutional database of 82 ET patients treated with MRgFUS was retrospectively studied. Subjects with <3mo follow-up were excluded, leaving 62 subjects. Analysis occurred as follows:1) Patients were categorized by postoperative QoL ("better," "same," or "worse"), determined from last available follow-up clinical visit. 2) Immediate pre/post MRgFUS CRST (Clinical Rating Scale for Tremor) hand tremor scores were compared for the "better," "same," and "worse" groups (Kruskal Wallis) 3) Patient-specific thalamic maps were determined through patient-fit normative tractography (Fig.1). Based on normative probabilistic tractography using the Human Connectome Project's (HCP) dataset, streamline probability maps were co-registered to each subject's pre-operative T1-weighted MRI: VIM(seed)precentral gyrus (M1, target). The VIM mask was derived from the DISTAL-atlas, while the M1 mask from the Harvard-Oxford Atlas. Streamline probability maps were determined using FMRIB Software Library (FSL) probabilistic tractography toolbox (FDT). The normative VIMM1 tract map was co-registered and warped onto each subject's preoperative MRI using Advanced Normalization Tools (ANTs). This workflow was based on a previously published method. 4) Ablations ("lesions") were manually segmented from immediate postoperative T2 weighted-MRI and co-registered with the patient-fit VIMM1 tract maps, again using ANTs (Fig.2). 5) Normative tractography coefficients (NTC) were calculated for each subject as the number of target voxels overlapping with HCP group-averaged streamline probability map. 6) "Better" and "Same" groups were combined to form a single "better/same" group, for performing two-group comparison testing with the "worse" group. 7) Optimal between-QoL-group segmented lesion volume thresholds were statistically identified based on bootstrapped maximization of Youden's Index (YI). Univariate logistic regression assessed predictiveness of lesion volume and NTC in predicting QoL.

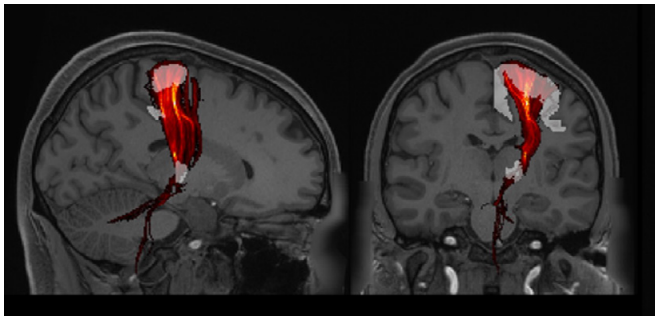

Figure 1. VIM—M1 normative tractography map fit to a patient by having been warped onto patient's own pre-operative T1-MRI. Tract (red),VIM seed-mask (grey within thalamus); M1 target-mask (grey in cortex).

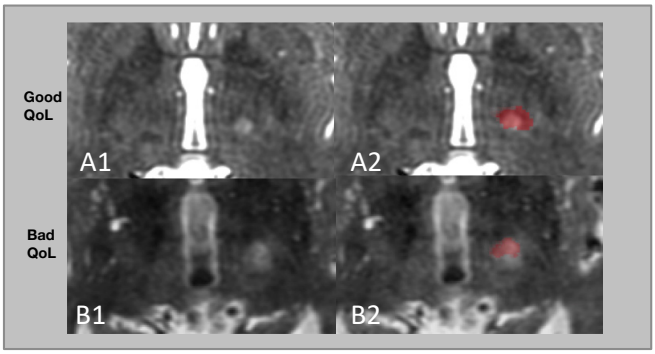

Figure 2. Good QoL patient (A) versus Worse QoL patient (B), both with similar tremor improvement. A's lesion (87.5 mm3) is smaller than B's (163.48 mm3). Patient-fit VIM—M1 normative tract overlapped (red) with differential overlap with lesion.

8) The "worse" versus "better/same" groups were compared for each of the variables of (i) Lesion-volume, and (ii) NTC (Mann-Whitney).

Results: 37 patients (59.7%) reported "better" QoL; 15 (24.2%) had "same" QoL; 10 (16.1%) reported "worse" QoL at latest follow-up (range 3-38mo; median 4.5mo). All three groups had substantial tremor reduction which did not differ between the three groups (p=0.45076), therefore tremor reduction alone failed to predict QoL outcomes (Fig.3). The "worse" versus "better/same" QoL groups differed when comparing each variable: (i) lesion volume (U=109, p=0.0040), and (ii) lesion:VIM—M1 NTC (U=383, p=0.019) (Fig.4). Cutoff points for each variable were calculated from ROC-curve points that maximized YI (balancing sensitivity & specificity). The following thresholds correlated with better QoL outcomes: Lesion-volume <143mm (AUC 0.79, YI 0.41, Sensitivity 60%, Specificity 81%); VIM—M1 NTC>895.4 (AUC 0.77, YI 0.48, Sensitivity 69%, Specificity 80%).

Conclusions: We observe that tremor reduction alone failed to predict QoL improvement after thalamotomy. The lesions that optimized QoL were smaller lesions that highly overlapped with patient-fit VIM—M1 normative tractography. Beyond tremor-improvement alone, QoL post-MRgFUS for ET should be emphasized. Utilizing patient-specific thalamic-mapping techniques (i.e. patient-fit VIM—M1 normative-tractography) during MRgFUS planning could help optimize QoL outcomes. Further validation of this technique may also eventually facilitate patient-asleep MRgFUS, enabling more comfortable and efficient procedures while optimizing outcomes.

Acknowledgment/Funding Sources: FUS Foundation Grant (McNab/Buch)

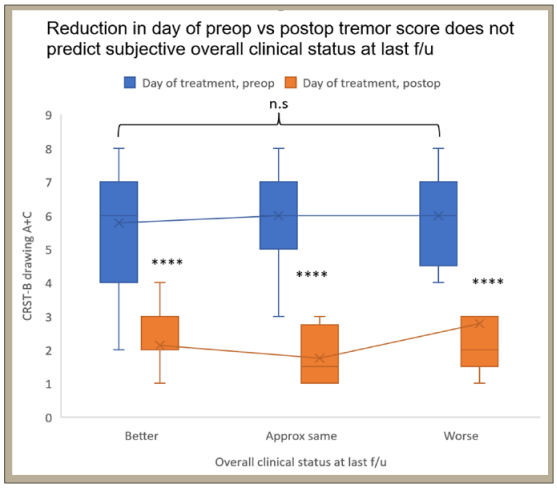

Figure 3. Comparison of QoL groups by change in tremor-scores on CRST for the treated side immediately pre-vs-post MRgFUS thalamotomy. All three groups had substantial tremor reduction, which did not differ between the groups (p=0.45076; Kruskal-Wallis).

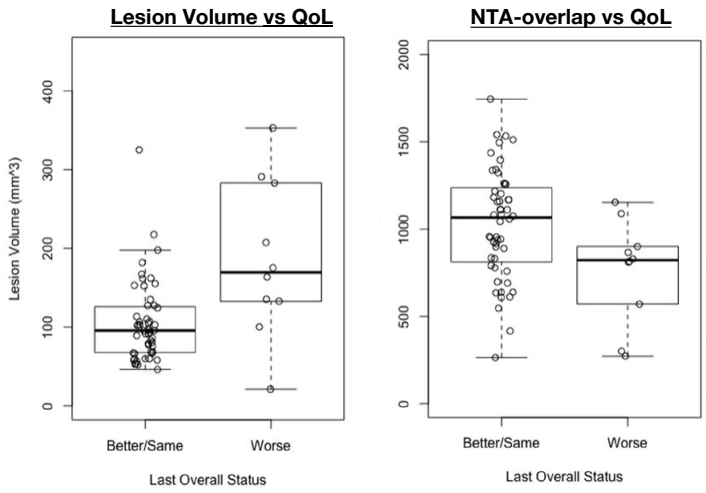

Figure 4. Comparing QoL to lesion volume and normative tract coefficient "NTC". The two groups were significantly different for each variable: (a) Lesion volume (p=0.0040), and (b) lesion:VIM—M1 NTC (p=0.019).

MOV-08

Topic: Movement Disorders
Presentation Type: Oral

Results from the Italian Group for Focused Ultrasounds in Neurosciences

Cesare Gagliardo[1], Federico Bruno[2], Giuseppe Kenneth Ricciardi[3], Silvia Marino[4], Marco D'Amelio[1], Alessia Catalucci[2], Patrizia Sucapane[2], Michele Longhi[3], Maria Grazia Bruzzone[5], Carmelo Anfuso[6], Domenico Gerardo Iacopino[1], Maurizio Marrale[7], Francesca Pistoia[8], Stefano Tamburin[9], Tommaso Bovi[3], Elisa F. Ciceri[5], Francesco DiMeco[10,11], Giuseppe Di Lorenzo[6], Domenico La Torre[12], Alessandro Napoli[13], Carlo Catalano[13], Roberto Eleopra[5]

[1]University of Palermo, Palermo, Palermo, Italy
[2]San Salvatore Hospital, L'Aquila, L'Aquila, Italy
[3]University-Hospital of Verona, Verona, Verona, Italy
[4]IRCCS Centro Neurolesi, Messina, Messina, Italy
[5]Fondazione IRCCS Istituto Neurologico Carlo Besta, Milan, Italy
[6]IRCCS Centro Neurolesi "Bonino-Pulejo", Messina, Messina, Italy
[7] Emilio Segrè, Palermo, Palermo, Italy
[8] University of L'Aquila, L'Aquila, L'Aquila, Italy
[9]University of Verona, Verona, Verona, Italy
[10]Fondazione IRCCS Istituto Neurologico Carlo Besta, Milan, Italy
[11]Johns Hopkins Medical School, Baltimore, MD, USA
[12]University of Catanzaro, Catanzaro, Catanzaro, Italy
[13]Sapienza University of Rome, Roma, Roma, Italy

Background: Magnetic resonance-guided focused ultrasound (MRgFUS) is one of the emerging non-invasive technologies offering both image guidance and thermal monitoring for new therapeutical approaches. In recent years transcranial application of this technology (transcranial MRgFUS, tcMRgFUS) is starting to heavily impact the neuroscience field for the treatment of a growing number of neurological disorders. In Italy, in the past eight years, five different clinical centers have invested in this rapidly expanding technology in both clinical care and research scenarios.

Materials and Methods: Following the installation of the world-first tcMRgFUS system ever integrated with a 1.5T scanner in the University-Hospital of Palermo in 2015 thanks to a key collaboration with the University of Rome "La Sapienza", two more systems have been installed and integrated with 3T MRI scanners in January 2018 in Verona and in February 2018 in L'Aquila respectively, and lastly, in 2019, two more 1.5T-integrated systems have been installed in Besta Institute of Milan and Bonino-Pulejo Institute of Messina. All the Italian centers are equipped with a tcMRgFUS system that consists of a hemispheric 1024-element phased-array transducer operating at 650kHz (INSIGHTEC ExAblate 4000 - Type 1). The authors present the results of tcMRgFUS procedures performed in Italy between Q1-2015 and Q2-2022 in patients with essential tremor (ET), tremor-dominant unilateral Parkinson Disease (PD), neuropathic pain (NP) and other clinical conditions not yet included in the current CE mark of conformity. The severity (mild, moderate or severe), number and kind (i.e.: paresthesia/numbness, taste, gait, dysmetria, weakness, dysarthria, disequilibrium sensation, other) of adverse events has been collected as well as the number of aborted or failed procedures.

Results: Although significantly affected by the more than two-year long COVID-19 pandemic, a total of 510 treatments have been carried out in Italy to date (n= 496 Vim thalamotomies for tremor, n=9 centrolateral thalamotomies for NP, n=5 GPi pallidotomies for dyskinesia in PD). Most of the treatments were performed on patients with ET (n=291) and tremor-dominant PD (n=181). The remaining treatments were performed on patients with dystonic tremor (n=15), NP (n=9), dyskinesias in PD (n=5) and a few other clinical conditions (n=9) such as vascular tremor, essential tremor in comorbidity with multiple sclerosis, tremor in multiple sclerosis, hemochromatosis-associated Parkinsonism, cerebellar tremor and spinocerebellar ataxia (type 2). The total percentage of relapse was 6,7% (3,8% for ET, 11% for PD and 6,7% for dystonic tremor and 22,2% for other tremors). No relapses were reported for NP and dyskinesia in PD. The percentage of aborted or failed procedures was 3,5% (n=18). No severe permanent adverse events were reported. The percentage of patients with mild or moderate adverse events, with no restrictions in daily life activities, was 14,5% in particular 13,4% for ET, 16% for PD and 66,6% for other tremors. No permanent

adverse events were reported for patients with NP, dystonic tremor and dyskinesias in PD. Six retreatments after symptoms relapse were reported. Three sites performed staged (after at least 6m from the first procedure) bilateral Vim thalamotomy in 12 patients with ET.

Conclusions: These results, even considering the certainly particular recent years due to the pandemic and the physiological learning curve to which all teams dealing with this emerging technology had necessarily to face, confirm the high safety profile and high success rate of tcMRgFUS procedures for the treatments of several neurological disorders. These results, even if influenced by the methodological modifications of FUS Neuro procedures over the last few years, nevertheless confirm the excellent results that can be obtained thanks to teamwork which, in all Italian centers, involves neuroscientists with complementary skills such as neurologists, neurosurgeons, neuroradiologists and physicists.

Acknowledgment/Funding Sources: Installation of the FUS equipment in Palermo was funded by "Programma Operativo Nazionale 2007–3013" (PONa3_00011). Research leading to the results from Palermo funded by the Italian Ministry of Health (Ricerca Finalizzata 2016 grant no. GR-2016-02364526)

MOV-09

Topic: Movement Disorders

Presentation Type: Oral

Thalamic Parcellation for Target Identification in Trans-cranial MR-Guided Focused UltraSound Thalamotomies: A Retrospective Probabilistic Tractography Study in Patients with Essential Tremor

Cesare Gagliardo, Giorgio Collura, Marco D'Amelio, Domenico Gerardo Iacopino, Massimo Midiri, Maurizio Marrale

University of Palermo, Palermo, Italy

Background: Trans-cranial MR-guided Focused UltraSound (tcMRgFUS) allows a neurofunctional exploration of the thalamus to confirm and optimize the target before inducing a permanent brain lesion. However, the choice of the target is based on atlas-based stereotactic coordinates that do not take into account the anatomical variability of each single patient. Thus, the final identification of the target is based on the patient's feedback during lower power sonications that can be time consuming in some cases, risking to lengthen the procedural times excessively. The aim of this work is to retrospectively evaluate the possible role of thalamic parcellation based on probabilistic tractography algorithm for the identification of the intermediate ventral nucleus (Vim) in patients with essential tremor (ET) underwent unilateral tcMRgFUS thalamotomy.

Materials and Methods: Screening brain MRI scan of twenty-seven ET patients (21♀, 6♂) was used for this retrospective study. Dataset were acquired with a 1.5T MR scanner (GE Signa HDxt) equipped with an 8-channel phased-array head coil. Imaging protocol included morphological (3D-BRAVO T1w; 1mm isotropic resolution) and ultrastructural (Diffusion Tensor Imaging, DTI; 2D echo-planar-imaging 3mm isotropic resolution, b=1000s♀mm-2, 64 gradient directions) pulse sequences. FreeSurfer workflow was used to segment both the cortical and deep gray matter from 3D-BRAVO T1w sequence. The segmented cerebral areas were then used as seed for a probabilistic tractography algorithm (FSL's probtractX) aimed at representing the cortical projections to and from the thalamus with particular reference to the primary (M1), the supplementary motor areas (SMA), the premotor cortex (BA6) and primary somatosensory cortex (S1). The distance from the maximum probability point (Tract_max) and the distance from the center of gravity point (Tract_COG) within the probability map were calculated with a 25% threshold and then compared with standard (atlas-based) coordinates and target coordinates after neurofunctional exploration (corresponding to the spot where the tcMRgFUS lesion was placed).

Results: In all cases it was possible to represent the major groups of thalamic nuclei that receive from or project towards brain cortex analyzing MR dataset achieved with a 1.5T scanner with particular reference to the above-named eloquent areas. We also found preliminary evidence of connectivity-based inter-individual variability of thalamic nuclei if compared to atlas-based coordinates. Moreover, it was possible to identify a good overlap between the thalamic parcellation maps thus obtained (with particular reference to the Vim nucleus) and the lesions induced by tcMRgFUS.

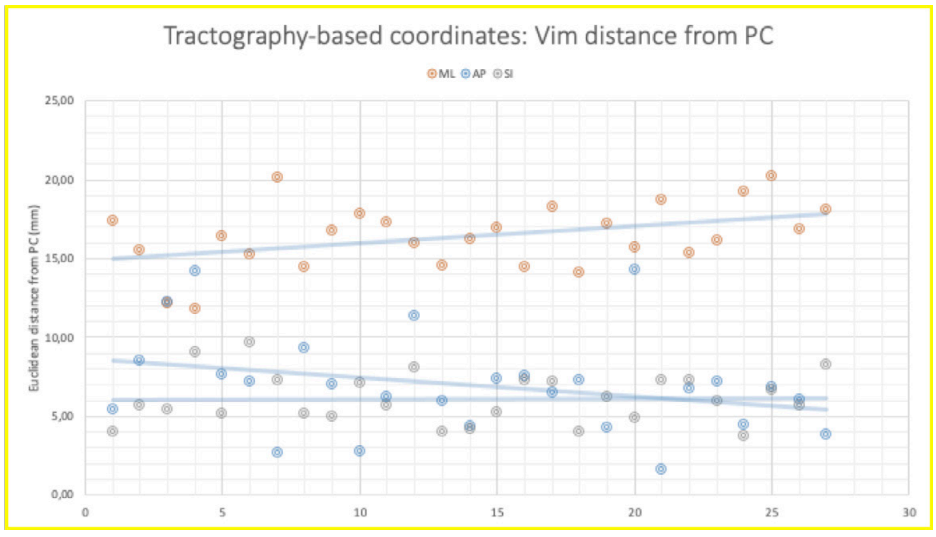

Figure 1. Tractography-based coordinates: Vim distance from the posterior commissure (PC)

Conclusions: These preliminary results are very encouraging. Even if the requested pre- and post-processing pipeline behind such an innovative approach are still extremely complex and time consuming, the use of such a technique could result very helpful during tcMRgFUS treatment target optimization, especially in those cases where the optimal treatment target does not perfectly match conventional stereotactic coordinates.

Acknowledgment/Funding Sources: The installation of the tcMRgFUS equipment used in this work was funded by the Italian Ministry of Education, University and Research (MIUR) within the project "Programma Operativo Nazionale 2007-3013" (PONa3_00011; Project Leader: Prof. Carlo Catalano).

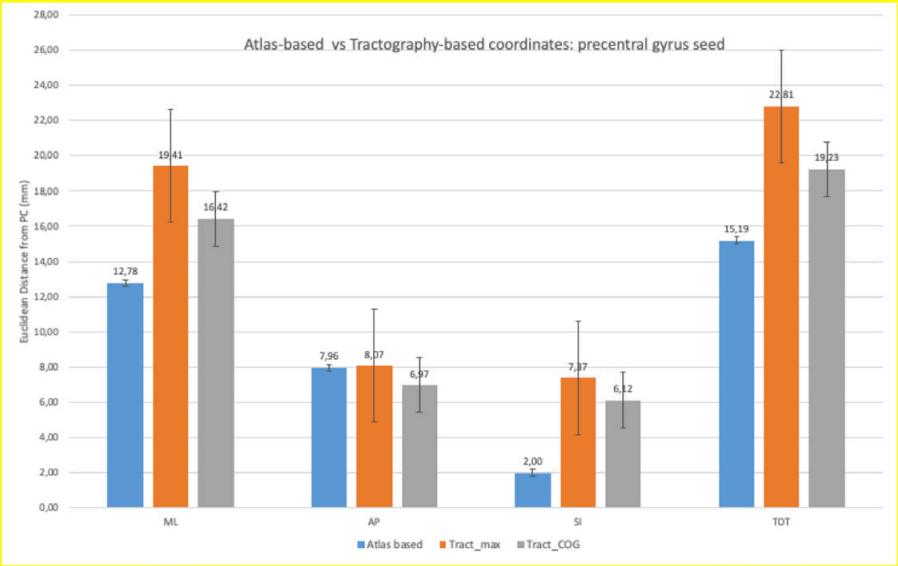

Figure 2. Atlas-based vs Tractography-based coordinates:precentral gyrus (M1) seed to the thalamus

MOV-11

Topic: Movement Disorders
Presentation Type: Oral

MRgFUS Thalamotomy Allows Sparing Dopaminergic Medication in Early-Stage Tremor-Dominant Parkinson's Disease: A Case-Control Pilot Study

Nico Golfre' Andreasi, Roberto Cilia, Luigi M. Romito, Salvatore Bonvegna, Giulia G. Straccia, Antonio E. Elia, Alessio Novelli, Giovanni Tringali, Giuseppe Massina, Vincenzo Levi, Grazia Devigili, Sara Rinaldo, Valentina Gasparini, Marina Grisoli, Mario Stanziano, Francesco Ghielmetti, Sara Prioni, Elisa Bocchi, Paolo Amami, Sylvie H. Piacentini, Elisa F. Ciceri, Maria Grazia Bruzzone, Roberto Eleopra

Fondazione IRCCS Istituto Neurologico Carlo Besta, Milan, Italy

Background: MRgFUS VIM thalamotomy is a safe and effective procedure for drug-resistant tremor in Parkinson's Disease (PD) patients. Tremor in PD patients may be difficult to treat and even high dosages of dopaminergic medication may provide little or no benefit. Dopaminergic medications are associated to the long term development of motor fluctuations and dyskinesias and increase the risk of impulse control disorders. To our knowledge, no study so far has specifically investigated how MRgFUS VIM thalamotomy may influence the following dopaminergic treatment. Our hypothesis was that MRgFUS VIM thalamotomy performed in early-stage tremor-dominant PD patients could be prospectively associated to a lower dopaminergic therapy daily dosage compared with a matched PD control population on standard medical therapy.

Materials and Methods: We included consecutive patients with early-stage tremor-dominant idiopathic PD who were evaluated in our outpatient clinic between 01 February 2019 and 31 March 2021. Patients who subsequently underwent MRgFUS VIM thalamotomy (PD-FUS) were matched by sex, age and disease duration in a 1:2 ratio with patients treated with only standard dopaminergic therapy (PD-ODT). We collected demographical and clinical [mainly levodopa-equivalent daily dose (LEDD), motor symptoms evaluation with the Movement Disorder Society Unified Parkinson's Disease Rating Scale part III (MDS-UPDRS-III) and adverse events] data at baseline and after 6- and 12-months follow-up.

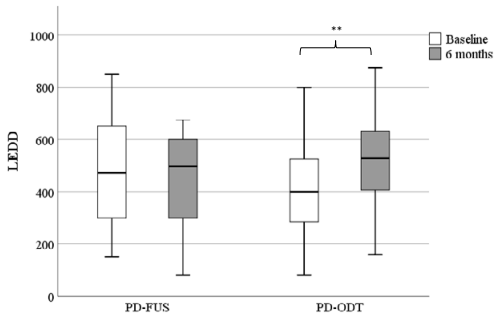

Figure 1. Change in LEDD between baseline and 6-months follow-up in PD-FUS (n=10) and PD-ODT (n=20) patients. **, p<0.01

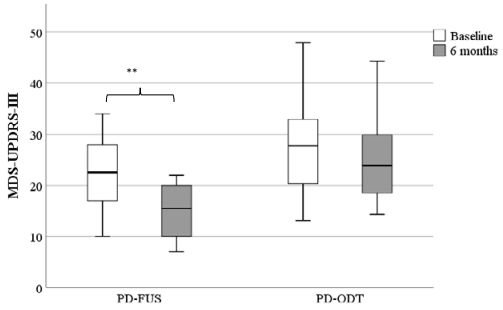

Figure 2. Change in MDS-UPDRS-III between baseline and 6-months follow-up in PD-FUS (n=10) and PD-ODT (n=20) patients.

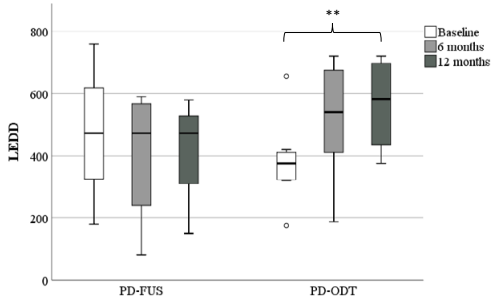

Figure 3. Change in LEDD at baseline, 6 and 12-months in PD-FUS (n=4) and PD-ODT (n=8) patients with 12-months follow-up. **, p<0.01

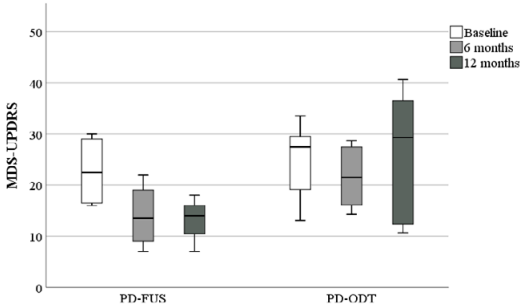

Figure 4. Change in MDS-UPDRS-III at baseline, 6 and 12-months in PD-FUS (n=4) and PD-ODT (n=8) patients with 12-months follow-up.

Results: We included 10 patients in the PD-FUS group and 20 patients in the PD-ODT group. We found a significant increase in total LEDD in the PD-ODT group compared to the PD-FUS group. In both groups, there was an improvement in the total MDS-UPDRS-III, but it was significantly more consistent in the PD-FUS group, mainly driven by the substantial improvement in tremor subscores. No serious adverse events were observed during the study and no statistically significant differences were found in the adverse effects profile between the two groups.

Conclusions: Our findings suggest that MRgFUS VIM thalamotomy performed in early-stage tremor-dominant PD patients allows to maintain low daily dosage of oral dopaminergic medications along with a good control of tremor. Prospective studies with larger cohorts and longer follow-up are needed to confirm these findings and to understand if this treatment may reduce the incidence of adverse effects and long-term motor complications of dopaminergic therapy.

MOV-12

Topic: Movement Disorders
Presentation Type: Oral

Volumetric and Topographic Analysis of Lesion and Edema Formation in MR-Guided Focused Ultrasound Thalamotomy for Essential Tremor Treatment: Relationships with Sonication Parameters and Adverse Events

Patrick R. Ng[1], Fardad Behzadi[2], Alfredo Morales Pinzon[3], Michele Cavallari[2], Andrzej Marciniak[4], Grégory Bliault[5], Kezia Irene[1], Clément Nicolas--Graffard[2], Sarah Blitz[1], Melissa M. Chua[2], David J. Segar[2], Bruno Madore[2], Matthew N. DeSalvo[2], Thomas Tourdias[6], Manojkumar Saranathan[7], Phillip J. White[2], Nathan McDannold[2], Rees Cosgrove[2], Charles R. Guttmann[2]

[1]Harvard Medical School, Boston, MA, USA
[2]Brigham and Women's Hospital, Boston, MA, USA
[3]Brigham and Women's Hospital & Harvard Medical School, Boston, MA, USA
[4]NA, Zielona Gora, lubuskie, Poland
[5]NA, Lyon, Rhône, France
[6]CHU de Bordeaux, Bordeaux, Gironde, France
[7]University of Massachusetts Chan Medical School, Worcester, MA, USA

Background: Associations between sonication parameters, lesion/edema volumes, and clinical outcomes have yielded important insights for MR-guided focused ultrasound (MRgFUS) thalamotomy for essential tremor (ET). Prior volumetric estimations assumed an ellipsoid lesion and did not account for irregular features. To enable voxel-based lesion-symptom mapping, we have reassessed these relationships with more accurate topographical segmentation of lesion and edema.

Materials and Methods: Lesion and edema were outlined on T2-weighted 3T MRI (24h post MRgFUS thalamotomy) in 125 ET patients using standardized, semi-automated segmentation workflows in our SPINE web-based laboratory. Lesion and edema volumes were aggregated into anatomical frequency maps, which were overlaid on human brain atlas images.

Results: Lesion volume was 364.32 mm3 +/- 142.21 mm3 (mean +/- SD). Edema volume was 1696.29 mm3 +/- 954.11 mm3. Lesion and edema volumes were significantly correlated. Lesion volume had a significant positive correlation with skull density ratio, thermal dose, and maximum temperature and a significant negative correlation with number of sonications. Edema volume had a significant positive correlation with maximum power. Median lesion volume was significantly larger for patients with acute dysarthria (430.77 mm3 vs. 322.68 mm3) and acute imbalance (400.81 mm3 vs. 309.02 mm3). Median edema volume was significantly larger for patients with acute imbalance (1626.83 mm3 vs. 1479.22 mm3). Anatomical frequency maps provided striking correlations between adverse events and involvement of critical structures, such as the internal capsule and adjacent thalamic nuclei (Figure 1).

Conclusions: High-resolution voxel-based volumetric analysis of lesion and edema in MRgFUS enabled correlation of lesion and edema volumes with sonication parameters and acute adverse events. Anatomical frequency maps provide striking correlations between adverse events and involvement of critical adjacent structures.

Acknowledgment/Funding Sources: This work is funded by the Focused Ultrasound Foundation

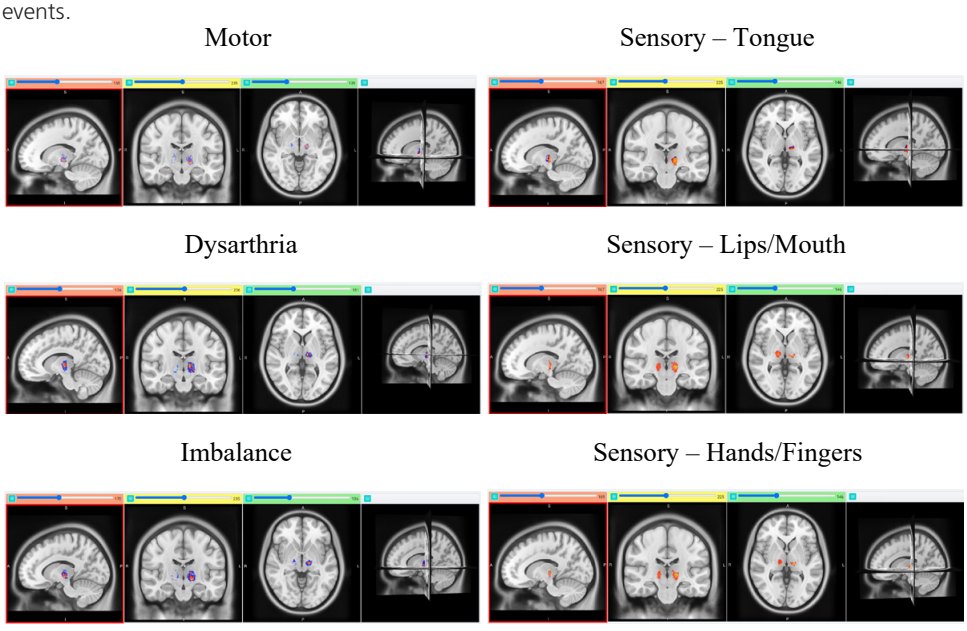

Figure 1. Frequency maps of lesion topology differences between patients with and without select acute adverse events.

MOV-13

Topic: Movement Disorders
Presentation Type: Oral

Preliminary Clinical Results of Magnetic Resonance Guided Focused Ultrasound Thalamotomy for Essential Tremor with Low Skull Density Ratio

Sakae Hino[1], Futaba Maki[1], Toshio Yamaguchi[2], Masayuki Nakano[1], Mayumi Kaburagi[1], Masahito Takasaki[1], Ken Iijima[1], Hirokazu Iwamuro[1], Yasuhiro Hasegawa[1], Jinichi Sasanuma[1], Yoshihisa Yamano[3]

[1]Shin-Yurigaoka General Hospital, Kawasaki, Kanagawa, Japan
[2]International Academia for Focused Ultrasound Therapy, Kawasaki, Japan, Kanagawa, Japan
[3]St. Marianna University School of Medicine, Kawasaki, Kanagawa, Japan

Background: Magnetic resonance guided focused ultrasound thalamotomy (MRgFUS) is generally considered to be clinically effective in patients with a skull density ratio (SDR) of 0.4 or higher because lesion is created with the elevated temperature in the targeted site. In Japan, however, there are many cases with relatively lower SDR, and therefore due to the failure of elevated temperature, appropriate lesioning may not be created, resulting in inadequate therapeutic effects. The purpose of this study is to describe our preliminary results of MRgFUS in patients with an SDR of 0.35 or less and discuss the issues in this difficult-to-perform group for MRgFUS.

Materials and Methods: Among 100 patients with essential tremor who underwent MRgFUS from June 2019 to March 2022, 21 consecutive patients (21%) with an SDR of 0.35 or less were included in this retrospective study. There were 15 male patients whose mean age at the operation of FUS was 67 years and mean disease duration was 23.5 years. The VIM target of MRgFUS was determined anterior to PC at the point of one-third (1/3) of the length of AC-PC line minus 1.5 mm from the PC, 12 mm lateral to the third ventricle, and 1.5-2 mm above the AC-PC plane. In the latter cases, the anteroposterior coordinate was based on one-fourth (1/4) of the length of AC-PC line and, in addition, the posterior border of the pyramidal tract as its MR imaging landmark was applied for the personal difference (Figure 1). To determine clinical effectiveness, the overall score of the clinical rating scale of tremor (CRST) and the CRST Part B score on the treated side were evaluated. In addition, the distance of pen tip movement needed to draw 150 mm was calculated using movement analysis software in two dimensions. The evaluation points were at baseline, 1 week and 3 months after FUS.

Results: Lesioning was created at VIM thalamus in 18 patients (86%) with the elevated temperature of 49 degrees or higher (Figure 2,3). However, in 3 patients below 47 degrees of temperature, lesioning was not achieved in MR imaging one day after MRgFUS (Figure 4). The mean total score of CRST was 37 at baseline, 22.6 at 1 week and 22.8 at 3 months post-operatively. Meanwhile, the mean CRST Part B score on the treated side was 8.5 at baseline, 3.3 at 1 week and 4.1 at 3 months post-operatively. The average distance of pen tip movement needed to draw 150 mm was 246 mm at baseline, 161.4 mm at 1 week and 224 mm at 3 months post-operatively. At 1 week post-operatively, 11 patients (52.4%) demonstrated an improvement of 75% or more; 4 patients (19%) showed an improvement of 51-74%, and 6 patients (28.6%) only achieved an improvement of 50% or less. At 3 months post-operatively, 4 patients presented recurrence. Mild adverse events included headache, numbness in the fingertips, facial edema, and one patient remained numbness in the fingertips at 3 months post-operatively. No patients with moderate or severe adverse events were observed. We had several difficult cases to evaluate, including tremor was induced in the other evaluation methods rather than writing, or strong tremor was not seen in writing in the absence of load, but was exacerbated by tension.

Conclusions: Because approximately 70 % of our patients showed the more than 50 % of improvement ratio even with low SDR in our preliminary

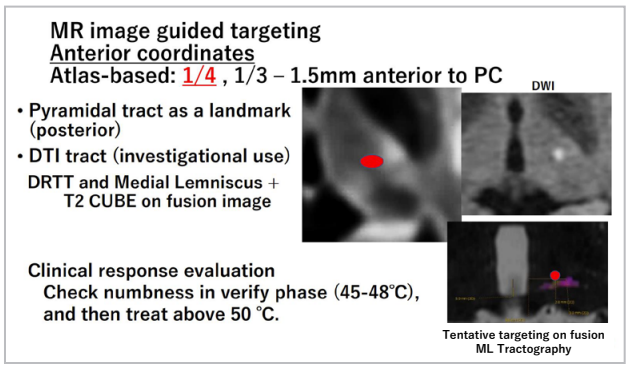

Figure 1. MR image guided targeting Anterior coordinates

study, low SDR alone should not be considered as one of absolute exclusion criteria. The issues to be solved may be addressed, 1) what kind of objective evaluations are appropriate for variable task-induced tremor specifically in MRgFUS thalamotomy, 2) which patients with lower SDR achieved lesion creation with high temperature and 3) how we should perform MRgFUS in these difficult patients with low SDR, including location, volume and strategy of temperature elevation.

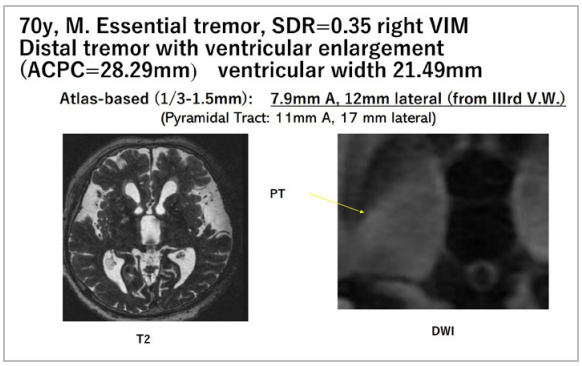

Figure 2. Effective case with low SDR 1

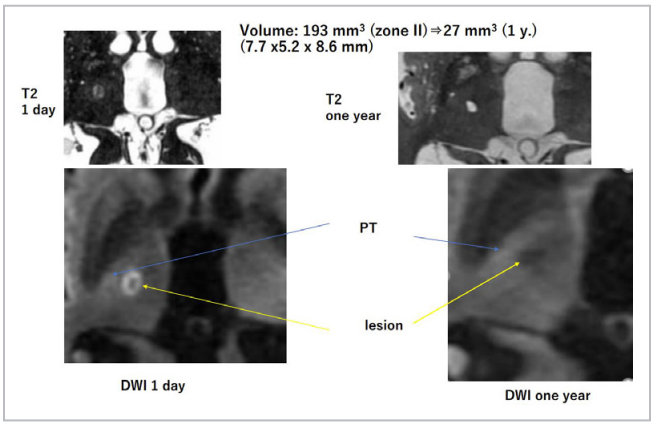

Figure 3. Effective case with low SDR 2

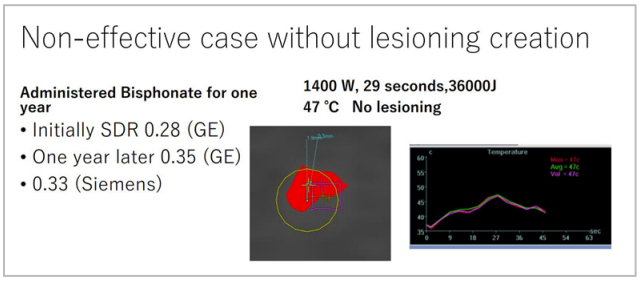

Figure 4. Non-effective case without lesioning creation

MOV-14

Topic: Movement Disorders

Presentation Type: Oral

Systematic Review of Cost Effectiveness Analyses of Magnetic Resonance Guided Focused Ultrasound vs Deep Brain Stimulation for Essential Tremor and Parkinson's Disease

Shuo Huang, Luisa Franzini

University of Maryland School of Public Health, College Park, MD, USA

Background: Medication-refractory essential tremor (ET) and Parkinson's disease are treated with medical interventions including both magnetic resonance guided focused ultrasound (MRgFUS) and deep brain stimulation (DBS). Cost effectiveness analysis could be used by payers and providers comparing the two interventions. Health economic evaluations reporting incremental cost effectiveness ratios (ICERs) could provide one direct comparison between MRgFUS and DBS. We describe the state of the literature on cost effectiveness analyses of MRgFUS versus DBS for medication-refractory, disabling, unilateral tremor and for Parkinson's disease.

Materials and Methods: We searched PubMed and Google Scholar using the search criteria: essential tremor, Parkinson's + MRgFUS + cost effectiveness analysis, cost utility analysis, ICER. Articles not related to cost effectiveness analyses, not original research, or duplicates were excluded. We extracted country of analysis, medical condition, analysis type, time horizon, analysis method, source for cost data, source for effect data, effect measure, and cost effectiveness measure. We also recorded the perspective used based on what costs and effects each study actually utilized rather than the perspective it claimed to utilize. We extracted and converted ICERs into 2021 US dollars (USD), using same-year currency exchange and year-over-year inflation.

Results: Our search returned 26 articles, three were retained. All studies were cost utility studies from the payer perspective. One study focused on Parkinson's disease, two on essential tremor. All three studies used modeled data, and none collected patient outcomes or cost data directly. The cost (2021 USD) of MRgFUS ranged from $11,860 to $23,732 and the cost of DBS ranged from $18,841 to $51,982. For ET, the ICER of DBS vs MRgFUS ranged from $111,109 per QALY gained to being dominated by MRgFUS. For Parkinson's disease, the ICER of DBS vs MRgFUS was $45,165 per QALY gained.

Conclusions: Research outputs on the cost effectiveness of MRgFUS vs DBS are still sparse. Future studies could focus on collecting cost and patient outcomes more directly to reduce sensitive assumptions.

Acknowledgment/Funding Sources: Focused Ultrasound Foundation

MOV-15

Topic: Movement Disorders
Presentation Type: Oral

The Cost Effectiveness of Unilateral Magnetic Resonance Guided Focused Ultrasound in Comparison to Unilateral Deep Brain Stimulation for the Treatment of Medically Refractory Essential Tremor in England

Ayesha Jameel[1], Anne Meiwald[2], peter bain[1], neekhil patel[3], Sena Akgun[4], dipankar nandi[5], brynmor jones, elisabeth adams, wladyslaw gedroyc[5]

[1]Imperial College, London, United Kingdom
[2]Aquarius Population Health, London, United Kingdom
[3]NHS, London, United Kingdom
[4]Imperial College NHS Trust, Rome, Italy
[5]Imperial College NHS Trust, London, United Kingdom

Background: Essential Tremor (ET) is the most common movement disorder affecting approximately 1 million in the United Kingdom causing considerable societal impact affecting patients, carers and the wider health service. Medical treatment has mixed efficacy with approximately 25%-55% of ET medication refractory. Deep Brain Stimulation (DBS), is a proven neurosurgical treatment the risks of surgery and anaesthesia mean some patients are ineligible. Magnetic Resonance Guided Focused Ultrasound (MRgFUS) is an emerging non-invasive technique to treat tremors. MRgFUS causes tremor suppression by thermal ablation of tremor-sensitive brain tissue. MRgFUS is performed without general anaesthesia and has been proven to be a safe and clinically effective treatment by several international clinical trials. The introduction of MRgFUS as a widely available ET treatment in the UK is currently undergoing the necessary stages of regulation and approval. However, to date, no cost-effectiveness study has been performed in the UK to assess MRgFUS in the treatment of Essential Tremor.

Materials and Methods: A Markov model was used to assess two sub-populations of mrET- those eligible and those ineligible for neurosurgery - in the context specific to England and its healthcare system. For those eligible for neurosurgery, MRgFUS was compared to the current standard treatment DBS. For those ineligible for neurosurgery, MRgFUS was compared to treatment with medication alone. The model calculated the Incremental Cost-Effectiveness Ratio (ICER) with appropriate sensitivity and scenario analyses.

Results: For those eligible for neurosurgery: In the model base case the MRgFUS strategy was economically dominant compared to DBS, as it was less costly with 53 additional QALYs over the 5-year time horizon. For those eligible for neurosurgery: In the model base case, MRgFUS cost £22 million more than medication alone but yielded 1,095 additional QALYs, producing an ICER of £20,718 per quality-adjusted life-year gained. This ICER of £20,718 per QALY falls within the NICE willingness to pay threshold of 20,000-30,000 demonstrating the cost-effectiveness profile of MRgFUS.

Conclusions: This study demonstrates the favourable cost-effectiveness profile of MRgFUS for the treatment of mrET in England; in both sub-populations assessed MRgFUS is

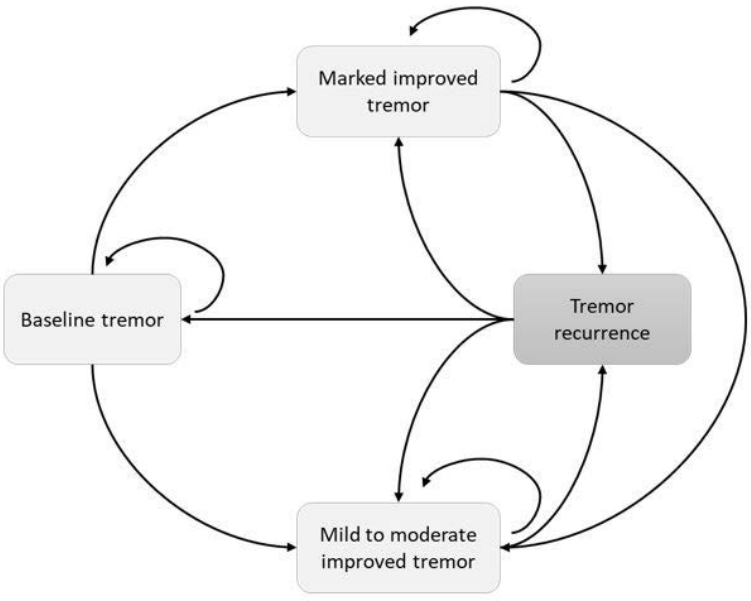

***Figure 1:** Markov model outlining the health states patients can move into post-procedure (DBS and MRgFUS). Grey boxes represent model health states with dark grey representing a temporary health state. Patients in the DBS strategy follow the same clinical pathway and model structure as those in the MRgFUS strategy.*

cost-effective (patients who are suitable and those who are not suitable for DBS. As the first European study, the outcomes demonstrated here, provide a basis for future commissioning of brain MRgFUS treatments in the UK, Europe and worldwide (including North America)

Acknowledgment/Funding Sources: Aquarius Population Health

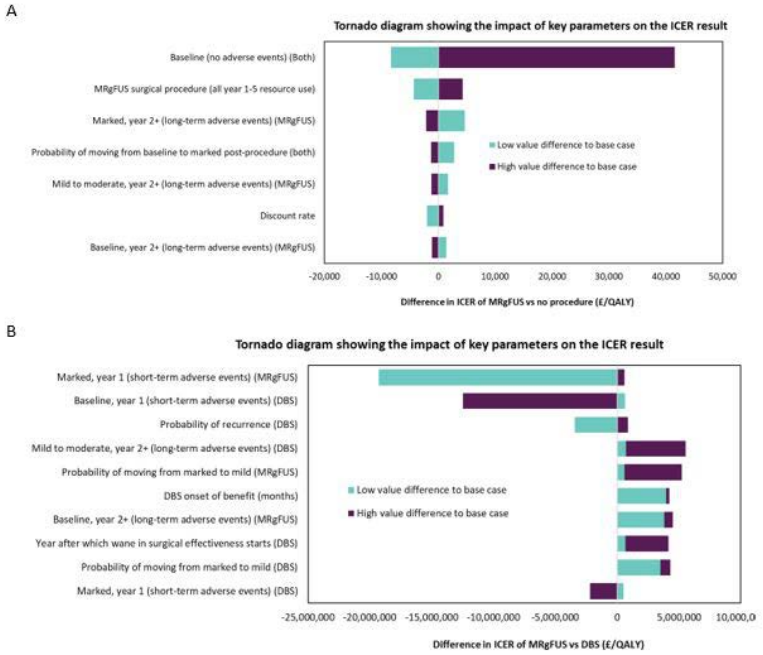

Figure 2: Results of the deterministic sensitivity analysis for A) MRgFUS vs No Procedure B) MRgFUS vs DBS: the impact on the ICER of varying each parameter individually to the high and low values in a one-way sensitivity analysis. (DBS, deep brain stimulation; MRgFUS, magnetic resonance-guided focused ultrasound; ICER, incremental cost-effectiveness ratio)

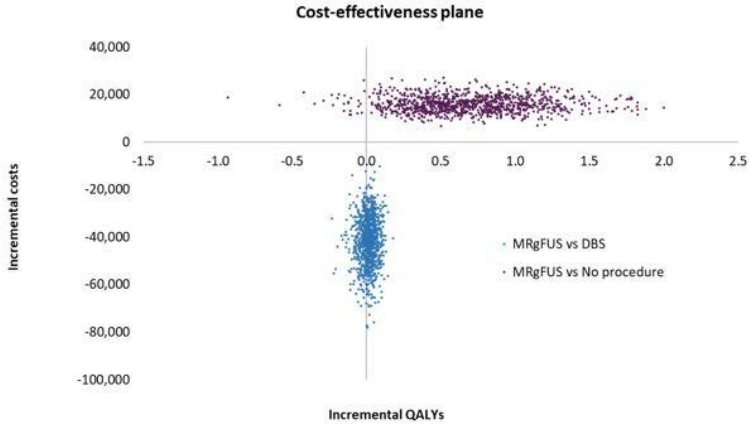

Figure 3: Result of probabilistic analysis for MRgFUS vs No Procedure and MRgFUS vs DBS: based on 1,000 iterations illustrating the distribution of the ICERs DBS, deep brain stimulation; MRgFUS, magnetic resonance-guided focused ultrasound; ICER, incremental cost-effectiveness ratio; QALYs, quality-adjusted life years

MOV-16-YI

Topic: Movement Disorders
Presentation Type: Oral

The Evolution of Thalamic Ventral Intermediate Nucleus Targeting in MRgFUS Thalamotomy for Tremor, an International Perspective 2019 to 2021

Ayesha Jameel[1], Sena Akgun[2], nada yousif[3], joely smith[4], brynmor jones, peter bain[1], dipankar nandi[4], wladyslaw gedroyc[4]

[1]Imperial College, London, United Kingdom
[2]Imperial College NHS Trust, Rome, Italy
[3]University of Hertforshire, London, United Kingdom
[4]Imperial College NHS Trust, London, United Kingdom

Background: Ventral Intermediate Nucleus (VIM) is the premier site for MRgFUS Thalamotomy in the treatment of Essential Tremor. VIM ablation has been used also for Deep Brain Stimulation, Gamma Knife and Radiofrequency ablation. However, targeting within the thalamus has always been a topic of debate, due to historical discussion on thalamic nucleic anatomy. The proximity of VIM to the Ventral Caudalis Nucleus (VC) and Internal Capsule (IC) means inaccurate targeting can lead to both sensory and motor adverse effects. As thalamic nuclei cannot be directly visualised on current clinical scanners (1.5T and 3T), anatomical landmarks such as the anterior commissure-posterior line (AC-PC) and the IC are often used to target the VIM. However there is currently no consensus, and as more centres adopt MRgFUS internationally, the methods of targeting VIM are yet unexplored. This study aims to ascertain any trend in VIM targeting approaches internationally between 2019 and 2021.

Materials and Methods: All 39 MRgFUS centres from Insightec?s 2019 international database who perform thalamotomies for tremor were invited to participate by sharing their VIM targeting approach (VIM-TA) in 2019 and 2021. Each centre was contacted at least 3 times. Results were analysed with regard to anatomical landmarks and use of tractography; and change in approach. Each VIM-TA was mapped in relation to the mid-commissural point (MCP) onto a 3D model of the thalamus based on the Schaltenbrand-Wahren Atlas.

Results: 30 centres participated across the study period; 26 centres reported 2019 VIM-TA, 23 centres provided 2021 VIM-TA, and 23 centres shared both. In 2019, 96.2% of centres (n=25) and in 2021 95.7% of centres (n=22) based targeting on anatomical landmarks rather than tractography. Although there was a definite trend to incorporate tractography (in research or as an adjunct to anatomical targeting) over the 2 year study period - the percentage of centres NOT using tractography in any role decreased from 65.4% to 21.7%. Across the study period, there was a notable superior trend in the anatomical method of targeting. In 2019, 28% VIM-TAs were level with the MCP and only 16% targeted 2mm above the MCP; however, in 2021 there was an evolution to target superiorly within the VIM with 40.9% centres targeting 2mm above MCP. In contrast, the VIM-TA medial-lateral and anterior-posterior positions remained stable across the study period.

Conclusions: In the 2-year interval from 2019 to 2021, many MRgFUS centers have evolved their VIM-TA with a notable move superiorly within the VIM (2mm above the MCP) and the introduction of tractography to aid VIM localisation. This pattern has been demonstrated internationally and independently across the participating MRgFUS tremor centres.

Acknowledgment/Funding Sources: Insightec for 2019 database

MOV-17

Topic: Movement Disorders
Presentation Type: Oral

Ultra High-Field MRI (7T) of the Thalamic Ventral Intermediate Nucleus (VIM) to Validate 3T Diffusion Tractography and 3T Anatomical Targeting for MR-Guided Focused Ultrasound (MRgFUS) of Essential Tremor (ET)

Ayesha Jameel[1], joely smith[2], Rebecca A. Quest[2], nada yousif[3], Sena Akgun[4], brynmor jones, peter bain[1], dipankar nandi[2], wladyslaw gedroyc[2]

[1]Imperial College, London, United Kingdom
[2]Imperial College NHS Trust, London, United Kingdom
[3]University of Hertforshire, London, United Kingdom
[4]Imperial College NHS Trust, Rome, Italy

Background: The Ventral Intermediate Nucleus is the premiere target in Magnetic Resonance guided Focused Ultrasound treatment of Tremors. Accurate targeting of VIM is crucial to both safety and efficacy of treatment, however, the VIM cannot be directly visualised on current clinical scanners (1.5T and 3T) there is much debate on the best targeting techniques in MRgFUS. The most commonly used method is anatomical targeting using local landmarks such as the anterior commissure - posterior commissure line. An alternative technique is using diffusion tensor imaging (DTI), locating the VIM at the intersection between the pyramidal tract (PT) and Medial Lemniscus (ML).

The aim of this proof of concept trial is to validate both anatomical and DTI targeting of the VIM against high resolution 7T MRI. Previous studies have shown that 7T SWI can be used to delineate individual thalamic nuclei (direct visualisation), including VIM. By comparison of these techniques on healthy volunteers, this study hopes to demonstrate the accuracy (or inaccuracy) of the current anatomical and tractography targeting methods on 3T.

Materials and Methods: Following local ethics approval, 3 healthy volunteers were scanned on 3T MRI including DTI, T2 and SWI sequences and subsequently on 7T MRI including SWI sequences. For each healthy volunteer, the VIM was located on 3T imaging using the anatomical and the tractographical method. For comparison, VIM was then located on 7T SWI. For each volunteer, the position of the two VIM targets on 3T (anatomical and DTI targeting) were compared against their delineated 7T VIM.

All results were mapped onto 3D models of the thalamus based on individualised MRI data.

Results: Imaging was successfully acquired for all healthy volunteers on both the 3T and 7T MRI scanners. DTI Mapping was successful. The VIM was located by anatomical and tractographical methods on the 3T imaging and delineated (direct visualisation) on 7T. For all 3 healthy volunteers, there was good correlation between the position of VIM on all three methods, thus demonstrating the accuracy of VIM targeting by tractography and anatomical mapping on current clinical (3T) scanners.

Conclusions: This study validates both the 3T anatomical and 3T tractographical methods of VIM targeting, providing reassurance that safe and effective VIM targeting can be performed on current clinical scanners (3T) for MRgFUS thalamotomy. This study adds further evidence to the body of work, demonstrating the safety and accuracy of MRgFUS in the treatment of tremor - accurate VIM targeting allows accurate VIM ablation and thus the efficacy of tremor impression is optimised. Furthermore, accurate VIM targeting minimises adverse effects associated with sonication of non-target tissue in MRgFUS thalamotomy for tremor.

Acknowledgment/Funding Sources: IPEM innovation grant - Institute of Physics and Engineering in Medicine

MOV-18

Topic: Movement Disorders

Presentation Type: Oral

First Steps towards an Automated and Generalized Definition of Target and Areas of Risk in TcMRgFUS for Tremor Therapy

Jan Klein[1], Annika Hänsch[2], Veronika Purrer[3], Neeraj Upadhyay[3], Carsten Schmeel[3], Yeruham Shapira[4], Ullrich Wüllner[3], Jürgen Jenne[1]

[1]Fraunhofer MEVIS, Bremen, Bremen, Germany
[2]Fraunhofer Insitute for Digital Medicine MEVIS, Bremen, Bremen, Germany,
[3]University Hospital Bonn, Bonn, Nordrhein-Westfalen, Germany,
[4]Insightec Ltd, Tirat Carmel, Haifa, Israel

Background: Ablative transcranial therapy with MR-guided focused ultrasound (tcMRgFUS) for the treatment of essential tremor (ET) and tremor in Parkinson's disease (MP) is becoming clinical reality.

As the targets for the ablation pulses cannot be visualized on the morphological images, their definition depends on the user's experience. The target regions have not yet been defined uniformly and vary among experts. The final positioning of the ablation focus is found by using multiple low-energy test pulses that cause transient, reversible effects on the patients. Once the right position is found, suppressing the tremor without adverse effects, the final pulse is applied.

The final aim of the project tcFUS-Control is to fully automate target finding for tremor treatment with tcMRgFUS based on pre-therapy MR images, as well as the automated identification of 'no-go' risk areas, that must not be ablated under any circumstances.

In this ongoing work, we concentrated on ET clinical cases, to be extended to MP-tremor therapy.

Materials and Methods: We used T1 MPRAGE MRI data (1 mm resolution) and diffusion tensor MRI data (2 mm, 56 gradient directions) from 45 pre-therapeutic ET patients treated with tcMRgFUS. A fully automatic DTI-based fiber tracking pipeline was set up, supported by deep learning (DL) based segmentation of ROI.

The target area for ET treatment, the nucleus ventralis intermedius (VIM) and the target bundles, cerebello-thalamic tract (CTT) and pallido-thalamic tract (PTT), are located nearby important fiber pathways, the corticospinal tract (CST), the medial lemniscus (ML) and the mammillothalamic tract (MT) which must be spared from lesioning by the FUS-pulse.

We developed a fiber tracking algorithm which is able to reconstruct crossing and kissing tracts and also allows for using clinically accepted DTI maps.[1] The main idea is that it locally adapts its parameters to specific brain regions of the JHU-MNI-ss atlas. The algorithm needs a seed region as input and further include and exclude areas to reconstruct the desired fiber bundle.

We used a DL-based algorithm to segment ROI for cerebral peduncle, dentate nucleus, globus pallidus interna, medial lemniscus seed, pre- and postcentral gyri, posterior limb of internal capsule, red nucleus, superior cerebellar peduncle, thalamus, and ventricles. Reference data for DL training were created using semi-automatic tools (gyri, ventricles) or registration of pre-defined ROI on an atlas (all other ROI). 3D U-Nets[2] were trained using the T1 data as input (gyri, ventricles) or T1 data and a color-coded direction map derived from DTI.[3]

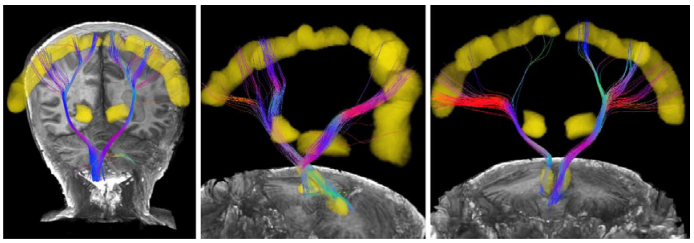

Figure 1. (from left to right): CST, CTT, ML correctly pass include ROIs and do not enter exclude areas. The CST was not fanned out quite as one might expect anatomically. However, this fanning out is not particularly relevant to the clinical question.

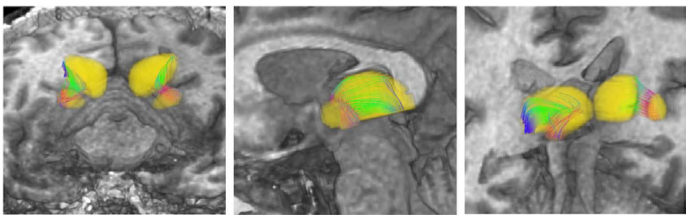

Figure 2. PTT bundle connecting thalamus and globus pallidus interna. The short bundle could be calculated for almost all patients. The clinical evaluation requires a careful approach, because the bundle is not only short but also very narrow.

Results: A well-known problem with fiber tracking is its evaluation due to a lack of ground truth. Clinical experts evaluated the bundles which showed that the reconstruction for the CTT, CST and ML provided good visual results (Fig. 1).

The PTT has not been evaluated in detail (Fig. 2). The MTT sometimes included fibers in the ventricular area. The evaluation of the automatic segmentation is also challenging due to the lack of ground truth for most ROI. We used automatically generated screenshots to visually assess their quality. We aim to improve the ROI quality and subsequent tracking by curating the training data or by improving the atlas-registration.

Conclusions: An automated DTI-based tractography of the most important tracts for target finding in tcMRgFUS for the therapy of ET was developed, including DL algorithms for the automatic and patient-specific segmentation of supporting ROI. However, this is only a first step towards a fully automated target and area of risk identification for ET therapy.

In the next step, these tractography data will be used to automatically determine the target coordinates in advance. For this purpose, the treatment data are analyzed with the coordinates of the applied test and ablation pulses and attempts are made to find reliable connections with tractography data. An extension to MP tremor data and the inclusion of the data from other working groups is planned to improve the methods developed and to consider the different approaches in target finding.

Acknowledgment/Funding Sources: The research presented in this paper was funded by the German Federal Ministry for Economic Affairs and Energy in the context of the project tcFUS-Control (ZF4173706CR9, ZF4801301CR9).

References

1. Klein J (2015) doi: 10.1117/12.2080765
2. Çiçek Ö (2016) doi: 10.1007/978-3-319-46723-8_49
3. Hänsch A (2022) doi: 10.1117/12.2611710

MOV-19

Topic: Movement Disorders
Presentation Type: Oral

Microbubble Drug Conjugate and Focused Ultrasound Blood Brain Barrier Delivery of AAV-2 SIRT-3

James Keenan

Artenga Inc., Ottawa, ON, Canada

Background: Delivery of viral vectors as gene therapies to treat neurodegenerative diseases has been hampered by the inability to penetrate the blood brain barrier (BBB) and invasive or non-targeted delivery options prone to inducing immune responses. MR guided focused ultrasound (MR-g-FUS) and microbubbles have demonstrated safe, temporary, targeted BBB permeabilization clinically.

Materials and Methods: We developed clinically-scalable, microbubble drug conjugates (MDCs) for the viral gene therapy, AAV.SIRT3-myc [adeno-associated virus expressing myc-tagged SIRT3], which has previously been shown to have disease modifying effects in animal models of Parkinson's disease (PD). The lipid shells of the perfluorocarbon gas MDCs were covalently conjugated to antibodies with binding specificity to AAVs. Following systemic (iv) delivery of AAV.SIRT3-myc MDCs, MR-g-FUS was used to deliver SIRT3-myc to brain regions affected in PD. SIRT3-myc expression was determined post mortem, using immunohistochemistry.

Results: An in vitro, SH-SY5Y cell culture model was used to show that the localized destruction of MDCs using ultrasound exposures within biological safety limits dissociated AAV2-GFP (green fluorescent protein) from the MDCs in the targeted area while maintaining their transduction capacity. In rats, MR-g-FUS resulted in BBB permeabilization in the striatum and substantia nigra (SNc). SIRT3-myc was expressed in the striatum, but not the SNc.

Conclusions: These studies demonstrate that MDCs combined with MR-g-FUS are an effective method for delivery of viral vector gene therapies, such as AAV.SIRT3, to brain regions affected in PD. This technology may prove useful as a disease-modifying strategy in PD and other neurodegenerative disorders.

Acknowledgment/Funding Sources: The Focused Ultrasound Foundation funded the study and funds we're supplemented by an Ontario Research Fund project.

MOV-20

Topic: Movement Disorders
Presentation Type: Oral

Site-Specific Symptom Improvement after Globus Pallidus Focused Ultrasound Ablation in Parkinson's Disease

Vibhor Krishna[1], Francesco Sammartino[2], Frank Yeh[3]

[1]University of North Carolina at Chapel Hill, Chapel Hill, NC, USA
[2]The Ohio State University, Columbus, OH, USA
[3]University of Pittsburgh, Pittsburgh, PA, USA

Background: Globus pallidus focused ultrasound ablation (GP-FUSA) was recently approved by the FDA to treat Parkinson's disease. However, clinically relevant lesion characteristics are yet to be determined. Specifically, the lesion location relative to the GP's motor subregion is not defined and it is unknown whether the improvements in bradykinesia and dyskinesia are site-specific within the GP. In this study, the authors hypothesize that the GP-FUSA lesions will overlap the motor subregion, and the improvements in bradykinesia and dyskinesia are site-specific.

Materials and Methods: Diffusion MRI from healthy controls (n=45) PD subjects (n = 33) were parcellated based on the magnitude of water diffusivity in the GP, as measured orientation distribution function (ODF). A clustering algorithm was used to identify GP parcels with distinct ODF magnitude. The individual parcels were used as seeds for tractography to distinguish motor from nonmotor GP subregions. In addition, the locations of focused ultrasound lesions relative to the GP parcels were analyzed in PD subjects (n=11). The hot spots for improvement in bradykinesia (measured by Unified Parkinson's disease Rating Scale subscale-III (UPDRS-III) in OFF state) and dyskinesia (measured by Unified Dyskinesia Rating Scale (UDyRS)) were statistically distinguished using a one-group general linear model.

Results: Radiologically, three distinct parcels were identified within the GP in PD patients: posterior, central, and anterior. The posterior and central parcels comprised the motor subregion based on the tractography connections, and the anterior parcel was classified as a nonmotor subregion. The mean improvement in OFF medication UPDRS-III score was 30.6% ± 7.9% and on the UDyRS was 54% ± 20.7%. The focused ultrasound lesions overlapped with the motor subregion (posterior more than central). Two distinct hotspots for improvement in bradykinesia and dyskinesia were identified within the GP motor subregion.

Conclusions: The improvements in bradykinesia and dyskinesia after GP-FUSA are site-specific in the GP motor subregion. These results have implications for stereotactic targeting in PD patients undergoing GP-FUSA.

MOV-21

Topic: Movement Disorders
Presentation Type: Oral

Multimodal Intraoperative Lesion Characterization after Focused Ultrasound Thalamotomy

Vibhor Krishna[1], Francesco Sammartino[2], Frank Yeh[3]

[1]University of North Carolina at Chapel Hill, Chapel Hill, NC, USA
[2]The Ohio State University, Columbus, OH, USA
[3]University of Pittsburgh, Pittsburgh, PA, USA

An accurate lesion characterization is crucial to optimize focused ultrasound (FUS) treatment parameters and ultimately improve clinical outcomes. This study found that intraoperative restricted diffusion imaging (RDI) accurately identified the volume and location of FUS lesions.

Background: Recent data demonstrate that quantitative diffusion MRI, specifically the restricted diffusion imaging (RDI), can accurately characterize focused ultrasound (FUS) lesions in the acute (24 hours) and delayed (one year) imaging. However, it is unclear whether RDI can reliably detect FUS lesions intraoperatively (i.e., within a few minutes of lesioning) and whether the intraoperative lesions predict delayed clinical outcomes.

Materials and Methods: In patients undergoing ventral intermediate nucleus (VIM) FUS ablation, an intraoperative imaging protocol was implemented to include RDI and T2-weighted imaging in addition to intraoperative MR thermography. Lesion characteristics (i.e., lesion volume and location) were defined with each sequence and then compared. In addition, an imaging-outcomes analysis was performed to determine lesion characteristics associated with delayed clinical outcomes (i.e., tremor improvement and postoperative ataxia).

Results: The mean tremor reduction at the last follow-up after VIM FUS ablation was 84.8% (SD:18.6). Four patients developed ataxia postoperatively. Intraoperative RDI accurately identified the volume and location of FUS lesions. Intraoperative T2-weighted imaging underestimated the lesion volume but accurately identified the location. In addition, intraoperative RDI revealed that lesions adjacent to the ventral border of the VIM were significantly associated with postoperative tremor improvement, while the lesions extending into the inferolateral white matter were associated with postoperative ataxia.

Conclusions: These data support the acquisition of intraoperative RDI to characterize FUS lesions. Future research should test the histological correlates of intraoperative RDI and test whether it can be implemented to optimize the current technique of FUS ablation.

MOV-22

Topic: Movement Disorders
Presentation Type: Oral

The Impact of Optimal Thermal Neuromodulation Parameters on the Efficiency of Focused Ultrasound Treatment

Vibhor Krishna[1], Francesco Sammartino[2], John Snell[3], Matthew Eames[3]

[1]University of North Carolina at Chapel Hill, Chapel Hill, NC, USA
[2]The Ohio State University, Columbus, OH, USA
[3]Focused Ultrasound Foundation, Charlottesville, VA, USA

Background: During ventral intermediate nucleus focused ultrasound ablation (VIM-FUSA), the presumed target is tested with subthreshold sonications before permanent ablation. This testing relies on ultrasound-induced thermal neuromodulation (TN). The TN parameters (i.e., the thermal dose and spot size) for optimal subthreshold testing were recently defined. However, it is unknown whether optimal subthreshold testing was associated with shorter VIM-FUSA treatments. We aimed to compare the number of sonications required to complete the VIM-FUSA treatment in patients who received optimal versus standard subthreshold testing.

Materials and Methods: We analyze the intraoperative data clinical and radiographic in essential tremor patients undergoing VIM-FUSA. The intraoperative writing samples were independently rated by two raters using the clinical rating scale for tremor. Intraoperative thermography data was analyzed to classify subthreshold sonications (thermal dose less than 25 cumulative equivalent minutes (CEM)) into optimal vs. standard based on the thermal exposure (0.67 CEM or greater as optimal) and spot size (2.46 mm or higher as optimal). The number of sonications required to complete the treatment were compared between patients that received optimal versus standard subthreshold testing.

Results: From the 331 sonications with associated writing samples, 97 were classified as sub-threshold sonications. TN was observed in 23 (24%) sub-threshold sonications, and the median tremor improvement during TN was 20% (inter-quartile range = 41.6). The sonication duration in optimal subthreshold testing was significantly longer (30 seconds or higher) than the standard technique (11-13 seconds). In VIM-FUSA treatments with optimal sub-threshold testing, significantly fewer sonications were required than the treatments with the standard technique (mean sonications, n (SD)=8.8 (2.8) vs. 11.7 (3.2), p=0.006).

Conclusions: We observed significantly shorter VIM-FUSA treatments when using the optimal subthreshold testing than the standard technique. We recommend long duration (>30 seconds) subthreshold sonications for intraoperative testing during VIM-FUSA based on these observations.

MOV-23

Topic: Movement Disorders

Presentation Type: Oral

Blood Brain Barrier Striatal Opening by Focused Ultrasound Allows AAV Vector Delivery into Monkeys

Javier Blesa[1], Jose A. Pineda-Pardo[1], Ken Ichi Inoue[2], Tiziano Balzano[1], Natalia L. del Rey[1], Alejandro Reinares-Sebastian[1], Noelia Esteban-Garcia[1], Ines Trigo-Damas[1], Masahiko Takada[3], Jose A. Obeso[1]

[1]HM CINAC, Mostoles, Madrid, Spain
[2]Kyoto University, Kyoto, Aichi, Japan
[3]Center for the Evolutionary Origins of Human Behavior, Kyoto University, Inuyama, Aichi, Japan

Background: Potentially promising drugs and antibody therapies for neurodegenerative disorders are often limited by their inability to efficiently cross the blood-brain barrier (BBB). Thus, gene therapy for central nervous system disorders currently requires direct injections into multiple brain regions. While FUS BBB opening has been recently used to successfully enhance antibodies or viral vectors delivery in rodents nobody has achieved to deliver any of these candidates with FUS in non-human primates. We aimed to evaluate whether systemically injected adeno-associated viral vectors (AAV) can be delivered safely, reliably, and in a controlled manner into non-human primates' brain by combining low-intensity magnetic resonance-guided focused ultrasound (FUS) and intravenous microbubbles.

Materials and Methods: BBB in the putamen of 6 macaques (Macaca fascicularis) was opened with FUS. Low-intensity sonication were applied transcranially under MRI guidance, targeting a grid of sub-spot locations in the whole putamen structure. Microbubbles (Luminity) were delivered continuously during sonication with intravenous perfusion using an infusion pump. Treatment effects were monitored using MRI T2*, FLAIR and T1-weighted imaging with Gadolinium contrast. Following confirmation of successful BBB opening, we injected intravenously a single dose of AAV9-GFP (Green Fluorescent Protein). After one-month animals were sacrificed and detailed immunohistochemical assessment of the brains was completed.

Results: After sonication the relative gadolinium signal enhancement was significantly higher in the putamen compared to any other brain area in each monkey, indicating the successful opening of the BBB. No edema or hemorrhage was found on magnetic resonance images after BBB opening. Postmortem analysis demonstrates successful neuronal GFP expression only in the contrast-enhanced regions observed in T1-MR images from the same animals in absence of any apparent tissue damage.

Conclusions: FUS is a viable tool to deliver focally and noninvasively AAV in non-human primate brain regions. This approach may be useful to alter the progression of several neurodegenerative diseases and improve therapeutic outcomes particularly in the prodromal stages.

Acknowledgment/Funding Sources: Focused Ultrasound Foundation;: Fundacion Tatiana Perez de Guzman el Bueno; Instituto de Salud Carlos III

MOV-24-YI

Topic: Movement Disorders

Presentation Type: Oral

Quantitative and Qualitative Tremor Evaluation after tcMRgFUS Thalamotomy in ET

Veronika Purrer[1], Neeraj Upadhyay[1], Tara Chand[2], Valeri Borger[1], Carsten Schmeel[1], Henning Boecker[1], Ullrich Wüllner[1]

[1]University Hospital Bonn, Bonn, Nordrhein-Westfalen, Germany
[2]University Hospital Jena, Jena, Thueringen, Germany

Background: Transcranial high-intensity Magnetic Resonance-guided Focused Ultrasound (tcMRgFUS) is a recently developed technique for treatment of severe, medication-refractory Essential Tremor (ET). Previous studies employed clinical rating scales to assess a putative benefit after tcMRgFUS. Although reasonable reproducibility has been reported, sensitivity leaves room for improvement and investigator bias can pose problems, too. More quantitative methods i.e. devices using accelerometers may offer better ways to identify even small changes in tremor intensity. Herein, we report quantitative and qualitative outcome measures and their respective efficacy in tremor assessment in clinical practice after unilateral tcMRgFUS thalamotomy in patients with ET using a triaxial accelerometer.

Materials and Methods: We examined 17 patients with ET prior, 1 day and 12 months after tcMRgFUS using the Clinical Rating Scale for Tremor (CRST) and a CE-approved triaxial accelerometer (SOMNOwatchTM plus®). Quantitative frequency and amplitude analyses of the upper extremity were obtained bilaterally in defined rest, postural and kinetic condition, respectively (Fig. 1). Efficacy of tcMRgFUS was evaluated using the Friedman's test. Spearman's rank correlation coefficients (rs) were used to calculate the correlation of quantitative and qualitative tremor measures.

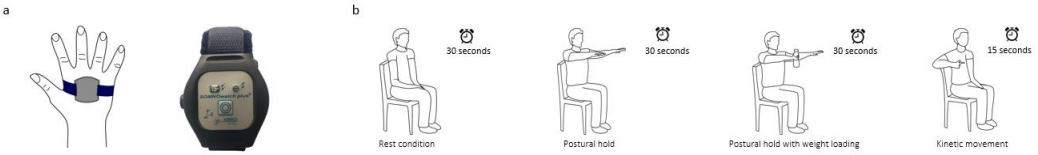

Figure 1. (a) Accelerometric recording using a triaxial accelerometer. (b) Recordings were obtained in rest, postural with and without weight loading of the outstretched arms and as kinetic condition for 30 and 15 seconds, respectively.

Table 1: Characteristics and quantitative and qualitative tremor outcome measurements of the study participants (n=17)

Age – yr[a]	68.4 ± 13.3							
Male sex–no. (%)	12 (71%)							
Age of onset[a]	34.4 ± 18.4							
Disease duration[a]	34.0 ± 13.4							
	Pre		**Post 1 day**		**Post 12 months**		**p-value[†]**	
CRST[a]	61.6 ± 15.9		28.8 ± 9.4		31.6 ± 10.4		<0.001	
	treated	**untreated**	**treated**	**untreated**	**treated**	**untreated**	**treated**	**untreated**
CRST subscores[a]								
Rest[b]	0.7 ± 0.7	0.7 ± 0.7	0.0 ± 0.0	0.8 ± 0.9	0.1 ± 0.2	0.8 ± 0.8	0.001	0.972
Postural[b]	3.1 ± 0.7	2.9 ± 0.7	0.4 ± 0.6	2.8 ± 0.8	0.8 ± 0.7	2.9 ± 0.9	<0.001	0.592
Kinetic[b]	3.5 ± 0.7	3.1 ± 1.0	0.5 ± 0.6	3.2 ± 0.9	1.2 ± 0.8	3.4 ± 0.9	<0.001	0.150
Drawing[c]	8.8 ± 3.1	8.2 ± 2.7	2.6 ± 1.4	8.8 ± 2.7	3.5 ± 1.4	9.0 ± 2.6	<0.001	0.301
Tremor intensity (m/s²)[a]								
Rest	28.6 ± 54.6	27.5 ± 54.2	6.8 ± 6.5	30.2 ± 55.1	3.9 ±2.1	22.7 ± 49.5	0.627	0.646
Postural	127.1 ± 138.7	96.9 ± 127.3	13.6 ± 16.5	82.6 ± 91.1	17.2 ± 16.3	79.2 ± 82.1	0001	0.005
Postural_weight	152.4 ± 108.6	111.5 ± 111.7	15.3 ± 13.9	111.5 ± 111.7	17.3 ± 10.3	147.6 ± 138.5	0.046	0.247
Kinetic	311.5 ± 322.0	192.2 ± 191.6	19.0 ± 25.3	190.4 ± 256.8	25.3 ± 28.3	150.7 ± 154.4	<0.001	0.943
Center frequency (Hz) [a]								
Rest	5.4 ± 0.7	5.3 ± 0.9	5.4 ± 1.0	5.5 ± 1.1	5.7 ± 1.0	5.6 ± 0.9	0.001	0.305
Postural	5.2 ± 0.9	5.3 ± 0.7	4.8 ± 1.0	5.4 ± 1.0	4.2 ± 0.7	4.9 ± 0.9	0.001	0.210
Postural_weight	5.2 ± 0.8	5.4 ± 0.9	5.9 ± 1.2	5.5 ± 0.8	5.1 ± 0.7	5.5 ± 0.8	<0.001	0.189
Kinetic	5.5 ± 0.8	5.4 ± 1.0	4.2 ± 1.0	5.6 ± 1.2	4.2 ± 1.2	5.4 ± 0.8	<0.001	0.291
Spearman's rank correlation coefficient (r_s)								
Rest		0.557*			0.661**		0.847**	
Postural	0.665**			0.754**		0.777**		
Postural_weight	0.607*			0.806**		0.651**		
Kinetic	0.798**	0.802**		0.756**		0.711		

[a] Values are means ± SD

[b] Item of Part A (clinical observation); range 0 to 4

[c] Item of Part B (motor tasks); range 0 to 12

[†] A p-value < 0.05 was considered statistically significant. Changes among all time points were calculated using Friedman's test

* $p < 0.05$

** $p < 0.01$

Abbreviations: CRST=Clinical Rating Scale for Tremor

Results: Details on demographic and clinical characteristics and tremor outcome parameters are reported in Table 1. Remarkable tremor improvement was evident in accelerometric measures and clinical rating after tcMRgFUS (Fig. 2). The congruence between tremor estimates on the CRST and the tremor intensity measures by accelerometry were relatively high in the postural and kinetic condition of the treated extremity prior and the untreated extremity prior and post tcMRgFUS (rs > 0.6) (Table 1).

Conclusions: Devices or wearables, i.e. simple and easy to use tools for quantitative measurements with an accelerometer, appear to be appropiate tools to measure tremor outcome after MRgFUS. The correlation with the standard clinical rating scale is high and the increasing use of similar systems to come will help to better characterize and compare the outcomes for the various treatment options available for movement disorders.

Acknowledgment/Funding Sources: The MRgFUS system was in part funded by the German Research Foundation (INST 1172/64-1) and the University of Bonn's Faculty of Medicine.

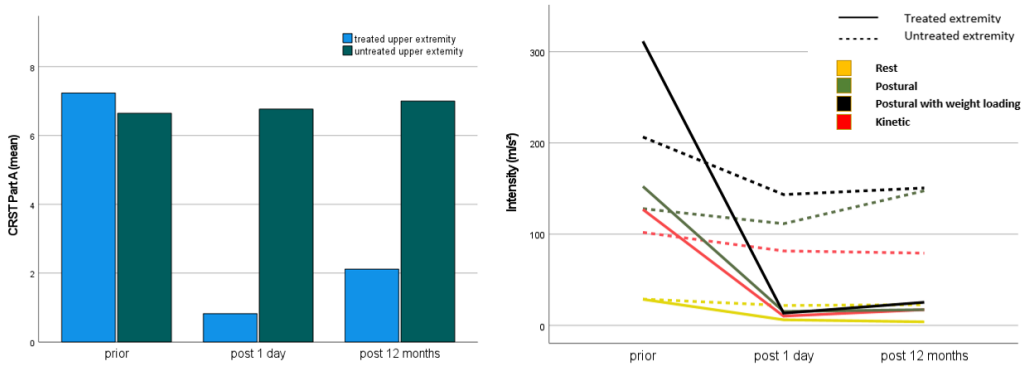

Figure 2. (a) CRST subscores for the treated and untreated upper extremity (Part A, clinical observation) prior and 1 and 12 months after tcMRgFUS. (b) Tremor intensity measures with a triaxial accelerometer in 4 different conditions

MOV-25

Topic: Movement Disorders

Presentation Type: Oral

Disrupted Rich-Club Organization Impacts Tremor Recovery after MRgFUS Thalamotomy in Patients with Essential Tremor

Xiaoyu Wang, Xin Lou

Chinese PLA General Hospital, Beijing, Beijing, China

Background: Magnetic resonance-guided focused ultrasound (MRgFUS) has become a research hotspot gradually in the treatment of essential tremor (ET). However, its impact on structural network is still unclear.

Materials and Methods: We constructed structural networks in 30 ET and 28 age- and gender-matched healthy controls (HC) using diffusion MRI and deterministic tractography. Meantime, 30 ET patients followed up on their clinical and imaging data from baseline to 6-month post-operation. Group differences in rich-club organization and other network topological metrics were investigated. The relationship between altered network topological metrics and clinical scores were calculated.

Results: In addition to increase for strength of rich-club (P = 0.034) connections, there were decreased values of the network topological metrics for strength of feeder (P = 0.000), local (P = 0.000) connections in ET compared with HC. The strength of rich-club (P = 0.000) and local (P = 0.010) connections were increased at the postoperative 6-month compared to pre-operative baseline, while no significant difference was found in the strength of feeder connections. Meantime, efficiency properties decreased in ET and increased after MRgFUS. Additionally, feeder connections were correlated with hand tremor score preoperatively (r = -0.406, P = 0.049) and postoperatively (r = -0.441, P = 0.031). Their pre-operative features act as post-operative tremor recovery prediction.

Conclusions: The rich-club organization was disrupted in ET patients compared with HC, which could be rescued by MRgFUS thalamotomy. These findings provided novel insight into a network mechanism and may work as a feasibility in the assessment of ET tremor control with MRgFUS thalamotomy.

Acknowledgment/Funding Sources: This work has been supported by the National Natural Science Foundation of China (Nos. 81825012, and 82151309). Xin Lou is the author who received the funding.

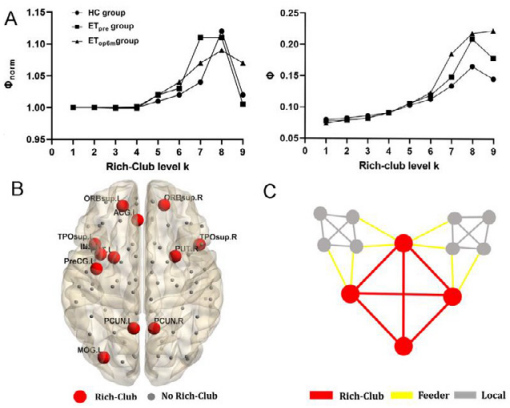

Figure 1. Rich-club organization of the healthy controls (HC) group and essential tremor (ET) group. (A) The figure shows normalized rich-club coefficients (?_norm) and actual rich-club coefficients (?). (B) The figure shows the distribution of rich-club

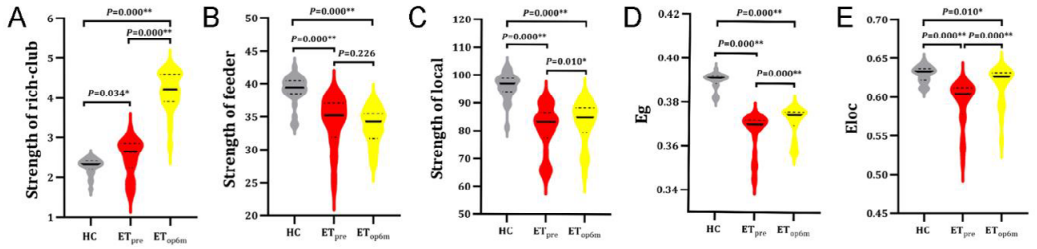

Figure 2. Between-group comparisons of rich-club organization and efficiency properties, including (A) strength of rich-club connections, (B) strength of feeder connections, (C) strength of local connections, (D) global efficiency (Eg), and (E) local efficiency (Eloc)

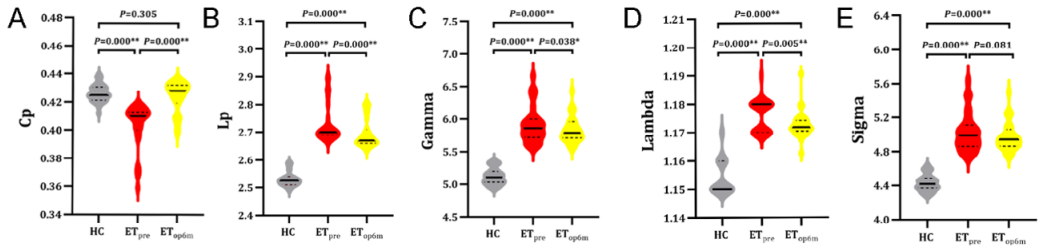

Figure 3. Between-group comparisons of small-world properties, including (A) clustering coefficient (Cp), (B) characteristic path length (Lp), (C) normalized clustering coefficient (Gamma), (D) normalized characteristic path length (Lambda), and (E) small-world coefficient (Sigma)

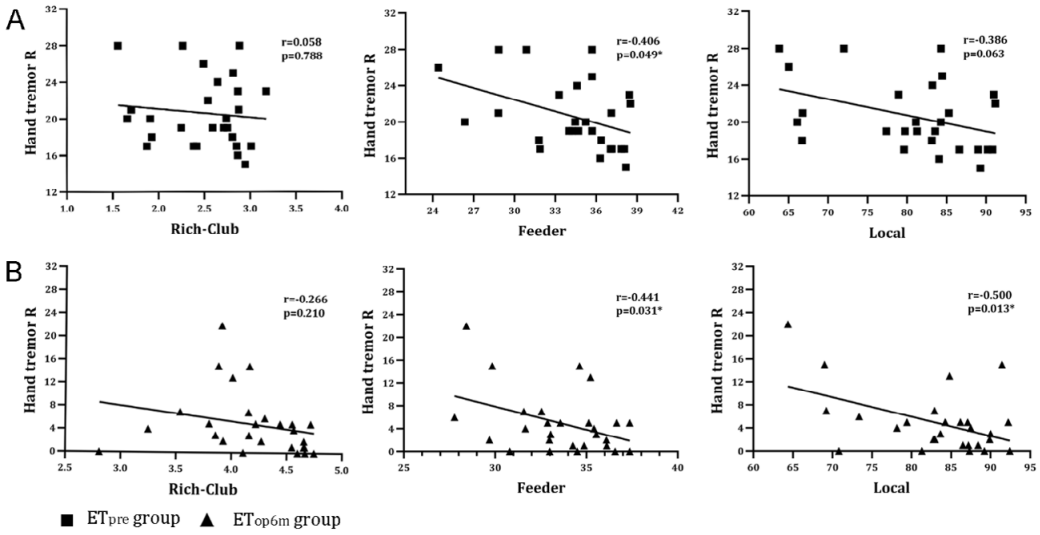

Figure 4. The correlations between the strength of rich-club, feeder, local connections and the clinical score for the right hand in ET_pre group (A) and ET_op6m group (B). ET_pre: ET patients at pre-operation, ET_op6m: ET patients at 6-month post-opera

MOV-26

Topic: Movement Disorders

Presentation Type: Oral

Comparison of the Impact of Skull Density Ratio to Alternative Skull Metrics on MRI-Guided Focused Ultrasound Thalamotomy for Tremor

Jason W. Yuen[1], Abhinav Goyal[1], Timothy Kaufmann[1], Lauren Jackson[1], Kai Miller[1], Bryan Klassen[1], Neha Dhawan[2], Kendall H. Lee[1], Vance T. Lehman[1]

[1]Mayo Clinic, Rochester, MN, USA
[2]Insightec, Dallas, TX, USA

Background: One of the key metrics that is used to predict likelihood of success of MR-guided focused ultrasound (MRgFUS) thalamotomy is the skull density ratio (overall calvarial SDR). However, this measure does not fully predict the sonication parameters which would be required or the technical success rates. We aim to assess other skull characteristics that may also contribute to technical success.

Materials and Methods: We retrospectively studied consecutive essential tremor patients who were treated by MRgFUS at our center, USA between 2017 and 2021. We evaluated the correlation between the different treatment parameters, particularly maximum power and energy delivered, with a range of patients' skull metrics and demographics. Machine learning algorithms were applied to investigate whether sonication parameters could be predicted from skull density metrics alone, and whether including combined local transducer SDRs with overall calvarial SDR would increase model accuracy.

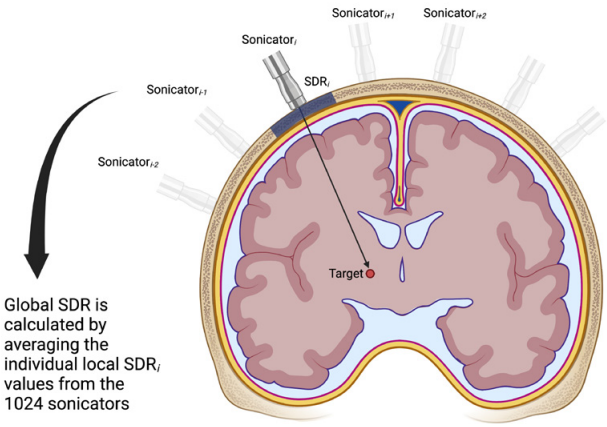

Figure 1. A schematic view of skull density ratio (SDR) measurements. Local SDR values from each of the 1024 sonicators are averaged to give a global SDR. Incidence angles not incorporated for simplification. Created with BioRender.com.

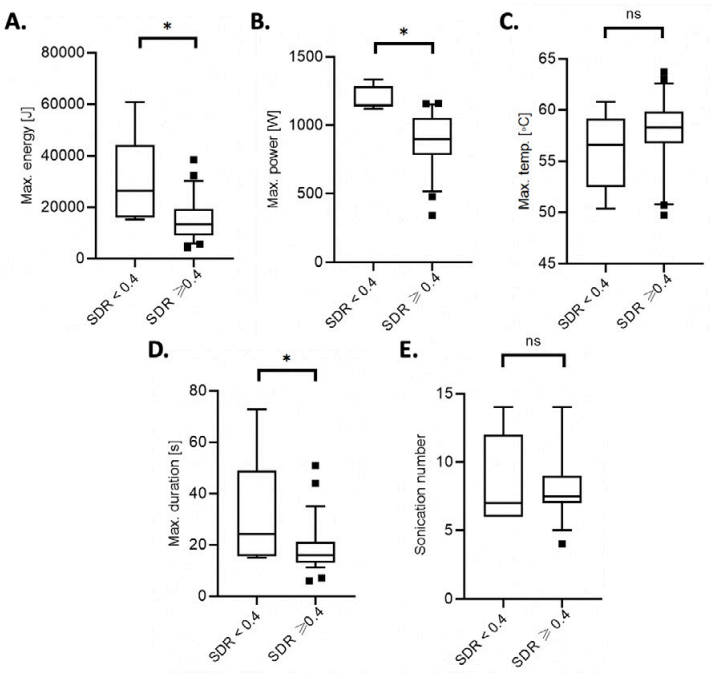

Figure 2. (A)-(E). Comparison of treatment parameters between those with SDR ⩾ 0.4 (N = 58) and those with SDR < 0.4 (N = 5) using Mann-Whitney U tests.

Results: 62 patients were included in the study. The mean age was 77.1 (S.D. 9.2) years and 78% (49/63) were male. The mean SDR was 0.51 (S.D. 0.10). Among the evaluated metrics, SDR had the highest correlation with the maximum power used in treatment ($r = -0.626$, $p < 0.001$; proportion of local SDR values ≤ 0.8 group also had $r = +0.626$, $p < 0.001$) and maximum energy delivered ($r = -0.680$, $p < 0.001$). Machine learning algorithms achieved a moderate ability to predict maximum power and energy required from the local and overall SDRs (accuracy of ~80% for maximum power, ~55% for maximum energy), and high ability to predict average maximum temperature reached from the local and overall SDRs (~95% accuracy).

Conclusions: We compared a number of skull metrics against SDR and showed that SDR was one of the best indicators of treatment parameters when used alone. In addition, we have proposed a number of other machine learning algorithms that may be explored to improve its accuracy when additional data is obtained. Additional metrics related to eventual sonication parameters should also be identified and explored.

Figure 3. Correlation of skull metrics with treatment parameters (N = 63). Spearman correlation coefficients are presented as the absolute value in the graph for clarity.

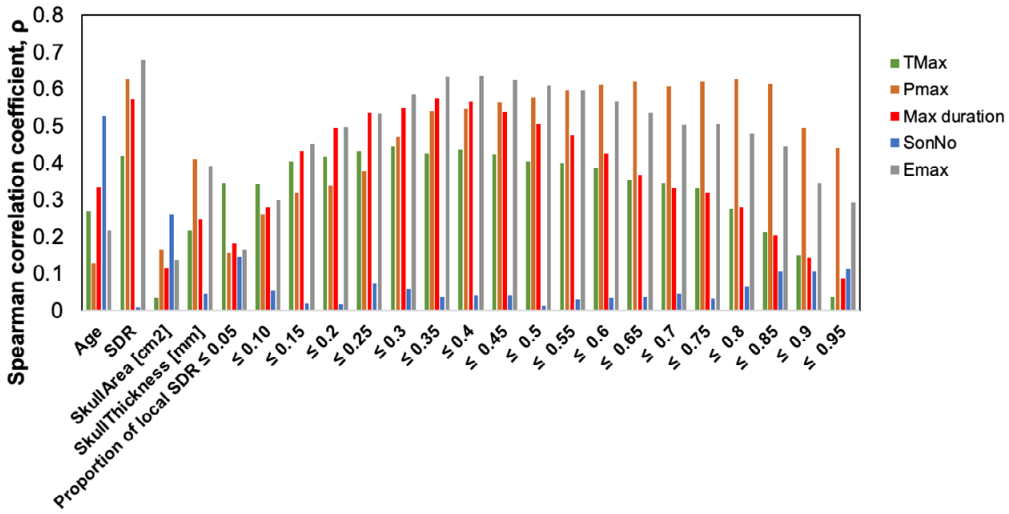

MSK-01

Topic: Musculoskeletal
Presentation Type: Oral

Limited Gender Differences in Gastrocnemius after Single LIPUS or pFUS Treatment

Chelsey L. Dunham[1], Scott R. Burks[1], Joseph A. Frank[2]

[1]NIH Clinical Center, Bethesda, MD, USA
[2]NIH, Bethesda, MD, USA

Background: Sonication treatments, especially pFUS (pulse focused ultrasound), have shown upregulated cytokine expression (e.g., MIP-1alpha, MCP-1, VEGF) in the hamstrings of control and dystrophic mice [1,2,3]. However, previous work has only evaluated this effect in females. The goal of this study was to determine if there are gender-based differences following single LIPUS (low intensity pulsed ultrasound) or pFUS treatment.

Materials and Methods: Right gastrocnemius of male and female C57BL6 mice (6 weeks) were sonicated with a single exposure of either LIPUS (2 W/cm2, 1 MHz, 10% duty cycle, 7 min) or pFUS (25 W, 1 MHz, 5 Hz repetition frequency, 10% duty cycle, 20 sec). Muscle was collected for cytokine analysis 1-, 8-, and 24-hours after treatment and for immunofluorescence 24-hours after treatment. Control mice were not treated. For cytokine analysis (5 muscles/group; 70 mice total), flash-frozen muscle was homogenized in protease inhibitor cocktail and centrifuged. Total protein was quantified using a BCA assay and a mouse cytokine panel quantified cytokine expression using 2 mg/mL sample. For immunofluorescence (3 muscles/group; 18 mice total), muscle mounted in tragacanth was flash-frozen in liquid nitrogen cooled isopentane and 10 um transverse sections were cut on a cryostat. Serial sections (3 sections/muscle) were incubated with primary antibody for laminin, F4/80, and CD206, followed by secondary and DAPI. Cells were counted on 5 images/section. A two-way ANOVA analyzed changes within each treatment due to gender and time (cytokine analysis) and gender and treatment (immunofluorescence) with post-hoc Bonferroni comparisons.

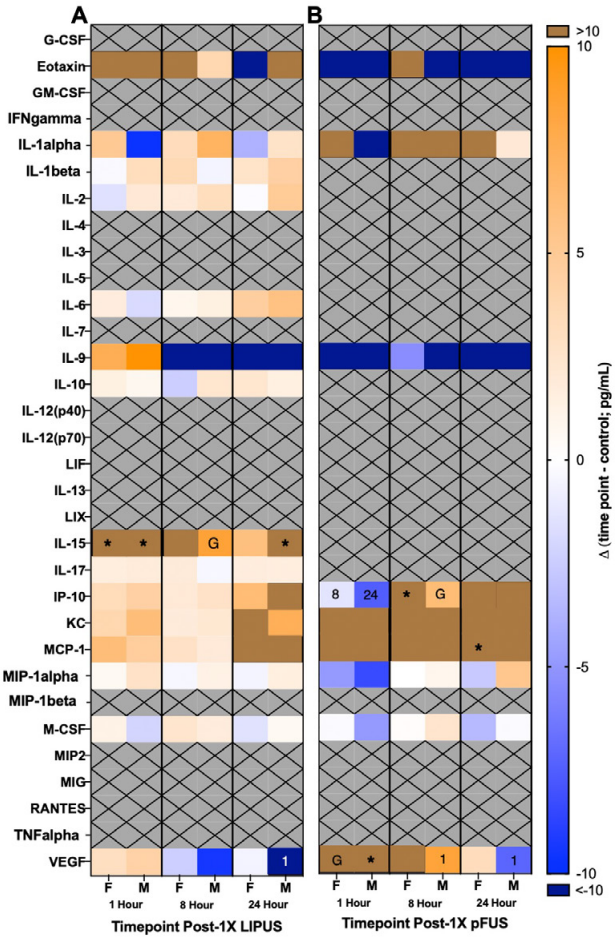

Figure 1. Cytokine analysis at 1-, 8-, and 24-hours after 1X LIPUS [A] or 1X pFUS [B]. Control expression was subtracted from each time point for normalization. (Not detected (X); Difference due to gender (G), control (*), or time point listed (#)).

Results: The number of cytokines that exhibited significance for gender or time were the same within each treatment. However, out of all possible post-hoc gender differences only 1/60 after LIPUS and 2/36 after pFUS were significant. There were no gender differences within the control group. Both LIPUS and pFUS regulated VEGF with a trend of upregulation at 1-hour and downregulation at 24-hours after treatment (Figure 1). pFUS males had increased VEGF compared to control and females at 1-hour. At 24-hours both LIPUS and pFUS males showed decreased VEGF compared to 1-hour. LIPUS had increased IL-15 at 1-hour in both genders and at 24-hours in males compared to control. At 8-hours, IL-15 expression in LIPUS females was increased compared to males. pFUS females at 8-hours had increased IP-10 compared to males and control. At 1-hour, IP-10 expression in pFUS females and males was decreased compared to 8-hour females and 24-hour males, respectively. MCP-1 was increased at 24-hours in pFUS females

compared to control. Total cell counts (DAPI+) exhibited significance due to gender and treatment but had no post-hoc gender differences. LIPUS males and females had increased cell infiltration compared to control (Figure 2). LIPUS males were also increased compared to pFUS males. M0 macrophages (F4/80+CD206-) had differences due to treatment with a significant interaction. The only post-hoc gender difference was LIPUS females showed increased M0 macrophages compared to males. LIPUS females M0 macrophages were also increased compared to control and pFUS females. M2 macrophages (F4/80+CD206+) exhibited no significant differences.

Conclusions: Overall, there are limited-to-no gender differences in gastrocnemius cytokine expression and cellularity after single LIPUS or pFUS treatment. LIPUS generally exhibited a constant upregulated pro-inflammatory response over time while after pFUS this response occurred later at 8- and 24-hours. LIPUS showed hypercellularity compared to control 24-hours after treatment, but not due to M2 macrophage infiltration. Therefore, other cell types likely contribute to this cellular influx (e.g., M1 macrophages, Pax7+ satellite cells) and will be evaluated in the future. pFUS likely presented no change in cellularity due to the delayed onset of its pro-inflammatory response and this could be studied by assessing cellularity 48- or 72-hours after treatment. Citations: [1] Burks+ Stem Cells 2013. [2] Frank+ Cytotherapy 2015. [3] Tebebi+ Stem Cells 2015.

Acknowledgment/Funding Sources: This research was funded by the Intramural Research Programs of the Clinical Center and the National Institute of Biomedical Imaging and Bioengineering at the National Institutes of Health.

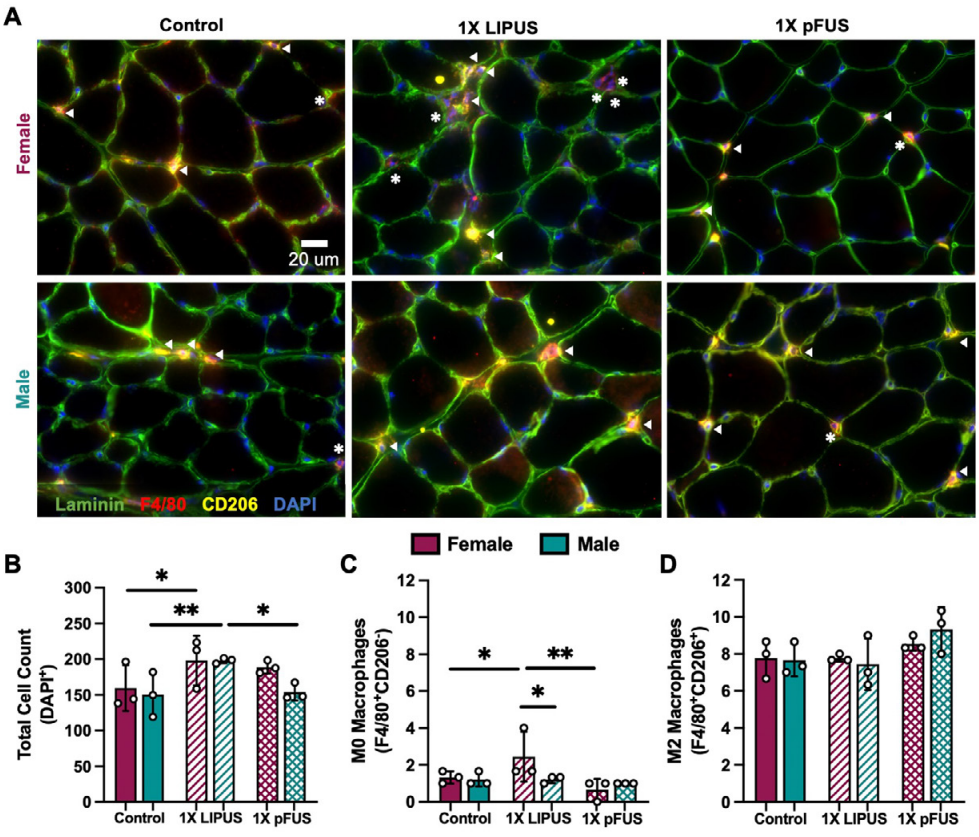

Figure 2. [A] Gastrocnemius stained 24-hours after 1X LIPUS or 1X pFUS. M0 macrophages = F4/80+CD206- (*). M2 macrophages = F4/80+CD206+ (triangle). Counted from these images: total cells [B] and M0 [C] and M2 [D] macrophages. (* $p < 0.05$, ** $p < 0.005$).

MSK-02-YI

Topic: Musculoskeletal
Presentation Type: Oral

A 10-Year Multicenter Experience of MR-Guided High Intensity Focused Ultrasound (MRgFUS) in 105 Patients with Extra-Abdominal Desmoid Tumors

Daniel Düx[1], Joe D. Baal[2], Rachelle Bitton[3], Joshua V. Chen[2], Ryan Brunsing[2], Vipul Sheth[2], Jarrett Rosenberg[2], Kisoo Kim[2], Eugene Ozhinsk[28], Raffi Avedian[4], Kirsten Ganjoo[5], Matthew Bucknor[2], Andrew Dobrotwir[6], Pejman Ghanouni[3]

[1]University of Hannover (MHH), Hannover, Niedersachsen, Germany
[2] University of California, San Francisco, San Francisco, CA, USA
[3]Stanford University, Palo Alto, CA, USA
[4]Stanford Medicine Outpatient Center, Stanford, CA, USA
[5]Stanford Health Care, Stanford, CA, USA
[6]MR Focused Ultrasound Center, Future Medical Imaging Group, Victoria, Victoria, Australia

Background: Desmoids are locally aggressive soft tissue tumors in mainly young patients, sometimes with highly progressive/recurrent growth (1-6). Observation, surgery (7, 8), radiation (9-11) and medication (12-18) may lead to high morbidity (18).

Materials and Methods: This multicenter 10-year retrospective review (2011-2021) of MRgFUS for biopsy-proven extra-abdominal desmoids was approved by the ethic committee at each institution. After multi-disciplinary evaluation, patients were treated with ExAblate 2100 (INSIGHTEC, Israel) coupled to a 3T MRI (GE Healthcare, USA). Patient demographics, prior/additional therapy, technical parameters, symptoms, tumor volume/diameter and complications were reviewed. Total tumor/viable tumor volume (TTV/VTV) were calculated on pre- and post-ablation MRI with Horos (Nimble Co LLC d/b/a Purview, USA). Response and progression-/recurrence-free survival were assessed with RECIST v.1.1 (19) and mRECIST (20), based on maximal and enhancing tumor diameter, respectively. Pain and quality of life were assessed via Numerical Rating Scale (NRS) (21) and RAND 36-Item Short Form Health Survey (22), respectively. Complications were graded per the Society of Interventional Radiology Adverse Event Severity Scale (23). Endpoints were evaluated with GraphPad Prism (GraphPad Software, USA) and Stata 16.1 (StataCorp LP, College Station, TX). Baseline was compared to the last available follow-up or date of tumor progression, when patients had subsequent therapy other than MRgFUS, and tested with a two-sided Wilcoxon matched-pairs signed rank test (p?0.05). SF-36 scores were evaluated with p-values adjusted using the Holm method.

Results: 105 patients (median age: 35, range 3-66, 79 females) were treated in 162 sessions (Figure 1). Median energy per sonication was 1727J (range 118-7897J). Therapies prior to MRgFUS and after (median 11 months) are summarized in Figure 2. The median TTV was 114mL (range 1-2000mL, n=161) at the day of MRgFUS, of which a median of 84.5mL (range 1-570mL, n=154) was targeted. 83% (IQR 31%) of the targeted tumor was ablated, representing 57% (IQR 45%) of the TTV. Follow-up is stated in Figure 3. At last follow-up (median 15 months (IQR 30 months)), median TTV decreased to 51mL (IQR 204mL, n=101, p<0.0001) and VTV decreased to 28.5mL (IQR 98mL, n=88, p<0.0001). For total tumor at last follow up (18 months), 86% of patients had stable disease or better response, although small viable tumor nodules were progressing in 50% (Table 1). Often, non-targeted or residual viable tumor regrew into the ablation cavity, while the overall tumor was stable or shrinking. At a median follow-up of 6 (range 1-84) months, the median NRS decreased from 6 (IQR 3) to 3 (IQR 4, p<0.001). Mental and physical health significantly improved from 49 (IQR 17) to 53 (IQR 9, p=0.02) and 41 (IQR 15) to 46 (IQR 12, p=0.05). The complication rate

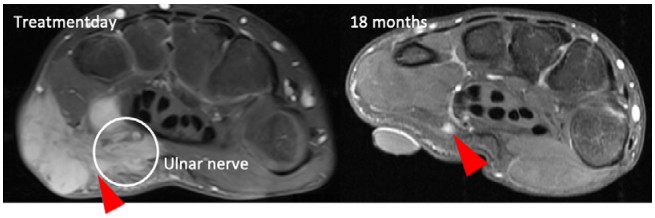

Figure 1. Post-contrast imaging at the treatment day and at last follow-up with MRI. 58% were ablated (area around ulnar nerve spared). Pain pre-MRgFUS: 2/10, pain at 5 years post-MRgFUS: 0/10.

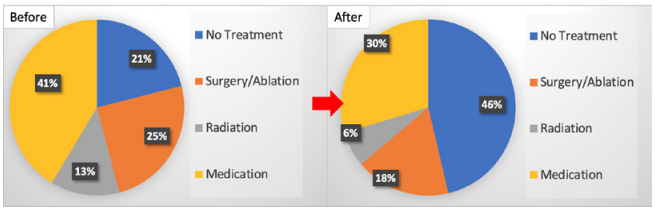

Figure 2. Shown are new therapies after MRgFUS (excluding repeat MRgFUS). After MRgFUS, surgery, medication and radiation were used less often. Patients often had multiple therapies in combination.

was 37% (79 complications in 60 treatments); 50/79 (63%) were mild, 15/79 (19%) moderate and 14/79 (18%) severe. Skin burns were the most common complication (43/79 (54%)). Passive skin cooling techniques during MRgFUS reduced this incidence by 46% (p=0.03). Nerve palsy occurred in 21/79 (27%), 4/21 (19%) of which were due to positioning. Complications resolved in all patients (3 lost to follow-up), with 7 needing surgery for severe burns.

Conclusions: MRgFUS is effective for desmoids, with reasonable safety profile compared to other therapies. Consistent insurance authorization might improve outcomes, as many with residual/recurrent viable tumor may have benefited from additional MRgFUS. The National Comprehensive Cancer Network (NCCN) included ablation as primary/salvage option for desmoids in 2020 (24). An active skin cooling device (not available in our cohort) has been introduced for skin burn reduction (25).

Acknowledgment/Funding Sources: I thank the Focused Ultrasound Foundation, who generously granted me a traveling scholarship as researcher in Stanford University 2021.

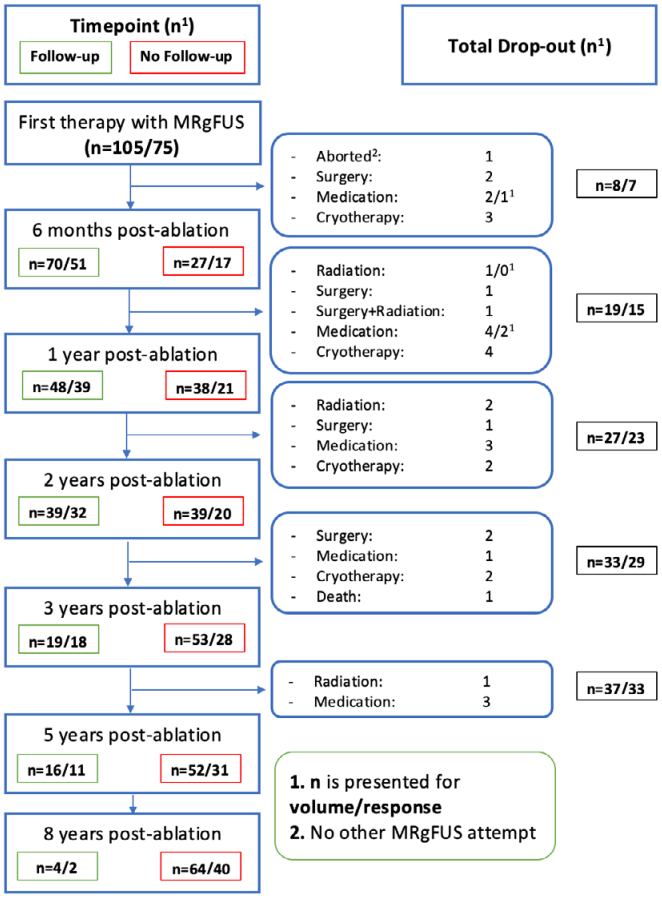

Figure 3. Follow-up (in green) and missing follow-up (in red) for both tumor volumes and response on the left side. Reason for exclusion in the middle. Total excluded patients at given time point on the right side.

RECIST	Best Response				Months	Latest Response				Months
	CR	PR	SD	PD		CR	PR	SD	PD	
n	5	18	44	2	16	5	16	38	10	18
%	7%	26%	64%	3%		7%	23%	55%	14%	
Progression-free survival										17
mRECIST	Best Response				Months	Latest Response				Months
	CR	PR	SD	PD		CR	PR	SD	PD	
n	12	36	2	18	11	9	23	2	34	17
%	18%	53%	3%	26%		13%	34%	3%	50%	
Progression-free survival										13
Recurrence-free survival										20.5

Figure 4. Complete response, partial response, stable disease, progressive disease and PFS are summarized for RECIST and mRECIST. 11 patients had PD in between sessions but ultimately responded with repetition of MRgFUS.

MSK-03

Topic: Musculoskeletal
Presentation Type: Oral

Histotripsy Bubble Dynamics in Anisotropic Hydrogels and Bovine Tendon

Jacob Elliott, Julianna Simon, Andrea Arguelles

The Pennsylvania State University, State College, PA, USA

Background: Collagenous, anisotropic tissues such as tendon have demonstrated resistance to liquefaction by histotripsy, despite the creation, oscillation and collapse of bubbles verified using B-mode imaging. The objective of this work is to evaluate effects of anisotropy on bubble dynamics in transparent, tissue-mimicking hydrogels and compare to anisotropic tissues.

Materials and Methods: Polyacrylamide (PA), fibrin, and collagen hydrogels were created, and ex vivo bovine deep digital flexor tendons were obtained. Using 1.0-MHz contact transducers, sound speeds were measured in each axial direction to determine degree of anisotropy (or the ratio of axial elastic moduli). Hydrogels and tendons were treated with 1.5-MHz focused ultrasound using conventional boiling histotripsy parameters of 10-ms pulses repeated at 1-Hz with p+=89 MPa, p-=26 MPa. For all hydrogel samples, cavitation activity was monitored using simultaneous high-speed photography and passive cavitation imaging with a Philips/ATL L7-4 transducer and Vantage® ultrasound system. Tendon samples were only monitored using passive cavitation imaging.

Results: Substantial cavitation activity (Fig. 1) and hydrogel fractionation was observed in PA, collagen, and fibrin hydrogels. PA gels demonstrated low elastic moduli (E = 2.54 GPa) compared to collagen (E = 4.86 GPa) and fibrin (E = 3.28 GPa), and all gels demonstrated low degrees of anisotropy (<1.2). This is highly dissimilar to what was observed in tendon (axial elastic modulus = 1.37 GPa, degree of anisotropy = 19.4). Dehydrating fibrin gels by evaporating >90% water content resulted in a 55% reduction in cavitation emission energy (0.66 ± 0.5 [x1010 V2])) compared to standard fibrin gel formulations (1.48 ± 0.6 [x1010 V2]), with a 43% increase in elasticity and 795% increase in degree of anisotropy (9.54 ± 4.18).

Conclusions: Dehydrated fibrin gels demonstrated similar cavitation emission energies to tendon (within 4%), although anisotropy was approximately 50% lower in dehydrated fibrin compared to tendon. These results suggest that dehydrated fibrin gels may allow for a thorough investigation of cavitation bubble dynamics in anisotropic tissues, like tendon, which is essential towards the development of histotripsy-based clinical treatments for these tissues.

Acknowledgment/Funding Sources: This work is supported by National Institutes of Health (Grant R21EB027886).

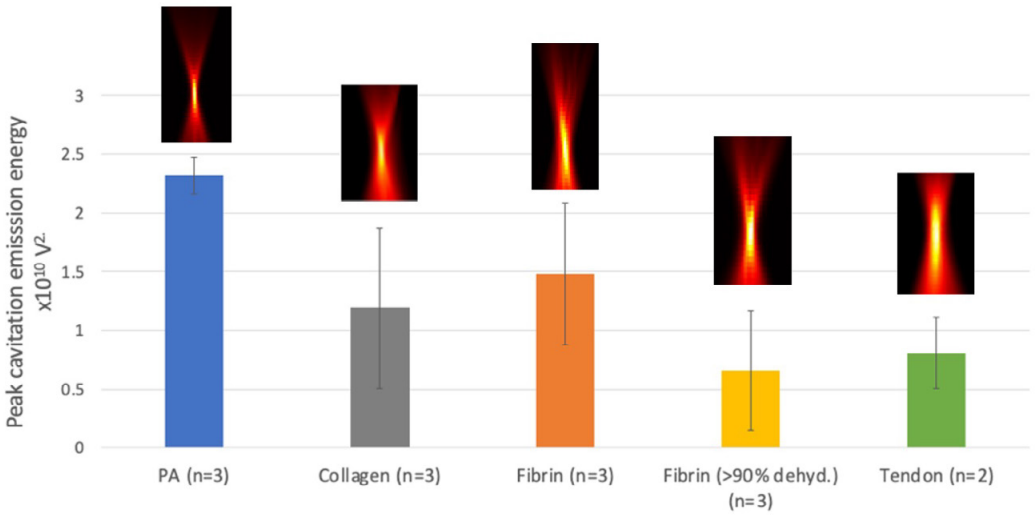

Figure 1. Peak cavitation emission energies for hydrogels and bovine tendons with representative passive cavitation images

MSK-04

Topic: Musculoskeletal
Presentation Type: Oral

Exploration of Patient Eligibility for the Palliative Treatment of Non-spinal Bone Metastases Using MRI-Guided High Intensity Focused Ultrasound (MR-HIFU)

Renée Hovenier[1], Jorik Slotman[1], Derek Mersch[1], Clemens Bos[1], Wilbert Bartels[1], Joost J. Verhoeff[1], Nicolien Kasperts[1], Erik Phernambucq[2], Martijn F. Boomsma[3], Chrit T. Moonen[1], Helena M. Verkooijen[1]

[1]University Medical Center Utrecht, Utrecht, Utrecht, Netherlands
[2]Isala Hospital, Utrecht, Utrecht, Netherlands
[3]Isala Hospital, Zwolle, Overijssel, Netherlands

Background: Cancer-induced bone pain is the most common symptom in patients with advanced cancer1-2. Bone pain limits daily functioning and reduces quality of life2-3. The current standard local treatment of painful bone metastases is external beam radiotherapy (EBRT), which takes up to four weeks to induce maximal pain relief3-5. Moreover, RT does not induce palliation in 30-40% of the patients3-5. Magnetic Resonance-guided High Intensity Focused Ultrasound (MR-HIFU), which has been shown to induce fast pain relief, may improve pain palliation in the non-spinal patient subpopulation6. Since the role of MR-HIFU as a first-line treatment option of bone metastases is still unclear, studies are being conducted to compare MR-HIFU with standard treatment (EBRT), including the FURTHER-trial (three-armed European multicenter randomized controlled trial)7-8. Compared to EBRT, MR-HIFU in bone metastases is more complicated due to the complexity of the intervention, the need for sedation or anesthesia, and the technical constraints of the treatment. Therefore, to assess the potential role of MR-HIFU in palliation of bone metastasis, ascertaining the proportion of eligible patients is important. Insight in the causes of ineligibility will help navigate further research and development aiming at increasing the availability and accessibility of MR-HIFU. The aim of this study was to estimate the proportion of all patients with non-spinal bone metastases eligible for MR-HIFU as an alternative to the standard local palliative treatment (EBRT), and examining causes of ineligibility.

Materials and Methods: In this prospective exploratory study, the Radiotherapy Departments in the University Medical Center Utrecht (UMCU) and Isala Hospital in Zwolle (Isala) participated, as part of the FURTHER-trial7-8. In UMCU, all patients referred for radiotherapy treatment of painful non-spinal bone metastases between January 2022 and May 2022 were included in the analysis. In Isala, patients referred for painful bone metastases between September 2020 and October 2021 were included in the analysis, after protocolled preselection by a medical planner who excluded spinal metastases, lymphoproliferative disorders or hospitalized patients. All patients were assessed for eligibility for MR-HIFU

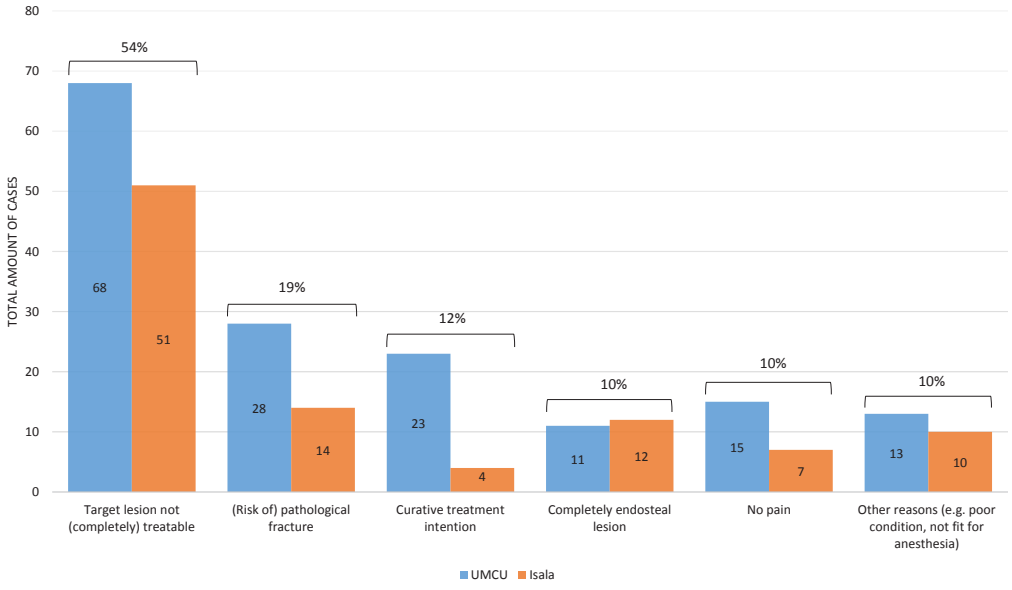

Figure 1. Ineligibility causes for MR-HIFU as alternative to EBRT for patients with painful non-spinal bone metastases in University Medical Center Utrecht (UMCU) and Isala Hospital (Isala). For each patient, the main reason(s) of ineligibility was/were reported.

by a team consisting of radiation oncologists, radiologists and clinical researchers. For each ineligible patient, the main reason(s) of ineligibility was/were reported.

Results: Overall, 246 non-spinal bone metastasis patients were screened for eligibility for MR-HIFU treatment (143 in UMCU, and 103 in Isala), resulting in 256 noted ineligibility causes. MR-HIFU could serve as an alternative treatment for EBRT in 24 patients (10%), of which 7 were not willing to undergo MR-HIFU. The other patients were ineligible based on one (or more) exclusion criteria, in which 'target lesion not (completely) treatable' (54%) concerned the largest group, followed by '(risk of) a pathological fracture' (19%), and 'oligometastasis with curative treatment intention' (12%). All other causes are categorized in Figure 1. Note that the total percentages add up to over 100%, because more than one reason could be noted for each patient.

Conclusions: In ten percent of patients with painful non-spinal bone metastases referred to two Dutch Radiotherapy Departments, MR-HIFU could possibly serve as a stand-alone treatment. The main causes for ineligibility seems to be related to inherent technical limitations of the MR-HIFU treatment modality (e.g. unreachable lesion, too extensive metastatic disease). During data acquisition of this exploratory study, only the most prominent appearing reason(s) of ineligibility has been collected. Therefore, these prominent causes may have caused underreporting of other less prominent ineligibility reasons, and a systematic study in a focused cohort is needed to assess the prevalence of these causes. In addition, the eligibility of patients for MR-HIFU combined with EBRT could be investigated to examine the potential of this combination treatment in local palliation of non-spinal bone metastases.

Acknowledgment/Funding Sources: Financial support for the FURTHER study was provided by the European Union's Horizon 2020 research and innovation programme under grant agreement No 825859.

References

1. Chow E, Harris K, Fan G, et al. Palliative radiotherapy trials for bone metastases: a systematic review. J Clin Oncol 2007;25(11):1423-36.

2. Han X, Huang R, Meng T, et al. The Roles of Magnetic Resonance-Guided Focused Ultrasound in Pain Relief in Patients With Bone Metastases: A Systemic Review and Meta-Analysis. Front Oncol 2021;11:617295.

3. Westhoff PG, de Graeff A, Monninkhof EM, et al. Quality of Life in Relation to Pain Response to Radiation Therapy for Painful Bone Metastases. Int J Radiat Oncol Biol Phys 2015;93(3):694-701.

4. Simoes Correa Galendi J, Yeo SY, Simic D, et al. A time-driven activity-based costing approach of magnetic resonance-guided high-intensity focused ultrasound for cancer-induced bone pain. Int J Hyperthermia 2022;39(1):173-80.

5. Linden YMvd, Lok JJ, Steenland E, et al. Single fraction radiotherapy is efficacious: a further analysis of the Dutch Bone Metastasis Study controlling for the influence of retreatment. Int J Radiat Oncol Biol Phys 2004;59(2):528-37.

6. Hurwitz MD, Ghanouni P, Kanaev SV, et al. Magnetic resonance-guided focused ultrasound for patients with painful bone metastases: phase III trial results. J Natl Cancer Inst 2014;106(5).

7. Verkooijen, H.M. (2020, March – 2024, June). *Focused Ultrasound and RadioTHERapy for Noninvasive Palliative Pain Treatment in Patients With Bone Metastases (FURTHER)*. Identifier NCT04307914. https://clinicaltrials.gov/ct2/show/NCT04307914.

8. Horizon 2020 (2018). *Focused Ultrasound and RadioTHERapy for Noninvasive Palliative Pain Treatment in Patients with Bone Metastasis (FURTHER)*. Grant agreement ID 825859. https://cordis.europa.eu/project/id/825859.

MSK-05

Topic: Musculoskeletal
Presentation Type: Oral

Investigation of Focused Ultrasound Therapy for Tendinopathies in an In Vivo Murine Model

Molly Smallcomb, Sujata Khandar, Jacob Elliott[3], Meghan Vidt, Julianna Simon

The Pennsylvania State University, University Park, PA, USA

Background: Over 30 million patients are diagnosed with tendinopathies in the US each year. Conservative therapies, like dry needling (DN), induce microdamage to promote healing but reported success rates are mixed. We recently reported a narrow range of focused ultrasound (fUS) parameters that create mild mechanical disruption in ex vivo murine tendons (Smallcomb, IEEE UFFC 2021). The objective of this study is to compare fUS to DN in an in vivo murine tendinopathy model.

Materials and Methods: Tendinopathy was induced in 28 rats by partially transecting the Achilles tendon in one randomly selected limb; the contralateral limb served as control. Tendons were treated one week post-surgery with either DN (30G needle, 5 fenestrations over 20 sec) or fUS (1.5 MHz, 1-ms pulses at 10 Hz for 106 sec with p+=49MPa, p-=19MPa) and survived for one week. Blood was collected immediately before and after treatment and before euthanasia for analysis of growth factors IGF-1, VEGF-A, and TGF-?. Tendons were harvested and prepared for mechanical testing (13 rats) or histological analysis (15 rats).

Results: No differences were observed between DN- and fUS-treated rats in the release of growth factors IFG-1, and TGF-? (Fig. 1a); VEGF-A levels were too low to be detectable for all time points in all animals. Histologically, DN- and fUS-treated tendon showed similar fibroblast infiltration (Fig 1b), indicative of the inflammatory stage of healing. Results from mechanical testing show stiffness and percent relaxation of fUS-treated tendons were similar to controls, whereas stiffness and percent relaxation of DN-treated tendons were lower than controls (p=0.0041 and p=0.0441, respectively; Fig 1c).

Conclusions: As fUS performed the same or better than DN in the release of growth factors, infiltration of fibroblasts, and maintenance mechanical properties, fUS may be a viable non-invasive alternative to DN for treatment of tendinopathies.

Acknowledgment/Funding Sources: This work was funded by the National Institutes of Health – National Institute of Biomedical Imaging and Bioengineering (R21EB027886); the NSF Graduate Research Fellowship (Smallcomb; Grant # DGE1255832).

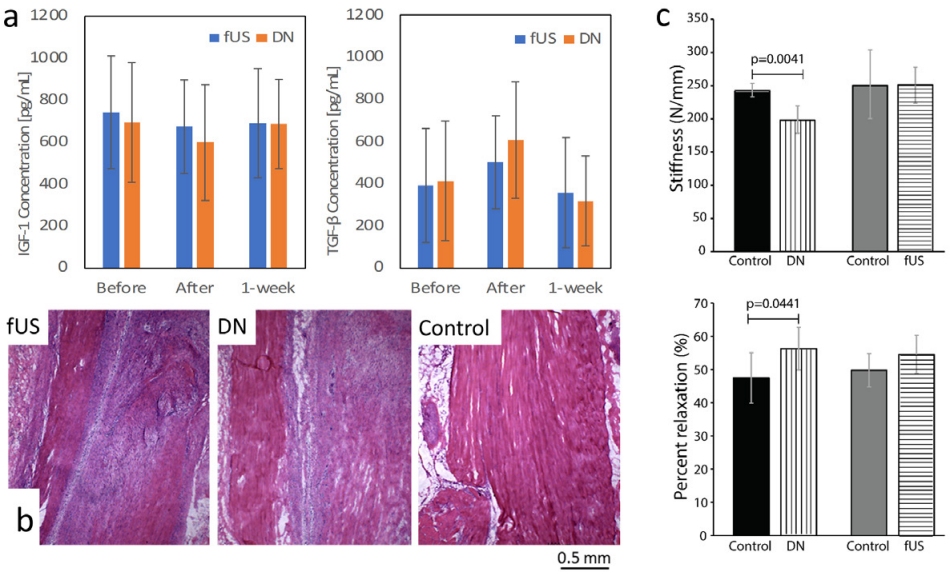

Figure 1. a) Concentration of IGF-1 and TGF-? growth factors immediately before, after, and 1-week after treatment. b) H&E histology images of fUS-, DN-treated, and control tendons. c) Stiffness and percent relaxation from mechanical testing of control, D

MSK-06

Topic: Musculoskeletal
Presentation Type: Oral

High Intensity Focused Ultrasound Thermal Ablation and Boiling Histotripsy in Combination with Checkpoint Inhibitors for the Treatment of Murine Sarcomas

Caitlin Tydings, Yarmolenko Pavel, Karun Sharma, AeRang Kim

Children's National Hospital, Washington, DC, USA

Background: Immunotherapy has revolutionized cancer therapy; however, pediatric solid tumors are largely considered to be nonimmunogenic and therefore less responsive to immunotherapy. High intensity focused ultrasound (HIFU) may amplify anti-tumor effects by causing a local inflammatory response, increasing antigen presentation and T cell activation against tumor antigens. Prior work showed a survival benefit with increased anti-tumor cytokine and cellular response treating refractory neuroblastoma with HIFU boiling histotripsy (BH) in combination with checkpoint inhibitors (CPI), ?CTLA-4 + ?PD-L1. However, a subsequent study using HIFU thermal ablation (ablation) in the same neuroblastoma model did not show a similar survival benefit. To determine if HIFU + CPI can also provide survival benefit in other pediatric tumors, we aimed to evaluate the effect of HIFU (BH and ablation) combined with CPI in a murine model of rhabdomyosarcoma (RMS), another common pediatric solid tumor.

Materials and Methods: RMS tumors were established following a subcutaneous injection of M3-9-M cell line (0.125 x106 cells) in the hind leg of C57BL/6J mice. Once longest tumor diameter reached 12mm-15mm, mice were treated with 1) ablation alone (n =40), 2) BH alone (n = 42), 3) ablation + CPI (n = 31), 4) BH + CPI (n = 34), 5) CPI alone (n = 33) or 6) control (n = 36). CPI (100?g per dose) were injected intraperitoneally on days 1, 4 and 7 after HIFU therapy or once tumors reached goal size in CPI only group. Mice were anesthetized, positioned on a holder stage and HIFU was performed with a 1.5 MHz transducer (BH using 13.33ms pulse at 1Hz pulse repetition frequency; ablation at 170mVpp). HIFU was guided by b-mode ultrasound imaging and was performed at three adjacent foci (5 sec/focus for ablation and 15 sec/focus for BH). Survival was measured for all treatment groups with endpoints being euthanasia due to deteriorating clinical status or tumor size >20mm in longest diameter. ELISA for cytokines was performed on serum obtained by cardiac puncture, and flow cytometry was performed on the tumors, draining and contralateral lymph nodes and spleen at 24, 48 and 72h after treatment.

Results: A long-term (>100 days) survival benefit was significant ($p<0.1$, log rank test) in mice treated with BH + CPI (64%) vs BH alone (10%) and control (0%); ablation + CPI (46%) vs ablation alone (0%) and control (0%); and CPI alone (31%) vs control (0%). CD8+T cells were upregulated in the tumor following all combination treatments and CPI alone at all time points, but not in the tumor following ablation and BH alone. PD1+ CD8 T cells were most notable in the spleen at all times following BH and ablation with CPI. Regulatory T cells (CD4+FOXP3+) were noted more in spleen following treatment used in combination with or CPI alone, including at 24 and 48 h after ablation + CPI as well as at all time points following BH + CPI and CPI alone. There was an upregulation of dendritic cells in the spleen after ablation and BH alone only at 24 h, but these effects were prolonged in the combination and CPI alone arms up to 72 h. Ablation alone led to a significant increase in CXCL10, IL-6 and KC/GRO. Combination of ablation with CPI increased IL-15, MCP-1, MIP-2 and VEGF-a were increased. BH alone increased CXCL10 and the combination of BH + CPI increased MCP-1. CPI alone increased IL17a/f, IFN-y, IL12p70 and IL-2.

Conclusions: Ablation and BH in combination with CPI led to a statistically significant survival benefit over HIFU alone (ablation or BH) and control animals. However, CPI alone also provided a statistically significant survival benefit, though inferior to that achieved with BH + CPI. Combinatorial approaches and CPI alone led to the upregulation of CD8+ T cells in the tumor, dendritic cells in the spleen, chemoattractants and proinflammatory cytokines. The findings of survival benefit after BH + CPI in rhabdomyosarcoma extend previous results seen in neuroblastoma. We are in the process of evaluating more aggressive/metastatic rhabdomyosarcoma cell lines as well as osteosarcoma cell lines to determine if there is broader applicability of this treatment in advanced pediatric solid tumors.

Acknowledgment/Funding Sources: Focused Ultrasound Foundation Center of Excellence Award

MSK-07

Topic: Musculoskeletal
Presentation Type: Oral

Preclinical and Clinical Assessment of Ultrasound Beam Shaping for MR-HIFU of Low Back Pain

Sin Yuin Yeo[1], Pia Rademann[2], Simo Kustaanheimo[3], Alexandra C. Simon[2], Simon Hubertus[3], Raimund Jung[3], Lukas C. Sebeke[2], Holger Grüll[2]

[1]University Hospital of Cologne/Profound Medical GmbH, Hamburg, Germany
[2]University Hospital of Cologne, Nordrhein-Westfalen, Germany
[3]Profound Medical GmbH, Cologne, Nordrhein-Westfalen, Germany

Background: Low back pain is the leading cause of disability worldwide with facet joint syndrome (FJS) being one of the main causes. Current treatments for chronic FJS include intraarticular injection of corticosteroids and/or analgesics, infiltration of the segmented medial branch nerves (MBNs) and intraoperative RF ablation of the MBNs. However, these treatments have mixed therapeutic outcome, expose patients to risks of infection and bleeding, ionizing radiation when fluoroscopic guidance is used and are invasive. As available treatments are strictly symptomatic treatments, recurrent pain and dysfunction are anticipated. Hence, it is important to provide an alternative non-invasive treatment option. Preliminary results have shown that Magnetic Resonance-guided High Intensity Focused Ultrasound (MR-HIFU) is a non-invasive, ionizing radiation-free thermal therapy that provides pain relief for patients with FJS. There are two MR-HIFU treatment approaches: targeting the facet joints (FJs) or medial branch nerves (MBNs). One of the clinical challenges for these approaches is the narrow acoustic access, for example at the L5/S1 FJ level, between the spinous process and pelvic bone or at the juncture of the superior articular process and transverse process, which has narrowed due to FJS-induced morphological changes (MBN targeting). The aim of this study is to assess the feasibility of an ultrasound beam shaping approach to efficiently ablate FJs and MBNs while sparing adjacent structures using a gel phantom, a preclinical swine model and a 3D-printed clinical lumbar spine model.

Materials and Methods: The experiments were divided into 3 parts. Firstly, using a polyacrylamide-based gel phantom, the feasibility to shape the HIFU beam, i.e. turning off <50% transducer elements, and the resulting focus quality were evaluated. Sonications were performed using 8mm treatment cells, different powers (40-190W), 20s sonication duration, and 1.2MHz sonication frequency on a Sonalleve V2 MR-HIFU system (Profound Medical, Canada). Then, the percentage of active transducer elements and sonication parameters that led to good focus quality were assessed in vivo in 3 landrace pigs. For each pig, 4-5 FJs or MBNs were sonicated with and without beam shaping using 8mm treatment cells, 100W acoustic power, 20s sonication duration, and 1.2MHz sonication frequency. T1-weighted contrast-enhanced images were used to evaluate intended and unintended non-perfused volume (NPV). Histology was performed to assess tissue damage. Finally, the feasibility to beam shape and ablate was investigated in a clinically relevant human lumbar spine model, which was 3D printed, cast with bone-mimicking polyurethane and embedded in tissue-mimicking material. FJs and MBNs were sonicated and the temperature increase and thermal dose in situ and on adjacent structures was evaluated.

Results: In the gel phantom study, good focus quality was observed at the target spot when <50% transducer elements were switched off. In vivo, ablative temperatures were noted in the soft tissue adjacent to FJs and MBNs. NPVs were present at the intended target location, while no NPVs were observed in structures, such as the spinous processes or pelvic bone, in the near-field beam path. Histology results confirmed tissue damage at FJs and MBNs. In the 3D printed spine, ablative temperatures of ? 57°C were reached at the MBNs and soft tissue adjacent to FJs. No ablative temperatures or thermal dose above 30CEM43 was seen on the pelvic bone and spinous processes, suggesting no thermal damage to these structures. Figure 1 shows

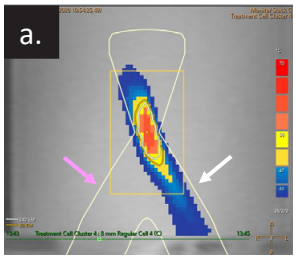

Figure 1. MR-HIFU ablation with beam shaping in a gel phantom. Pink arrows = absence of temperature increase in the beam path with transducer elements switched off. White arrows = temperature increase in beam path with transducer elements switched on.

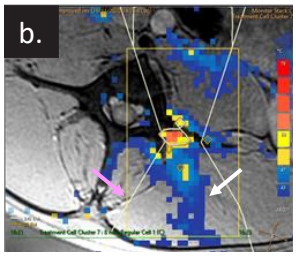

Figure 2. MR-HIFU ablation with beam shaping in swine model. Pink arrows = absence of temperature increase in the beam path with transducer elements switched off. White arrows = temperature increase in beam path with transducer elements switched on.

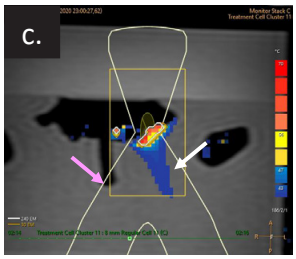

Figure 3. MR-HIFU ablation with beam shaping in 3D-printed lumbar spine model. Pink arrows = absence of temperature increase in the beam path with transducer elements switched off. White arrows = temperature increase in beam path with transducer elements switched on.

representative images of ablation with beam shaping in gel phantom, in vivo and in clinically relevant model.

Conclusions: Beam shaping is feasible and led to more focused ablation at the target while sparing the structures along the beam path. A clinical trial evaluating MR-HIFU for non-invasive thermal therapy of FJS will start patient recruitment at the University Hospital of Cologne. Depending on patient enrollment, preliminary clinical data may be presented.

Acknowledgment/Funding Sources: This work was supported by the German Federal Ministry of Education and Research ("Schmerz im Fokus", FKZ: 13GW0337A and 13GW0337D).

NDG-01

Topic: Neurodegenerative Disorders

Presentation Type: Oral

Achieving Controllable In-Vitro FUS Neurostimulation for Investigation of Its Underlying Mechanisms through Calcium Fluorescence Imaging

Tom Aubier[1], Ivan M. Suarez Castellanos[1], Magali Perier[1], Alexandre Carpentier[2], W. Apoutou N'Djin[1]

[1]LabTAU, INSERM, Université Lyon [1], Lyon, Rhône, France
[2]Hôpitaux Universitaires La Pitié Salpêtrière, Paris, Paris, France

Background: Focused UltraSound (FUS) has the potential of offering a minimally-invasive and targeted alternative to standard neurostimulation strategies. The nature of the mechanisms underlying the effects of FUS stimulation on neural structures remains however largely unknown. To investigate the nature of these mechanisms at the cellular level, an experimental approach was established to achieve highly repeatable and spatially selective single pulse stimulations on in-vitro human neural cells. Calcium ions being one the most prevalent secondary messenger in living cells, the spatiotemporal dynamics of Ca2+ mobilization is studied to assess the signaling processes occurring after FUS stimulation.

Materials and Methods: Experiments were performed on Human neural progenitors (ReNcell-VM) plated on 35mm Petri dishes and labelled with a Ca2+-sensitive fluorescent marker (Fluo-4). The experimental setup was built on an inverted microscope allowing the assessment of the cellular network calcium signaling activity. FUS stimulations consisted of a single-pulse (pRMS < 2.5 MPa), applied using a custom-made focused transducer (øTX : 15mm) capable of being driven at various harmonic frequencies (~n·f0 with n = [1, 3, 7, 11] and f0 = 727 kHz). To achieve the induction of neural activity in a controllable manner, FUS stimulation parameters were determined to promote the generation of neural responses through radiation force effects rather than cavitation. While both of these effects are discussed in the literature as being potentially involved in the occurrence of ultrasound neurostimulation, radiation force based processes are much less challenging to control, setting the stage to better repeatability and spatiotemporal selectivity.

Results: Using a fixed pulse duration of 400µs across a range of frequencies from 0.73 to 8.14 MHz, FUS stimulation parameters have been identified to achieve the quasi-systematic triggering of neural responses while minimizing the applied acoustic power (success rate: 80% over the 45 latest trials). At equivalent neuron activation success rates, it was found that the use of higher frequencies allows for a reduction of the area undergoing the mechanical effects of the radiation force (fig a1-a3) while significantly decreasing the occurrence of cavitation events (fig b). These parameters allowed for the immediate activation of clusters of cells (øcluster: 1.96mm - 205µm) located within the FUS focal spot (øFUS-focal: 2mm - 181µm respectively) which were manifested by strong and sustained elevations in intracellular Ca2+ (fig c1). Omnidirectional Ca2+ fluxes were subsequently observed extending around the initial response and propagating throughout the neural network at an estimated velocity of 6 µm·s-1(fig c2 and d).

Conclusions: The preliminary results obtained in this study indicate that FUS is capable of inducing causal neural activity repeatedly and with acute spatiotemporal selectivity. Over the course of a few tens of seconds, network-wide effects on neurons located beyond the targeted region were also be observed. Overall, the spatial-temporal control achieved with this setup should provide meaningful insights on the nature of the mechanisms involved in ultrasound neurostimulation.

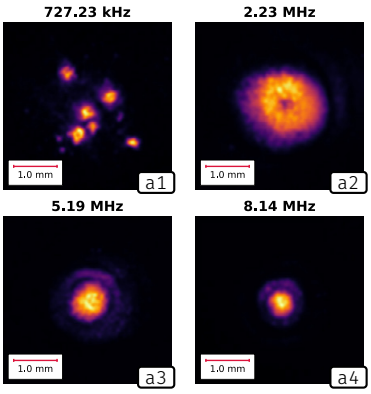

Figure a. Spatial distribution of the displacement caused by the acoustic radiation force estimated within the microscope field of view by particle image velocimetry. a1 illustrates the occurence of inertial cavitation taking place at low frequency.

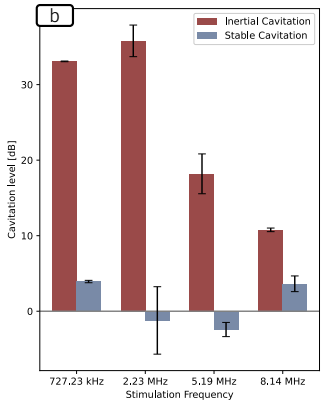

Figure b. Inertial and stable cavitation indexes estimated on successful stimulations events for a range of transducer harmonic frequencies.

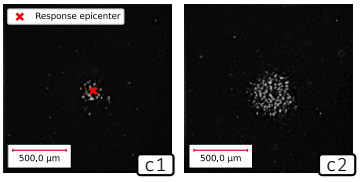

Figure c. FUS-induced Ca2+ fluxes in in vitro Human neural cells at t = 1s (c1) and t = 10s (c2).

Acknowledgment/Funding Sources: This project was supported by the French National Research Agency (ANR-16-TERC-0017 & ANR-21-CE19-0007-01), the Focused UltraSound Foundation (LabTAU, FUSF Center of Excellence), LabEx DevWeCan and LabEx Cortex.

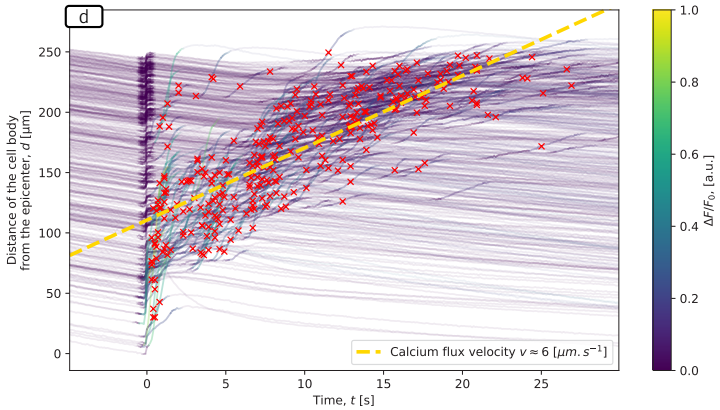

Figure d. Network-wide flux velocity estimated (in yellow) from the spatiotemporal distribution of the cell Ca2+ responses (red crosses).

NDG-02

Topic: Neurodegenerative Disorders

Presentation Type: Oral

Effects of Focus Ultrasound on CNS Uptake and Efficacy of an Anti-pyroGlu3 Abeta Antibody in Aged Alzheimer's Transgenic Mice

Praveen Bathini[1], Tao Sun[1], Qiaoqiao Shi[1], Yongzhi Zhang[2], Nadine Taudte[3], Mathias Schenk[3], Thore Hettmann[4], Stephan Schilling[5], Nathan McDannold[3], Cynthia A. Lemere[1]

[1]Brigham and Women`s Hospital/Harvard Medical School, Boston, MA, USA
[2]Brigham and Women's Hospital, Boston, MA, USA
[3]Fraunhofer Institute for Cell Therapy and Immunology, Leipzig, Sachsen, Germany
[4]Vivoryon Therapeutics AG, Halle (Saale), Sachsen-Anhalt, Germany
[5]Fraunhofer Institute for Cell Therapy and Immunology, Halle (Saale), Sachsen-Anhalt, Germany

Background: Currently, therapeutic agents targeting amyloid appear promising for Alzheimer's disease (AD), however, treatment options have limited efficacy and transiently improve cognitive symptoms in a minor of patients. Also, delivery of such therapeutics to the brain is limited due to the blood-brain barrier (BBB), stressing the need for effective dosing protocols without any side effects related to amyloid-related imaging abnormalities (ARIA). The failure of many anti-amyloid trials stimulated research on alternative treatments, of which Focused ultrasound (FUS) is one such method to induce a temporary opening of the BBB to enhance the delivery of therapeutic agents to CNS. Previously, we demonstrated that passive immunotherapy with an anti-pyroGlu3 A? antibody, 07/2a, lowered plaques and lessened cognitive decline in an AD-like mouse model. Here, we used FUS with intravenous injection of microbubbles, to open the BBB transiently and focally to enhance the intravenous delivery of the antibody. We studied the effect of single treatment and 3 weekly treatments of FUS and antibody combination treatment to understand the antibody delivery to the brain, its effect on plaque clearance, cognition and associated immune responses.

Materials and Methods: First, 24 mo-old APP/PS1dE9 mice were i.v. infused with a single dose of 300 ?g 07/2a (a gift from Probiodrug AG, Halle, Germany) with or without cerebral FUS sonication (n=5/group). These mice were assigned into two groups 1) "Unilateral FUS" where mice received 07/2a mAb i.v. and sonication on the mouse's right hemisphere. Mice were euthanized either 4 hr (n=5) or 72 hr (n=4) after mAb infusion. 2) "Bilateral FUS" where mice received 07/2a mAb with or without bilateral sonication and euthanized 4 or 72 hrs later (n=5). Controls received mAb alone. For all experiments, FUS was applied under anesthesia using an 837 kHz transducer in conjunction with intravenous 100 µl/kg Optison microbubbles. Burst sonications (10ms at 2 Hz) were applied for 100 s. Brain levels of antibodies were measured by ELISA followed by immunohistochemical analysis on another half hemisphere. Secondly, 16 mo-old APP/PS1dE9 mice were treated weekly for 3 weeks with PBS (n=9), 500 ?g 07/2a alone (n=9), FUS alone (n=7) or 07/2a + FUS combination (n=6). Sonication was applied at two locations in each hemisphere in

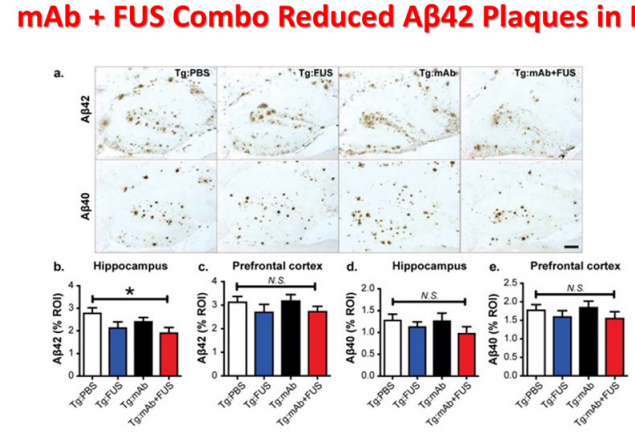

Figure 1. Combination treatment reduced Abeta42 levels in the hippocampus. No significant difference in prefrontal cortex and no change in A?40 deposition was observed

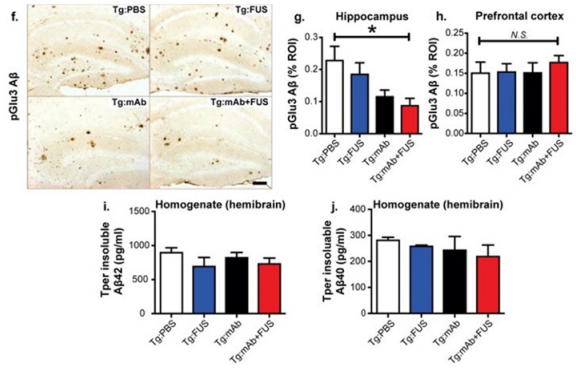

Figure 2. Combination treatment lowered pGlu3-A? in hippocampus without any changes in prefrontal cortex. No change in insoluble Abx-42 or Abx-40 was observed in hemibrain homogenates.

the hippocampus. Behavioral testing in the Water T Maze (WTM) was performed 1-2 week later followed by euthanasia. Brains were examined for amyloid burden, inflammation, and microhemorrhages.

Results: In our single-dose mAb and FUS combination treatment study, sonication increased 07/2a mAb levels in the brain by 5.9-fold after 4 hr ($p<0.005$) and 5.5-fold ($p<0.05$) 72 hr post-treatment. Brain-to-Blood ratio of the antibody was elevated at 4 hr and a significant increase was seen by 72 hr in the mice that received combination treatment. Immunohistochemistry confirmed an increase in antibody staining in the combination-treated mice at 4 hr and 72 hrs vs mAb alone treated mice. Increased Iba-1 & CD68 glial immunoreactivity was observed after combination treatment and such response was clearly observed in unilateral FUS cohort along with signs of transient recruitment of Ly6G+ monocyte/granulocyte/neutrophils. There was no significant increase in microhemorrhages. Three weekly treatments of 07/2a mAb treatment improved cognition and when combined with FUS, this improvement occurred faster while lowering A?42 and pGlu3-A? plaque load and increased synaptic markers in the hippocampus of AD mice compared to PBS control AD mice. Iba-1-positive, plaque-associated microglia/macrophages were observed in all treatment groups, while mAb+FUS also induced infiltration of Ly6G+ immune cells. Microhemorrhages were not increased following FUS, mAb, or the combination treatment.

Conclusions: Our results suggest that FUS may be a useful tool for facilitating the efficacy of anti-pyroGlu3 A? mAb immunotherapy presumably by enhancing delivery to the brain, with better A? clearance, synaptic protection, and hippocampal function. Combination treatment resulted in the presence of peripheral immune cells within plaques. Thus, FUS may have therapeutic potential when used in combination with anti-pyroGlu3 A? mAbs for AD treatment.

Acknowledgment/Funding Sources: NIH NIA RF1 XXX (CAL) and SSSSSSSS (NJM)

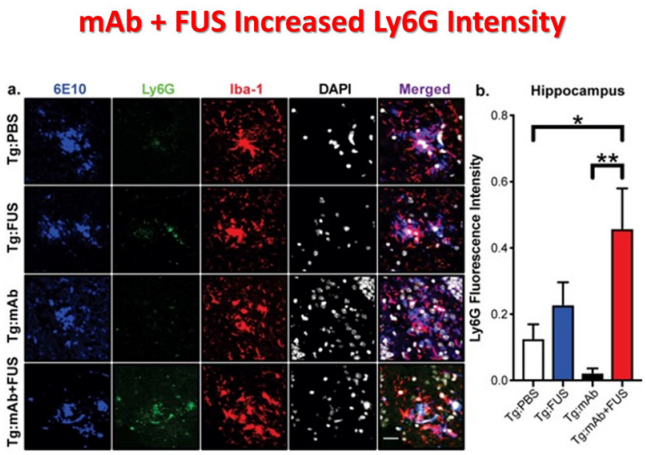

Figure 3. Combination treatment is associated with increased infiltration of Ly6G-positive immune cells

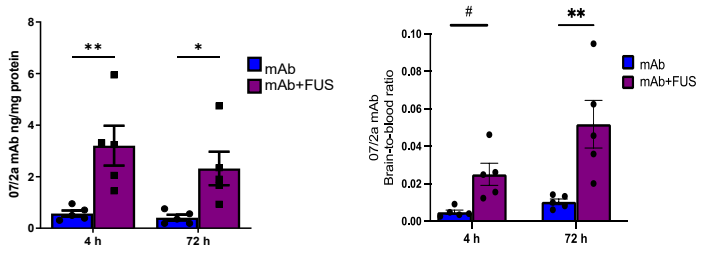

Figure 4. After acute single dose combination treatment, levels of 07/2a mAb levels in the brain were increased after 4 and 72 h post-treatment. Ratio of Brain-to-blood levels of 07/2a mAb indicating equilibrium across BBB.

NDG-03

Topic: Neurodegenerative Disorders

Presentation Type: Oral

Extensive Frontal Focused Ultrasound Mediated Blood-Brain Barrier Opening for the Treatment of Alzheimer's Disease

Jin Woo Chang

Yonsei University College of Medicine, Seoul, Seoul Teugbyeolsi, South Korea

Background: Focused ultrasound (FUS) mediated blood brain barrier (BBB) opening demonstrated the removal of amyloid plaque and the improvement of cognitive functions in preclinical studies, but there are a few clinical studies on this. This study was conducted to evaluate the safety, feasibility and potential benefits of repeated extensive BBB opening. Focused ultrasound (FUS) mediated blood brain barrier (BBB) opening demonstrated the removal of amyloid plaque and the improvement of cognitive functions in preclinical studies, but there are a few clinical studies on this. This study was conducted to evaluate the safety, feasibility and potential benefits of repeated extensive BBB opening.

Materials and Methods: This study was an open-label, prospective study. Six patients with Alzheimer's disease (AD) were enrolled at Severance hospital in Korea between March 2020 and August 2020. Five patients completed the study. FUS mediated BBB opening, targeting the bilateral frontal lobe regions over 20?, was performed twice at three-month intervals. Magnetic resonance imaging (MRI), 18F-Florbetaben (FBB) positron emission tomography (PET), Caregiver-Administered Neuropsychiatric Inventory (CGA-NPI) and comprehensive neuropsychological tests were performed before and after the procedures.

Results: We targeted a mean volume of 21·1±2·7? and BBB opening was confirmed at 95·7±9·4% of the targeted volume. The ratio of frontal to other cortical regions FBB Standardized Uptake Value Ratio (SUVR) after the procedure was significantly decreased compared to the pre-procedure (1.002 vs 0.986, P=0·043). CGA-NPI scores at two weeks after the second procedure significantly decreased compared to baseline (8.6±6.0 vs 2.2±3.0, P=0·042), but recovered after 3 months. No adverse effects were observed.

Conclusions: The repeated and extensive BBB opening in the frontal lobe was safe, feasible, resulting in decreased SUVR and temporary improvement in related symptoms. Future studies combining adjuvant therapeutics with BBB opening are needed to enhance the effect and lower the adverse effect of therapeutics.

Acknowledgment/Funding Sources: This study was supported by a grant from the Brain Research Program through the National Research Foundation of Korea(NRF) funded by the Korean Ministry of Science, ICT, and Future Planning, a government department (2016M3C7A1914123).

NDG-04

Topic: Neurodegenerative Disorders

Presentation Type: Oral

Improving the Safety Profile of Focused Ultrasound for Blood-Brain Barrier Opening by Applying a Combinatorial Strategy That Involves a Claudin-5-Specific Binder

Juergen Goetz[1], Liyu Chen[2], Jonathan Lee[2], Tishila Palliyaguru[2], Arnaud Gaudin[2], Jae Song[2], Gerhard Leinenga[2]

[1]University of Queensland, Brisbane (St Lucia Campus), Queensland, Australia
[2]University of Queensland, Queensland Brain Institute, Brisbane, Queensland, Australia

Background: Treatment strategies for neurological disorders such as Alzheimer?s disease are hampered by the fact that the blood-brain barrier (BBB) establishes an efficient barrier for therapeutic agents. An emerging technology to overcome this limitation is focused ultrasound (FUS). When FUS interacts with intravenously injected microbubbles (MB), FUS+MB, the BBB opens, transiently allowing access of therapeutic agents into the brain. However, the ultrasound parameters need to be tightly tuned: when the acoustic pressure is too low there is no opening, and when it is too high, tissue damage can occur. We therefore asked whether barrier permeability can be increased by combining FUS+MB with a second modality such that in a clinical setting lower acoustic pressures could be used.

Materials and Methods: Given that FUS+MB achieves BBB opening by disruption of tight junction (TJ) proteins such as claudin-5 of brain endothelial cells, we generated a stable MDCK (Madin-Darby Canine Kidney) II cell line (eGFP-hCldn5-MDCK II) that expresses fluorescently tagged human claudin-5. Two claudin-5 binders, the peptide mC5C2 and cCPEm (truncated form of an enterotoxin), reported previously to weaken the barrier (Dithmer et al., Ann. NY Acad 2017, Protze et al., CMLS 2015)), were synthesized and assessed for their abilities to enhance the permeability of cellular monolayers. We then performed a comparative analysis of single and combination treatments, measuring transendothelial electrical resistance (TEER) and cargo leakage, combined with confocal image analysis. We also performed in vivo experiments by pre-treating C57Bl/6 mice with cCPEm together with FD10 dextran as cargo, followed by FUS+MB treatment in order to determine whether the findings obtained in vitro can also be replicated in vivo.

Results: We successfully generated a novel cell line that formed functional monolayers as validated by an increased TEER reading (622.9 ± 129.1 Ohm·cm2) and a low (< 0.2%) permeability to sodium fluorescein (376 Da). We found that the binders exerted a time- and concentration-dependent effect on barrier opening when incubated over an extended period, whereas FUS+MB caused a rapid opening followed by recovery after 12 hours within the tested pressure range. Importantly, preincubation with cCPEm prior to FUS+MB treatment resulted in greater barrier opening compared to either FUS+MB or cCPEm alone as measured by reduced TEER values and an increased permeability to fluorescently labelled 40 kDa dextran (FD40). For example, preincubation with cCPEm for 12 h reduced TEER reduction for the combination treatment a further 166.5% and 160.6%, compared with cells treated with 0.1 and 0.2 MPa FUS+MB alone, respectively. The changes in TEER were reflected by changes in permeability in that the leakage of FD40. Segmentation analysis of confocal images revealed that while the TJ protein ZO-1 displayed a constant stability across all treatment conditions, the eGFP-hCldn5 signal initially detected in the plasma membrane was relocated and clustered in the cytoplasm after 12h GST-cCPEm and 12h GST-cCPEm + FUS+MB conditions (Chen et al., Theranostics 2022). To determine whether the in vitro findings can be translated in vivo, C57Bl/6 mice were i.v. injected with cCPEm and FD10 dextran followed 2.5 h later by FUS+MB treatment (1 MHz centre frequency, 10 Hz PRF, 10 ms PL, 10 % duty cycle, 2 min sonication, testing a PNP range) using FUS+MB only as control, using the TIPS 1 MHz annular array system (Philips). Our preliminary analysis reveals increased uptake of the cargo for the combination treatment compared to ultrasound on its own.

Conclusions: In conclusion, we have generated a novel combinational strategy utilizing a claudin-5 specific binder, GST-cCPEm, together with FUS+MB to weaken the BBB, and thereby enhance BBB permeability. The data suggest (in vivo data pending) that pre-incubation with clinically suitable binders to TJ proteins is a suitable strategy to facilitate safer and more effective ultrasound-mediated BBB opening in cellular and animal systems and potentially also for the treatment of human diseases of the brain.

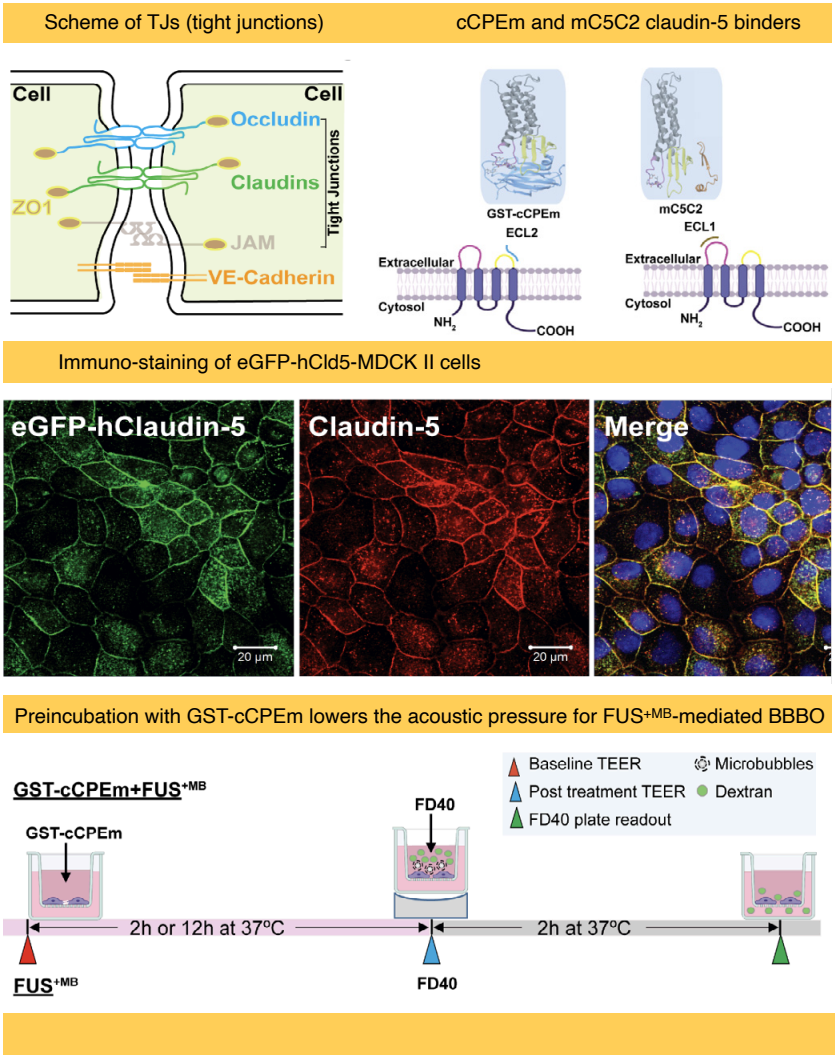

Figure 1. Scheme of TJs (tight junctions); cCPEm and mC5C2 claudin-5 binders; Immuno-staining of eGFP-hCld5-MDCK II cells; Preincubation with GST-cCPEm lowers the acoustic pressure for FUS+MB-mediated BBBO (blood-brain-barrier opening)

NDG-05

Topic: Neurodegenerative Disorders

Presentation Type: Oral

Low-Intensity Ultrasound Restores Long-Term Potentiation and Memory in Senescent Mice through Pleiotropic Mechanisms including NMDAR Signaling

Juergen Goetz, Daniel Blackmore

University of Queensland, Brisbane (St Lucia Campus), Queensland, Australia

Background: The major risk factor for Alzheimer s disease (AD) is age, and it is therefore not surprising, that the pathology in, for example, transgenic mouse models expressing mutant forms of APP and Tau progresses with age, as does the ensuing cognitive impairment. Nonetheless, many analyses in these models are conducted at an early age, not only in absolute terms given an average life span of around 26 months for C57Bl/6 mice, the inbred strain on which most AD transgenic mouse strains have either been generated or onto which they have been backcrossed, but also in relative terms. While this is a reasonable approach to understand pathogenic processes, for therapeutic strategies it depends on whether the objective is to slow down the pathogenic process, to cure the disease, or to ask whether the treatment is also effective at an advanced age. Given that cognitive functions become impaired in physiological ageing and not just AD, the question can be asked whether US (having shown efficacy in AD mouse models) would also improve cognitive functions in senescence.

Materials and Methods: 20-22 month-old senescent C57Bl/6 wild-type mice were treated weekly over six scanning ultrasound (SUS) sessions with SUS+MB and also SUSonly (with ultrasound in the presence and absence of microbubbles), i.e. with and without blood-brain-barrier (BBB) opening. The animals all underwent behavioral testing, using an accelerated active place avoidance (APA) paradigm. A subset of mice was used to obtain slice cultures for electrophysiological recordings to measure induction of long-term potentiation (LTP): The remainder of the mice were perfused, and their brains dissected, for histological analysis (neurogenesis, extracellular matrix) or biochemical analysis (western blotting, SWATH quantitative proteomics).

Results: To our surprise, LTP induction was rescued in both the SUS+MB and SUSonly groups. In the APA spatial memory paradigm, the SUS+MB group showed a trend towards improved cognition, whilst SUSonly resulted in statistically significant improvements in spatial learning. Synaptic plasticity and cognitive function are both associated with alterations of the extracellular matrix (perineuronal nets) of the brain. Our study revealed a significant reduction of these nets using WFA as a marker in the dentate gyrus in SUSonly mice compared to naïve, sham or SUS+MB animals. Moreover, given the tight link between the extracellular matrix and neurogenesis, both SUS paradigms were found to massively induce neurogenesis (13-fold for SUSonly). We next examined whether the two SUS treatment paradigms altered the levels and activities of key proteins in the hippocampus compared to sham. Phosphorylation of the NMDA receptor subunit 2B (pNR2B) by the kinase CaMKII has been found to play a critical role in learning and memory storage, and importantly, pNR2B levels were also increased following the SUSonly treatment. No change was observed for NR2A, but the NR2A/B ratio was significantly reduced after SUSonly treatment. Lowering this ratio has been shown to reduce the threshold for LTP induction in the murine visual cortex. Taken together these findings

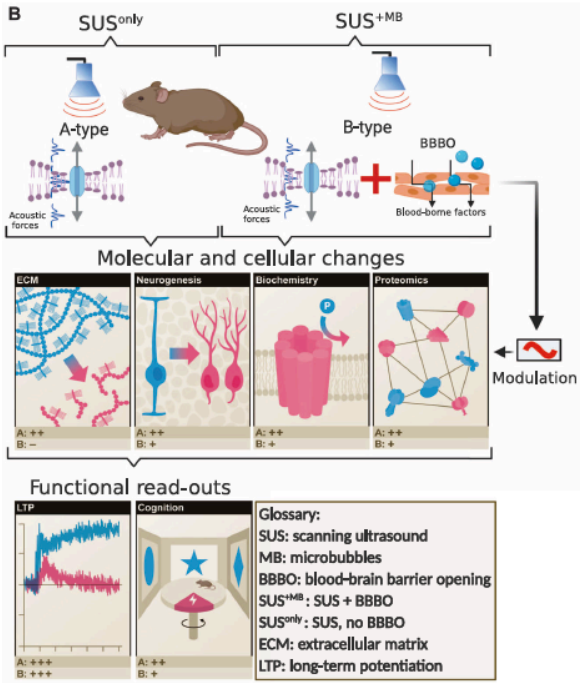

Figure 1. Integrated model differentiating A-type effects of SUS due to a pressure wave (SUSonly) and B-type effects, adding modulatory effects due to BBB opening and the uptake of blood-borne factors by the brain (SUS+MB).

demonstrate that therapeutic ultrasound leads to significant, activating changes in synaptic signaling. The proteomic analysis identified a cluster of proteins associated with synaptic signaling, including an increase in both mGluR1 which has been shown to be associated with spatial learning and Lrrtm4, which is critically involved in synapse development.

Conclusions: Together, our work suggests that US exerts its neuromodulatory effects via pleiotropic mechanisms which may converge on the NMDA receptor. It adds to several studies that highlight the neuromodulatory potential of therapeutic ultrasound in different species and experimental paradigms. With the observed changes associated with synaptic plasticity, SUS may therefore be an additional non-invasive modality, as to some extent shown for repeated transmagnetic stimulation, transdural electric nerve stimulation and direct current stimulation, to induce LTP or LTP-like plasticity, which have been suggested to hold promise for the treatment of a variety of neurological conditions.

Acknowledgment/Funding Sources: National Health and Medical Research

NDG-06

Topic: Neurodegenerative Disorders

Presentation Type: Oral

Transcriptional Signature in Microglia Isolated from an Alzheimer's Disease Mouse Model Treated with Focused Ultrasound-Mediated Blood-Brain Barrier Opening

Gerhard Leinenga[1], Liviu-Gabriel Bodea[2], Jan Schröder[3], Jae Song[1], Alexandra Grubman[4], Jose M. Polo[3], Juergen Goetz[5]

[1]University of Queensland, Queensland Brain Institute, Brisbane, Queensland, Australia
[2]The University of Queensland, Brisbane, Queensland, Australia
[3]Monash University, Melbourne, Victoria, Australia
[4]Monash University, Brisbane, Queensland, Australia
[5]University of Queensland, Brisbane (St Lucia Campus), Queensland, Australia

Background: In the brain of a person with Alzheimer's disease, amyloid beta plaques are present and are surrounded by microglia, the brain's resident immune cells. Microglia assume both a protective role (through shielding, recognition, and removal of amyloid beta) and a detrimental role (through removal of synapses or the release of neurotoxic factors), in AD. it has been shown that amyloid-beta containing microglia differ in their transcriptional signature in comparison to microglia that have not internalized the peptide. Studies in animal models of AD have indicated that repeated treatments with focused ultrasound and microbubbles (SUS+MB) open the blood-brain barrier temporarily and cause reduction in amyloid plaques through their phagocytosis by microglia. To gain a better understanding of how the combination of SUS+MB treatment and amyloid-beta internalization affects microglial physiology, we analyzed the transcriptional profile of microglia isolated from APP23 mice (a model of AD) that had been subjected to SUS+MB.

Materials and Methods: Wild-type (WT) and APP23 mice were subjected to SUS+MB treatment, using non-sonicated mice as sham controls. After 48 h, the APP23 mice were injected with methoxy-XO4 to label amyloid-beta aggregates, followed by microglial isolation into XO4+ and XO4- populations using flow cytometry. Both XO4+ cells containing phagocytosed amyloid plaques and XO4- cells were subjected to RNA sequencing and transcriptome profiling and cluster analysis and interrogation of differentially expressed genes and pathways were carried out.

Results: The analysis of the microglial cells revealed a clear segregation depending on genotype (AD model vs. WT mice) and Aβ internalization (XO4+ vs. XO4- microglia in APP23 mice), but interestingly, no differences were found between SUS+MB and sham in WT mice at a two days post SUS+MB. Differential gene expression analysis in APP23 mice detected 278 genes that were significantly changed by SUS+MB in the XO4+ cells (248 up/30 down) and 242 in XO- cells (225 up/17 down). Pathway analysis highlighted differential expression of genes related to the phagosome pathway and marked upregulation of cell cycle-related transcripts in XO4+ and XO4- microglia isolated from SUS+MB-treated APP23 mice.

Conclusions: In this study, we sought to investigate the changes to the microglial transcriptomic profile induced by the application of BBB opening achieved with therapeutic ultrasound in conjunction with

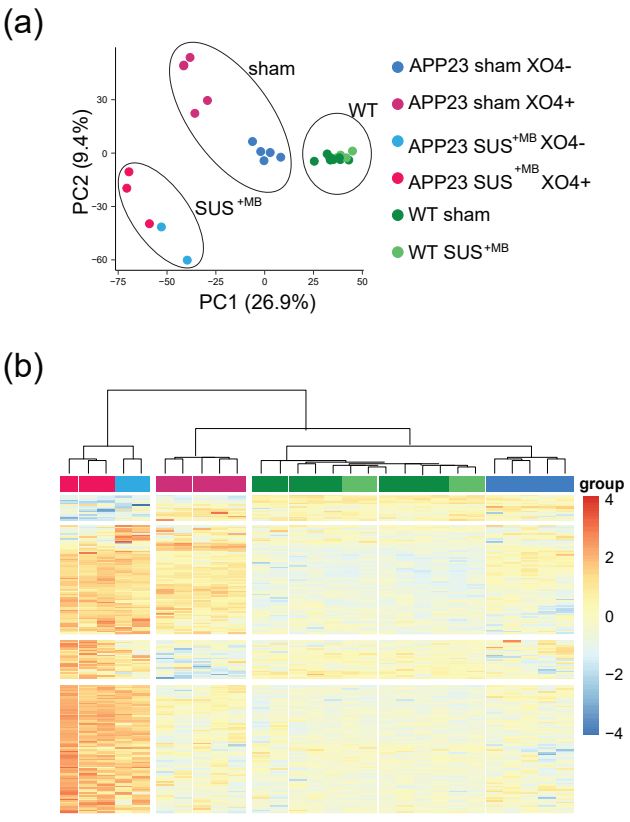

Figure 1. Cluster analyses distinguishes between genotype-, treatment-, and Aβ-dependent microglial phenotypes

intravenously injected microbubbles in a mouse model of AD. By analyzing the microglial transcriptome and correlating it with the presence or absence of amyloid-beta in the microglia at two days after treating amyloid-depositing APP23 mice with SUS+MB. This allowed us to identify several cellular functions that were increased by SUS+MB application in microglial populations that contained amyloid-beta or not, such as the phagosome (reflecting uptake of amyloid-beta plaques for degradation), as well as the cell-cycle pathway. Focused ultrasound has a relatively larger effect than A? plaque internalization on upregulating transcripts associated with the cell cycle and proliferation and this occurred independently of A? internalization. Together, this highlights the complexity of the microglial response to focused ultrasound mediated blood-brain barrier opening, with potential applications for the treatment of AD.

Acknowledgment/Funding Sources: Estate of Dr Clem Jones AO, the National Health and Medical Research Council of Australia

NDG-07 -YI

Topic: Neurodegenerative Disorders

Presentation Type: Oral

Safety and efficacy of single-treatment neuronavigation-guided FUS to induce blood-brain barrier opening in Alzheimer's disease patients

Katherine Liu[1], Antonios Pouliopoulos[2], Robin Ji[1], Sua Bae[1], Lawrence S. Honig[3], Elisa Konofagou[1]

[1]Columbia University, New York, NY, USA
[2]King's College London, London, London, United Kingdom
[3]Columbia University Irving Medical Center, New York, NY, USA

Background: Targeted, non-invasive blood-brain barrier opening (BBBO) achieved through microbubble (MB)-mediated focused ultrasound (FUS) has been studied for its effects on beta-amyloid plaque reduction in Alzheimer's disease (AD). In this phase-1 clinical trial (NCT04118764), one treatment session was given to each patient using neuronavigation-guided FUS to temporarily open the BBB in the right prefrontal cortex (PFC). The trial's primary objective is to assess safety and feasibility of FUS-induced BBB opening, while the secondary objective is to assess changes in beta-amyloid load using standard uptake value ratio (SUVR) values calculated from PET scans.

Materials and Methods: Two AD patients (P1: Patient 1, P2: Patient 2) have completed the study so far. Treatment with a single element transducer targeting the right PFC was performed following FDA-approved parameters (Fc: 0.25 MHz, pulse length: 10 ms, PRF: 2 Hz, derated peak-negative pressure: 200 kPa, treatment duration: 2 min, Definity MB clinical dose: 10 ?l/kg). Contrast-enhanced T1-weighted MRI scans were acquired to confirm successful BBB opening. A baseline PET scan with 18F-florbetapir tracer and an MMSE test were acquired before treatment, followed by a short-term PET scan after treatment, and a long-term PET scan after treatment with a final MMSE test. For P1, the 3 PET scans were acquired 1 month prior, 3 days after, and 5 months after treatment. For P2, the PET scans were acquired 2 months prior, 3 weeks after, and 3 months after treatment. SUVR values were found by normalizing the SUV in the frontal lobe (FL) by the mean SUV of the cerebellum and pons. SUVR asymmetry ratios (SUVRasym) in the FL were obtained by dividing the SUVR of the treated FL in the right hemisphere (FLright) with that of the untreated FL in the left hemisphere (FLleft), and their changes relative to baseline SUVRasym (dSUVRasym) were found.

Results: Both patients showed successful BBBO (opening volumes – P1: 318mm3, P2: 257mm3), as seen in Fig 1(a) and 2(a). For each patient, SUVR maps were calculated and overlaid onto the T1-weighted MRI, as seen in Fig 1(b)-(d) and Fig 2(b)-(d) for P1 and P2, respectively. P1's baseline and final MMSE scores were both 18, and P2's baseline and final

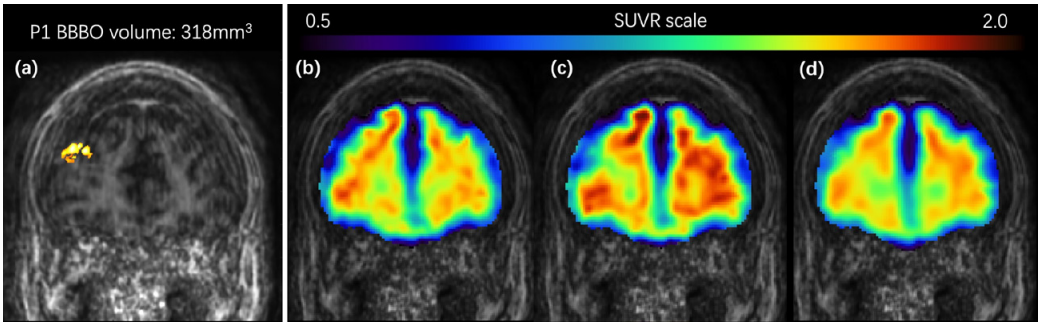

Figure 1. Patient 1 (P1) contrast-enhanced T1 scan (a) indicating BBBO (highlighted) and overlaid with PET SUVR (b) 1 month before treatment, (c) 3 days after treatment, and (d) 5 months after treatment.

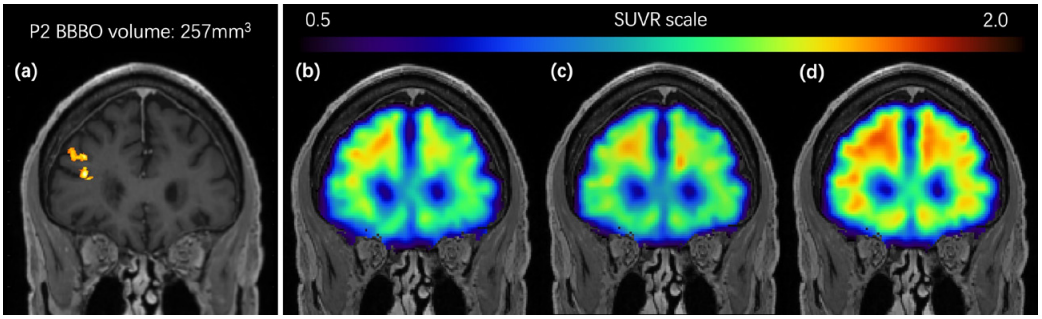

Figure 2. Patient 2 (P2) contrast-enhanced T1 scan (a) indicating BBBO (highlighted) and overlaid with PET SUVR (b) 2 months before treatment, (c) 3 weeks after treatment, and (d) 3 months after treatment.

MMSE scores were 20 and 22, respectively. Fig 3(a) and 3(b) show the dSUVRasym in the FL of P1 and P2, respectively. dSUVRasym in P1's FL revealed a consistent decrease relative to the baseline, both 3 days after treatment (-1.51%) and 5 months after treatment (-1.38%). P2 saw a similar short-term decrease in SUVRasym 3 weeks after treatment (-0.96%) but it was not sustained at the long-term time-point of 3 months after treatment (+3.17%).

Conclusions: Short-term and long-term changes of dSUVRasym in the FL showed varying degrees of amyloid load changes. dSUVRasym over time would indicate a change in the rate of beta-amyloid accumulation in the treated and untreated regions. Therefore, a decrease in SUVRasym (i.e. negative dSUVRasym) would indicate a slower beta-amyloid progression in the treated region relative to that in the untreated region. Both subjects exhibited negative dSUVRasym at the short-term timepoint, suggesting that there was a greater reduction in beta-amyloid load in the treated FL relative to the untreated FL. However, assessment of SUVRasym at the long-term timepoint indicates that the reduction stagnated (P1) or was only temporary (P2). Thus, the dSUVRasym observed on the short-term suggests that the efficacy of FUS-induced BBBO to reduce beta-amyloid may be transient, and could require multiple session to cause a greater reduction. Additionally, the BBBO volume sizes could also influence the extent and sustainability of treatment effects. The sustained decrease of SUVRasym in the FL of P1 over the course of several months, which was not observed in P2, could be explained by the larger BBBO in P1. While the negative dSUVRasym showed potential treatment efficacy, significant beta amyloid changes after BBB opening have yet to be established due to the limited sample size of 2 patients and different individual PET scan timelines. Future analysis with additional patients would offer more insights into potential efficacy trends in beta-amyloid changes as a result of FUS-induced BBB opening.

Acknowledgment/Funding Sources: This work was supported by the National Institutes of Health (R01AG038961) and the Focused Ultrasound Foundation.

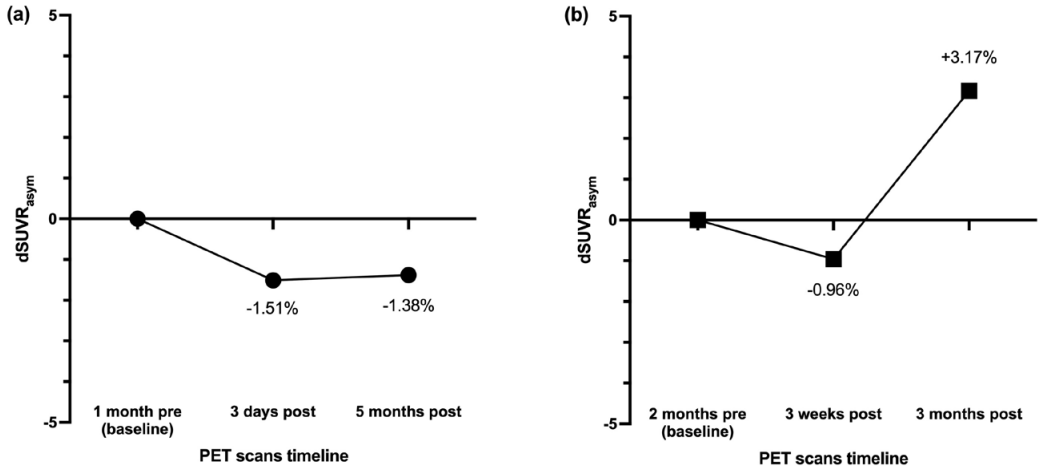

Figure 3. (a) P1 and (b) P2 dSUVR_asym in the FL across PET scans timeline. Baseline PET scans were acquired before FUS (labeled 'pre'), follow-up PET scans were acquired after FUS (labeled 'post').

NDG-09

Topic: Neurodegenerative Disorders

Presentation Type: Oral

Neuromodulation with Transcranial Pulse Stimulation (TPS) or with Transcranial Focused Ultrasound (tFUS): What Is the Difference?

Pavel Novak

Storz Medical AG, Tägerwilen, Thurgau, Switzerland

Background: Transcranial Pulse Stimulation uses focused shockwave pulses, which are transmitted to the brain through the skull. The TPS was introduced in 2018. It replaced the term TESWT (Transcranial Extracorporeal Shock Wave Treatment), which emerged on behalf of the first shockwaves applications to the brain in 2005 (unresponsive wakefulness syndrome). Low-intensity shockwaves (ESWT) are used in orthopedic, cardiology, urology, dermatology, and aesthetics since 1990. Next to shockwaves, there is another focal, mechanical stimulation tool in medicine, the focused ultrasound. FUS is used for tissue ablation and drug delivery. There is an emerging neurological application with tFUS for neuromodulation.

Materials and Methods: Shockwaves are single pulses with high positive amplitude, very steep leading edge and short duration. The asymmetrical pulse shape results in very broad frequency spectrum (up to 20MHz), Fig.1: In spite of the high-pressure amplitude, the average power density is less than 0.1 W/cm2 due to the low repetition pulse rate. Thus, there is no heating and no micro lesions. Typical focal zone of an electromagnetic generator is an ellipsoid with 5mm diameter and 20-30mm length. TPS shockwave pulses have Energy Flux Density (EFD) of up to 0.25 mJ/mm2. Due to the application through the skull, 85% energy and correspondingly 65% pressure are absorbed. Compared to shockwaves, ultrasound is a continuous train of sinusoidal pressure oscillations with typical frequency of 0.5 to 5MHz. The frequency spectrum contains only the main frequency with its harmonics, Fig.2 Focused ultrasound can have focal area similar to the focal size of an electromagnetically generated shockwaves. The pressure amplitude is often not explicitly mentioned. The intensity is expressed as power density (W/cm2). The skull attenuates transcranial FUS in a similar way like shockwaves. For minimizing the tissue heating capacity of the FUS, the continuous ultrasound train is applied intermittently with repeated pulse bursts.

Results: The key stimulation parameters are listed in Table 1. The TPS is used for experimental treatment of Alzheimer's and Parkinson's disease since 2010 with positive results. The Alzheimer's disease treatment with TPS (Neurolith) is approved in Europe (CE

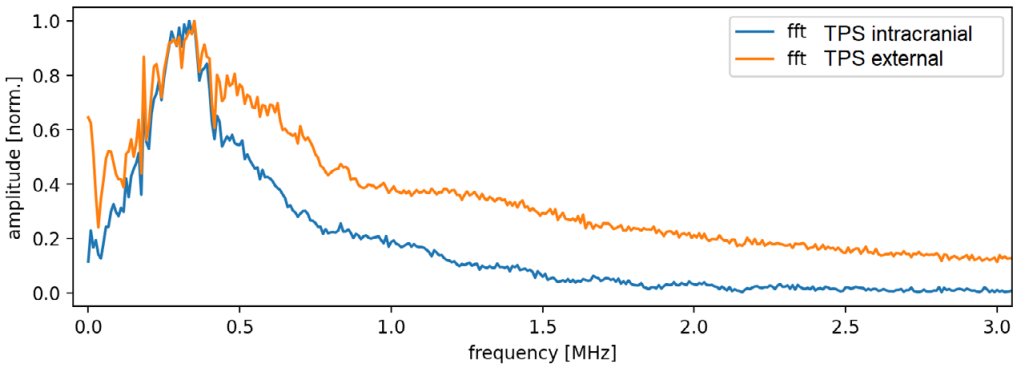

Figure 1. TPS frequency spectrum, extracorporeal and intracranial.

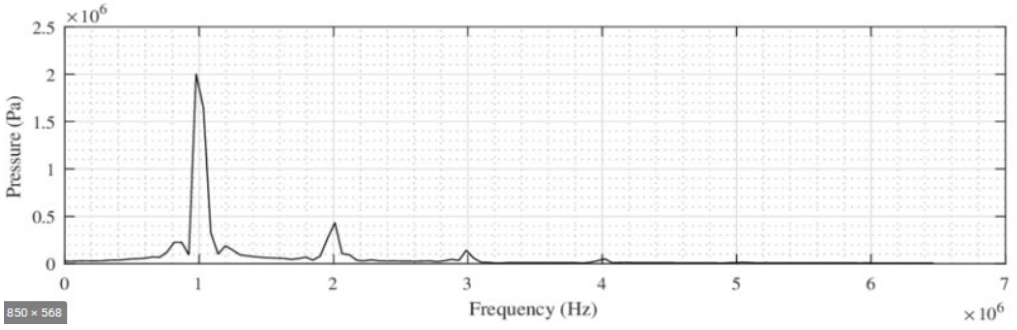

Figure 2. Frequency spectrum of focused ultrasound

mark) since 2018. Infrared Camera based navigation and documentation system (BodyTrack) together with MRI images allows precise and homogenous acoustic energy delivery to the targeted brain tissue. tFUS applications are still experimental.

Conclusions: The high frequency of the ultrasound pulses compared to the single shockwave pulses (1'000'000 times) results in tissue temperature increase. The formation of bursts is a compromise between biological effect (neuromodulation) and tissue heating. Based on the long-term experiences with shockwaves, a minimal pressure amplitude of 5MPa is considered necessary for biological effects. This might explain the significantly higher capability and efficacy of shockwaves in generating biological effects.

Table 1.

	TPS	**tFUS**
Pulse repetition frequency	4-8 Hz	0,5-5 MHz
Pressure amplitude	5-25 Mpa	0,1-3 Mpa
Energy Flux Density (EFD)	0,01-0.25mJ/mm^2	---
Average power density	0,1 W/cm^2	25 W/cm^2
Biological effects	many	few
max. intracranial values		
Pressure amplitude	8,75 Mpa	---
Energy Flux Density (EFD)	0,04 mJ/mm^2	---
Average power density	16 mW/cm^2	6 W/cm^2

NDG-10

Topic: Neurodegenerative Disorders

Presentation Type: Oral

Long-Term Safety and Outcomes of Focused Ultrasound Mediated Blood-Brain Barrier Opening in Alzheimer's Disease

Ali Rezai[1], Manish Ranjan[1], Jeffrey Carpenter[2], Marc W. Haut[1], Pierre F. D'haese[1], Rashi Mehta[1], Victor S. Finomore[1], Daniel O. Claassen[3], Peng Wang[2], Sally L. Hodder[4], Michael G. Kaplitt[5]

[1]West Virginia University Rockefeller Neuroscience Institute, Morgantown, WV, USA
[2]West Virginia University, Morgantown, WV, USA
[3]Vanderbilt University Medical Center, Nashville, TN, USA
[4]West Virginia Clinical and Translational Science Institute, Morgantown, WV, USA
[5]Weill Cornell Medical College, New York, NY, USA

Background: MRI-guided low intensity focused ultrasound (FUS) reversibly opened the blood-brain barrier (BBB), reduced beta-amyloid plaque, and improved memory in preclinical Alzheimer's disease (AD) models. Previously, we reported short-term safety and feasibility of FUS BBB opening (BBBO) in the hippocampus and entorhinal cortex (EC) in patients with Alzheimer's disease (AD). Here we report the long-term safety, clinical, and imaging outcomes of BBBO of larger brain areas in hippocampus/EC, frontal, and parietal lobes in participants with mild AD.

Materials and Methods: In this open-label, multi-center trial, participants with mild AD underwent MRI-guided FUS sonication to open the BBB in beta-amyloid positive regions of the hippocampus, entorhinal cortex, frontal, and parietal lobes. Participants underwent three separate FUS treatment sessions, 2 weeks apart. BBB opening and closure were assessed with gadolinium contrast enhancement on MRI brain following FUS treatment. Clinical outcomes included safety, neurological and cognitive evaluations with MMSE and ADAS-Cog, while Florbetaben PET measured levels of beta-amyloid deposition in target regions before and after FUS mediated BBB opening.

Results: Ten participants (55-73 years old) completed 30 separate FUS treatments at two participating institutions with 6-12 months follow-up. All FUS treatments were well tolerated, with no serious adverse events related to the procedure. All participants had immediate BBB opening after FUS, with a contrast enhancement of an average of 82% (range 53%-99%) of the FUS treated brain parenchyma, and BBB closed within 24-48 hours. Change on the ADAS-Cog and MMSE was similar to controls from the Alzheimer's Disease Neuroimaging Initiative (ADNI). PET scan demonstrated an average beta-amyloid plaque decrease of 5% SUVr and 14% in Centiloid scale in the beta-amyloid in the FUS treated regions.

Conclusions: We demonstrate that FUS BBB opening in AD is safe and reversible across multiple brain regions. There was no apparent cognitive worsening. Concomitant reduction of beta-amyloid in the FUS targeted regions was observed. The non-invasive and reversible opening of the BBB offers a unique opportunity for a novel approach to treatment as well as the possibility of targeted delivery of therapeutics to meaningful volumes of brain structures in AD and other neurodegenerative conditions.

Acknowledgment/Funding Sources: Insightec

NDG-11

Topic: Neurodegenerative Disorders

Presentation Type: Oral

Enhancing Delivery of Molecular Therapies to the CNS for Genetic Neurological Disorders

Nick Todd[1], Sneham Tiwari[2], Yongzhi Zhang[1], Christina Hung[2], Olaf Bodamer[2]

[1]Brigham and Women's Hospital, Boston, MA, USA
[2]Boston Children's Hospital, Boston, MA, USA

Background: Disease-specific molecular therapies for neurodegenerative monogenic disorders are particularly attractive due to well-studied disease mechanisms. Niemann-Pick Type C (NPC) is a rare lysosomal storage disorder caused by a single gene mutation in the NPC1 gene, which encodes a membrane protein that regulates the homeostasis and transport of unesterified cholesterol. Modified messenger RNA (modRNA) is emerging as a promising therapeutic with applications in vaccination, protein replacement therapy and treatment of genetic diseases. Preliminary animal studies using a lipid nanoparticle (LNP)-packaged modRNA for NPC show that current nanoparticle formulations are unable to penetrate the BBB. Here we propose to use focused ultrasound (FUS)-mediated disruption of the BBB to improve delivery of an LNP-modRNA therapy to the brains of NPC disease model mice

Materials and Methods: Preliminary experiments have been carried out to validate: 1) the effectiveness of the LNP-packaged modRNA therapy in lowering cholesterol storage in human cells; 2) that LNP formulation does not cross the BBB on its own; 3) FUS-BBB opening is feasible in the cerebellum of mice; 4) The LNP formulation will penetrate into the brain at the site of FUS-BBB disruption. Experiments to be performed next will be organized in a 3x2 factorial design study consisting of IV vs IV+FUS vs Cisterna Magna Injection administration and Therapy (1.5 mg/kg) vs No therapy, for a total of 6 groups. FUS-BBB opening will be targeted to the cerebellum: 690 kHz, 10 ms bursts applied at 1 Hz for 120 s, 0.34 MPa, and 20 ?L/kg Definity. The modRNA therapy will be given immediately after and T1-weighted contrast enhanced MRI images will be acquired. For cisterna magna (CM) injection, a 30-second injection of the modRNA formulation will be done to avoid sudden increases in intracranial pressure. The amount of therapy delivered to cerebellar (FUS-targeted) and cortical (non-FUS targeted) regions will be quantified by NPC1 mRNA levels (qPCR) and NPC1 protein translation levels (western blot). Safety metrics will assess inflammation by qPCR using a standard panel of markers and signs of potential tissue damage using H&E stained sections.

Results: 1) Figure 1 demonstrates therapy efficacy in vitro as measured by the level of unesterified cholesterol storage in human fibroblast cell lines. The control cell lines all had similar low levels of cholesterol storage for the no treat, mock treated (LNP-eGFP) and treated groups (hNPC1_06, hNPC1_07 and hNPC1_10). The NPC1 cell line had significantly elevated levels of cholesterol storage in the mock and untreated groups, as expected. Application of the three therapy formulations significantly reduced the cholesterol storage level. 2) Figure 2 shows western blot analysis of NPC1 protein expression in cerebellum 24h after therapy given by retro-orbital injection. NPC1 protein expression is observed in WT mice, but not in either the mock-treated (eGPF) or treated NPC homozygous mice, indicating that the therapy does not penetrate the BBB. 3) Figure 3 shows results from contrast MRI images of five WT mice following FUS-BBB opening targeted to the cerebellum. Hyperintense regions in each mouse show evidence of BBB disruption in the cerebellum. 4) Figure 4 shows GFP protein expression in cerebellum of mice 48 hours after treatment as measured by western blot. GFP signal intensity was significantly greater for the FUS group compared to the No FUS group (for both left and right hemisphere), showing that GFP-LNP crosses the BBB following FUS

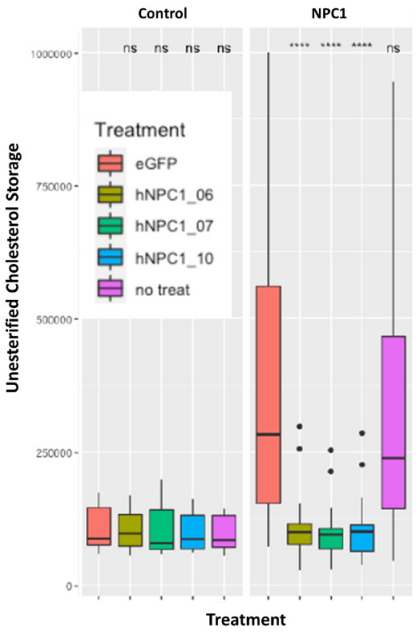

Figure 1. Cholesterol levels in Control and NPC1 deficient human cells.

disruption and is successfully translated into protein in the target organ.

Conclusions: The preliminary results indicate that the LNP particles can enter the brain parenchyma following FUS-BBB opening and that the modRNA therapy is successful in replacing the lost function of the NPC1 gene. We will now proceed to experiments that will answer the questions of FUS-BBB opening provides better CNS therapy distribution than another route of administration that could be used (IV injection alone or cisterna magna injection) and whether the therapy delivered by to the brain has the same therapeutic effect on CNS cells as what has been seen in peripheral organs.

Acknowledgment/Funding Sources: Focused Ultrasound Surgery Foundation

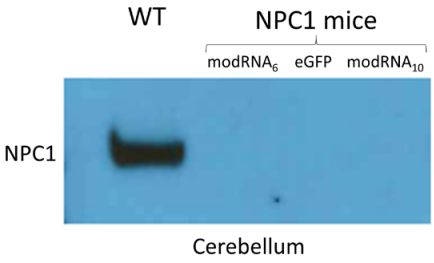

Figure 2. Protein levels of NPC1 in cerebellum follwing IV delivery alone of modRNA therapy.

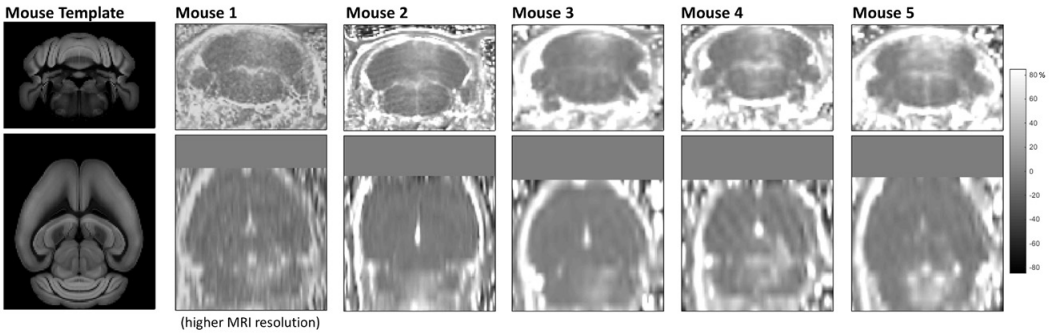

Figure 3. FUS-BBB opening in mouse cerebellum.

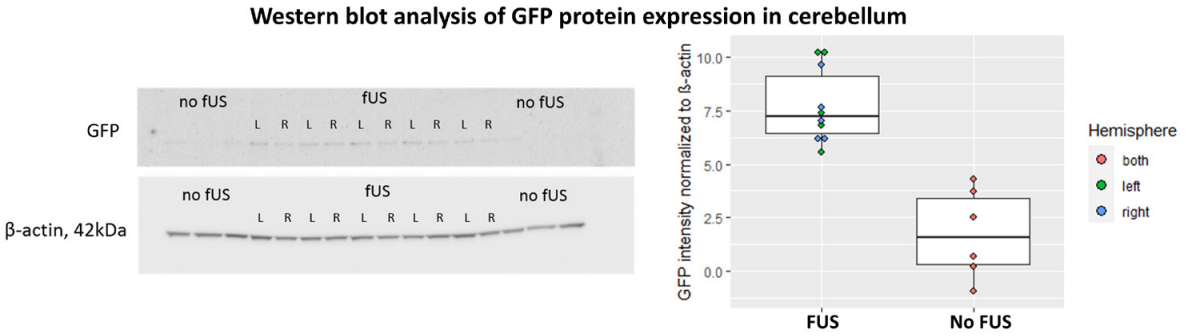

Figure 4. Protein levels of LNP-packaged GFP delivered to cerebellum with and without FUS.

NMD-01 -YI

Topic: Neuromodulation
Presentation Type: Oral

Examination of Low-Intensity Focused Ultrasound (LIFU) Parameters and Longevity of Effect for Human Neuromodulation

Areej N. Ennasr[1], Wynn Legon[2]

[1]Virginia Tech Carilion School of Medicine, Fairfax, VA, USA
[2]Fralin Biomedical Research Institute, Roanoke, VA, USA

Background: Low-intensity focused ultrasound (LIFU) has been well-studied in animals with conflicting reports on the role of specific parameters. A study in mice concluded intensity and duration were predictors for desired neuromodulation. However, duty cycle (DC) and pulse repetition frequency (PRF) were the best predictors in studies in rats, rabbits, and sheep. It is unclear if studies in small animal translate well to human due to differences in cranial volume, skull morphology, and the use of anesthetics. There is no evidence in humans of the best LIFU parameters to achieve clinically meaningful results that are robust, reproducible, and lasting.

Materials and Methods: This study examines a full parameterization design of LIFU parameters in humans using 3 intensity settings (6, 12, and 24 W/cm2), 6 DC settings (1%, 5%, 10%, 30%, 50%, and 70%), 4 PRF settings (10, 100, 500, and 1000 Hz), and 3 duration settings (100, 500, and 1000 msec), resulting in a total of 216 conditions. The second portion of the study analyzes LIFU application of varying durations delivered either intermittently or continuously, using optimal inhibitory and excitatory parameters from the full parameterization design. Prior to LIFU application, brain and skull images were collected for each participant using magnetic resonance imaging (MRI) and computed tomograhy (CT) scans, respectively. The primary outcome measure is the motor-evoked potential (MEP) generated using transcranial magnetic stimulation (TMS) of the first dorsal interosseous (FDI) muscle representation of the primary motor cortex (M1).

Results: Preliminary data has been collected in 6 participants for the full parameterization design. Analysis revealed DC to be a critical parameter. A DC = 30% resulted in ~10-15% suppression of MEPs, while a DC = 50 – 70% resulted in ~15 – 25% facilitation of MEPs. Moreover, DC appears to interact with duration, but not with intensity, as seen in Figure 1. These effects are independent of PRF. In 3 participants, inhibitory effects from LIFU application for 5-, 10-, and 20-minutes were analyzed. The inhibition of signal from the 20 minutes protocol lasted out to 60 minutes after

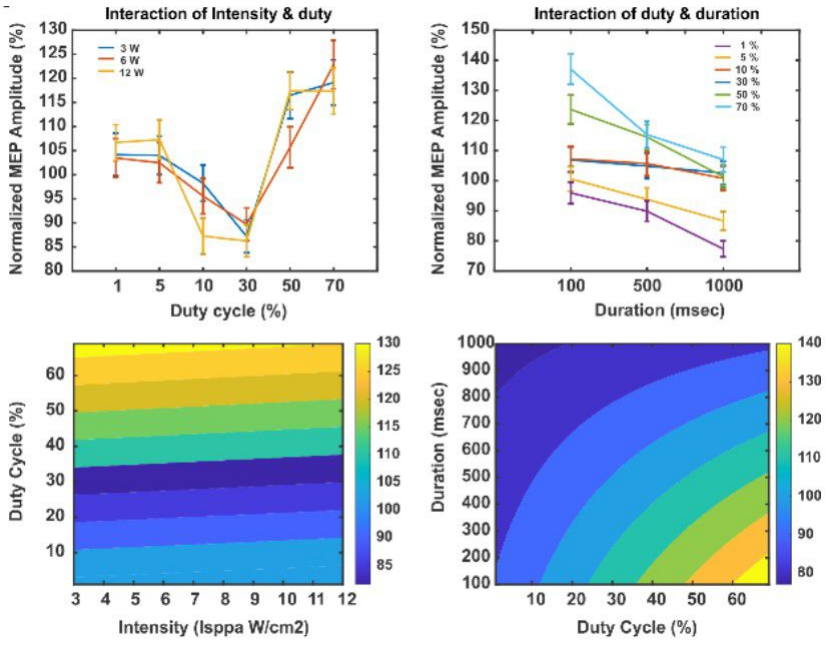

Figure 1. Interactions of duty cycle with intensity and duration. DC operates independently of intensity, while duration and DC do interact.

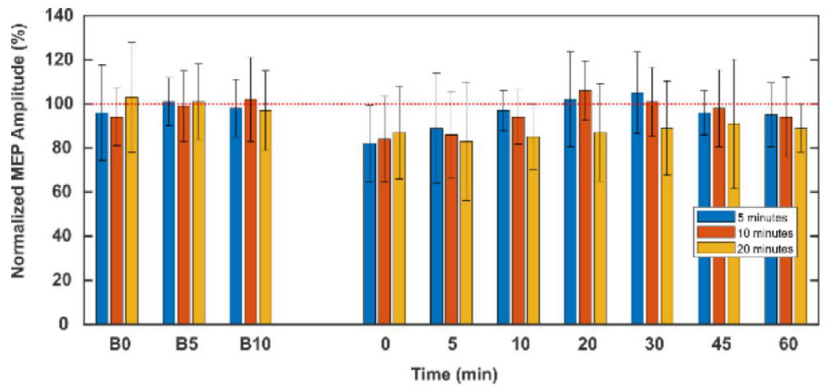

Figure 2. Longevity of LIFU effects after stimulation. N=3 exploring the impact of 5-,10-,20-minutes of LIFU application on the longevity of LIFU effect out to 1-hour post sonication. B0, B5, B10= baseline measurements.

application while 5 and 10 minutes did not, as seen in Figure 2. Therefore, longer applications of LIFU result in longest lasting effects.

Conclusions: Altering LIFU parameter settings looks to have a differential effect on MEP amplitude in healthy human volunteers. DC between 10-30% causes inhibition, while DC greater than 50% causes excitation, but this interacts with the duration of stimulation. Longer lasting effects are achieved with longer LIFU applications. . This study provides a precise way to define effective parameters for LIFU application, which is necessary before it can be translated as a neuromodulatory tool in the clinic.

NMD-02

Topic: Neuromodulation
Presentation Type: Oral

Durable Modulation of Deep Brain Circuits

Jan Kubanek, Taylor Webb, Matthew G. Wilson, Henrik Odéen

University of Utah, Salt Lake City, UT, USA

Background: Transcranial focused ultrasound has shown a unique potential for noninvasive and targeted repair of deep brain circuits.

Nonetheless, Previous studies have applied to the brain limited energies and thus could not investigate this capacity.

Materials and Methods: We developed a 256-element phased array that enables us to deliver ultrasound into specific deep brain targets of task-performing non-human primates (Fig 1).

We specifically targeted the lateral geniculate nucleus---a primary relay nucleus of visual information into the brain (Fig. 2)---while the subjects engaged in an established visual discrimination task.

We delivered into deep brain targets 30 s of pulsed ultrasound.

Results: Stimulation of the LGN (16 sessions, 2 animals) evoked substantial and significant bias (up to 2:1) in the animals' choice behavior in the discrimination task (Fig. 3).

The effect outlasted the stimulus for at least 10 minutes.

Moreover, as expected, the effect reversed polarity upon stimulation of the opposite LGN (left vs right), thus controlling for potential artifacts that can be associated with transcranial ultrasound.

Conclusions: These data demonstrate that low-intensity ultrasound can be used to induce sustained yet reversible effects in deep brain circuits of primates.

Acknowledgment/Funding Sources: This work was supported by the NIH grants R00NS100986 and F32MH123019.

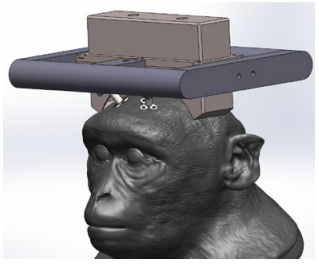

Figure 1.

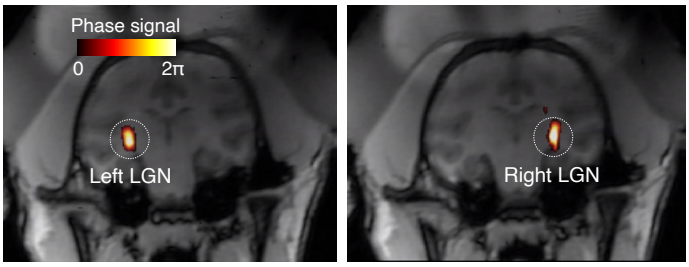

Figure 2.

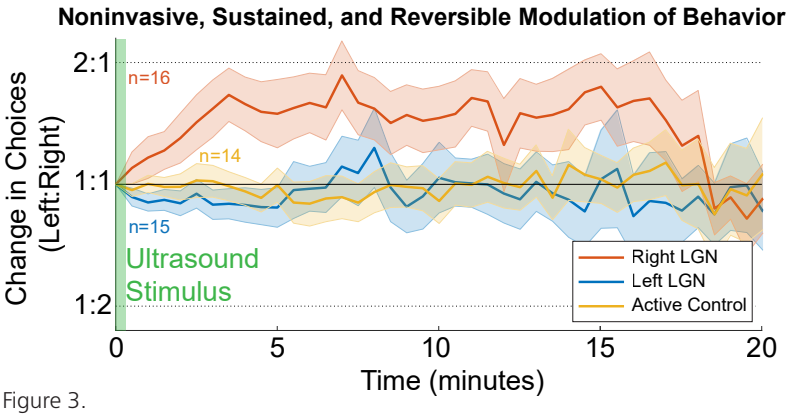

Figure 3.

NMD-03

Topic: Neuromodulation
Presentation Type: Oral

Single-Element Low-Intensity Focused Ultrasound to the Left Dorsal Anterior Insula Increases Coupling of the Human Salience Network

Andrew C. Strohma, Jessica Florig[1], Brighton Payne, Wynn Legon

Fralin Biomedical Research Institute, Roanoke, VA, USA

Background: Low-intensity focused ultrasound (LIFU) is an emerging non-invasive brain stimulation (NIBS) tool with significantly improved spatial resolution and targeting to deeper cortical structures compared to other forms of NIBS like transcranial magnetic stimulation (TMS). The insula, located deep to the Sylvian fissure and covered by the overlying frontal opercula is a promising target for neuromodulation for chronic pain as the posterior insula receives the majority of direct di-synaptic spinothalamic inputs while the dorsal anterior insula (dAI) integrates this nociceptive information and serves as a key node in the salience network. This network, comprised of the dAI and the dorsal anterior cingulate cortex (dACC), is critical for engaging attentional networks in response to salient noxious and innocuous stimuli. Functional and structural aberrations in the salience network have been implicated in a variety of centralized pain and neuropsychiatric conditions, making it a strong candidate target for these patient populations.

Materials and Methods: A 500kHz single-element focused transducer was stereotaxically targeted to the left dorsal anterior insula in four healthy participants (2 male, 2 female, mean age = 27.5 ± 3.2 years) using co-registered MRI/CT scans. Participants first underwent a pre-LIFU resting-state fMRI (rsfMRI) scan and a heat evoked Quantitative Sensory Testing (QST) protocol used to elicit 40 noxious stimuli to the dorsum of the right hand. Each stimulus was randomly separated by 10-20 seconds and rated on a 0-9 pain scale. 100 total stimulations of LIFU (pulsed repetition frequency = 1000 Hz, sonication duration = 1s, duty cycle = 36%) each separated by 5s was applied over 10 minutes followed by an identical post-LIFU rsfMRI and QST protocol. Resting-state fMRI and QST protocols were counterbalanced across participants. Physiologic data including continuous heart rate and respiration rate and pre/post blood pressure were collected. Resting-state fMRI connectivity data was analyzed using the CONN toolbox for Matlab. Seed regions of interest (ROI) included the left dAI, dACC, and amygdala.

Results: Seed-to-voxel analysis of the time-series data was compared pre/post-LIFU and revealed LIFU to left dorsal anterior insula increased local connectivity compared to pre-stimulation. Additionally, seed-based functional connectivity revealed increased coupling with the contralateral insula and dACC. There was no evidence for altered coupling with the amygdala.

Conclusions: Preliminary data analysis demonstrates that single-element LIFU is an effective means to non-invasively target the dorsal anterior insula in humans to affect resting-state functional connectivity of the salience network. The ability of LIFU to the left dAI to alter both network connectivity may have clinical applications for chronic pain and neuropsychiatric populations.

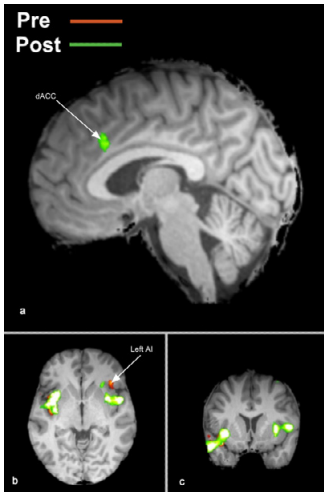

Figure 1. Coronal view of functional connectivity in an example participant. The left AI as the seed ROI was used to evaluate gray matter functional connectivity before and after a LIFU protocol.

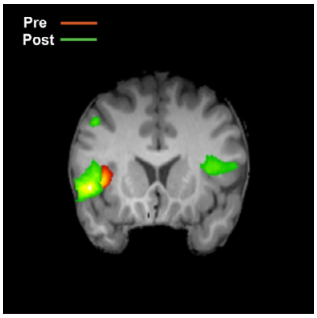

Figure 2. Sagittal, axial and coronal views of seed-based functional connectivity analysis following sonication using LIFU. a) Sagittal view demonstrating functional connections to the left AI and post LIFU coupling in the dACC. b) Transverse view c) Coronal view

OPE-01

Topic: Open Science
Presentation Type: Oral

Open Science Initiative at the Focused Ultrasound Foundation: Update

Charlie Manning

Focused Ultrasound Foundation, Charlottesville, VA, USA

Two years on from the 2020 launch of the FUSF open science initiative, the program has been successful in progressing FUSF open science policy and establishing dialogues with top publishers on increasing openness in the field. This update covers that work and plans going forward.

OPT-01

Topic: Opthalmic
Presentation Type: Oral

Shear Wave Passive Elastography for Crystalline Lens Elasticity Measurement in the Context of Cavitation-Mediated Presbyopia Treatment

Maxime Lafond[1], Alice Ganeau[1], Gabrielle Laloy-Borgna[1], Olfa Ben Moussa[2], Sylvain Poinard[2], Frédéric Mascarelli[2], Gilles Thuret[2], Philippe Gain[2], Stefan Catheline[1], Cyril Lafon[1]

[1]LabTAU, INSERM U1032, Lyon, Rhône, France
[2]BiiGC, University of Saint-Etienne, Saint-Priest-en-Jarez, Loire, France

Background: Presbyopia is the progressive rigidification and loss of accommodation of the crystalline lens, inducing loss of near vision. It affects everyone from age 40 to 45. Ultrasonic cavitation is being investigated in our group to soften the lens and treat presbyopia. The lens is a challenging organ: it is a sanctuary, remote from blood circulation. Thus, cavitation nucleation agents cannot be used. Additionally, it does not scatter ultrasound except at its interfaces. The classic elastography methods are inapplicable in this case, due to the lack of speckle to track. We are presenting the preliminary results of cavitation nucleation and methods of elasticity measurement in the lens. First experiments show the feasibility and the repeatability to nucleate cavitation inside the lens. We then propose a non-invasive method of elasticity monitoring by curvilinear shear wave elastography.

Materials and Methods: Experiments to show the feasibility of nucleating cavitation in the lens were implemented. Four transducers, focused at 50 mm and operating at 1.11 MHz were positioned in such a way that their foci were crossing at a same point. We obtained a small focal volume (1.2 mm3), well adapted to create cavitation in a small organ at a precise location. A 15 MHz clinical imaging array at the center of the therapy probe enabled precise targeting in the lens. We determined the cavitation threshold using passive cavitation imaging. We repeated exposures in 8 porcine whole eyes. For shear wave elastography, we developed a method around the only speckle available: the anterior interface of the lens. Gelatin spheres, mimicking the ultrasound transparency of the crystalline lens, were used as an experimental model to evaluate the feasibility of curvilinear elastography. Sweeps of vibrations (0.1–3.5 kHz) were induced to the sample with vibrators and displacements were tracked by ultrafast ultrasound imaging along the interface. We calculated the propagation velocity of waves by two methods: the time of flight and the noise correlation algorithm. Results were compared to indentation where the Young modulus was calculated from a compressive strength applied to the sample. The same experiments were conducted on ex vivo porcine lenses.

Results: Figure 1 shows the intrinsic cavitation threshold in the lens. Using the higher end of our system, we induced cavitation

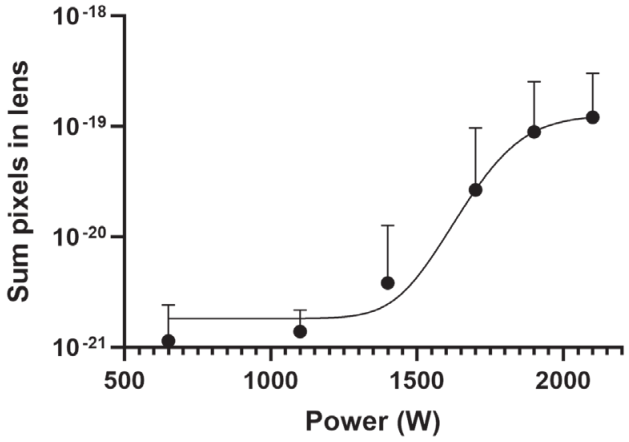

Figure 1. Intrinsic cavitation threshold in the lens.

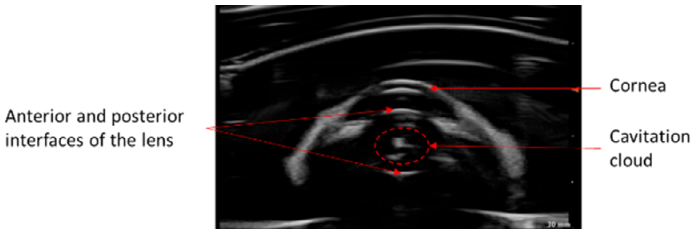

Figure 2. B-mode imaging of cavitation cloud nucleated in lens

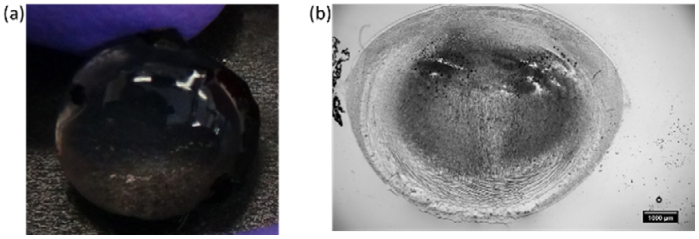

Figure 3. Photo showing the conservation of lens transparency (a) and macroscopic image of histological section of lens exposed to ultrasound cavitation, presenting no damages (b)

clouds in the lens with an average initiation time of 1.3 seconds, as seen on B-mode (Figure 2). Cavitation was confined in the target organ without damaged other parts of the eye as the cornea or the retina. No damages were observed on histology and the transparency was conserved (figure 3.a et 3.b). The measured Young moduli in the gelatin spheres were consistent across the three methods: 50±13kPa, 69±12kPa, and 42±4.6kPa for the time of flight, noise correlation, and indentation, respectively. Spectral analysis indicated only a small dispersive effect. The same acquisitions were realized on pig lenses by putting in vibration the entire eye. The time of flight and the correlation method gave 1.1±0.8kPa (0.6±0.2 m/s) and 0.9±0.1kPa (0.6±0.3 x 10-1m/s), respectively. These values are comparable with the literature that show Young moduli of the kPa order for young crystalline lens. However, spectral analysis showed a marked dispersion, likely because of the complex inhomogeneous structure of the lens. Further studies are necessary to understand its impact on elasticity.

Conclusions: First experiments to nucleate cavitation clouds in lenses show its feasibility and its repeatability in several samples of different ages. It remains to study the impact of this ultrasound treatment on the lens elasticity. The experiments implemented on the gelatin spheres validated the curvilinear shear wave elastography method. However, spectral analysis of propagating waves along the interface shows the complexity to deduce a global elasticity of a 3D object from 1D data. Furthermore, the crystalline lens is an inhomogeneous multilayer medium that can impact the propagation of waves. Additional studies, through numerical simulations of propagating waves in complex medium, are in progress for a better understanding of the phenomenon.

Acknowledgment/Funding Sources: This work was supported by the French Research Agency (ANR-21-CE19-0059-02) and the Focused Ultrasound Foundation (FUS).